NBER WORKING PAPER SERIES

ADAPTING TO FLOOD RISK: EVIDENCE FROM A PANEL OF GLOBAL CITIES

Sahil Gandhi
Matthew E. Kahn
Rajat Kochhar
Somik Lall
Vaidehi Tandel

Working Paper 30137
http://www.nber.org/papers/w30137

NATIONAL BUREAU OF ECONOMIC RESEARCH
1050 Massachusetts Avenue
Cambridge, MA 02138
June 2022, Revised March 2025

The authors thank and acknowledge financial support from the World Bank though its Vibrant Cities project as well as the UK FCDO's program on Climate Compatible Economic Growth. We also thank Sam Asher, Ludovica Gazze, Michael Greenstone, Forhad Shilpi, Ruozi Song, Sameh Wahba, Niels Holms Neilson, and participants at Delhi School of Economics seminar and the USC Environmental Economics Reading Group for constructive comments. We thank Adam Dessouky, Nadia Filanovsky, Xiaoqian Zhang, Suyang Wang, Yang Peng, David Krieger, Emma Cockerell, Divyam Jindal, and Robert Huang for excellent research assistance. The findings, interpretations, and conclusions expressed in this paper are entirely those of the authors. They do not necessarily represent the views of the International Bank for Reconstruction and Development/World Bank and its affiliated organizations, or those of the Executive Directors of the World Bank, the governments they represent, or the National Bureau of Economic Research.

NBER working papers are circulated for discussion and comment purposes. They have not been peer-reviewed or been subject to the review by the NBER Board of Directors that accompanies official NBER publications.

Adapting to Flood Risk: Evidence from a Panel of Global Cities
Sahil Gandhi, Matthew E. Kahn, Rajat Kochhar, Somik Lall, and Vaidehi Tandel
NBER Working Paper No. 30137
June 2022, Revised March 2025
JEL No. Q5, R1

ABSTRACT

We assemble a global dataset capturing the universe of major floods in 9,468 cities across 175 countries to estimate flood damage and test adaptation hypotheses. Analyzing 3,931 major floods (2000–2023) and monthly night lights data (2012–2023) as a proxy for urban economic activity, we present three key findings. First, floods lead to a 3.5-times larger decline in night lights in cities in low-income countries compared to cities in high-income countries. Second, the impact of floods on economic activity and mortality has decreased over time. Third, we explore the mechanisms driving this adaptation. Cities with greater prior flood exposure experience smaller impacts, supporting experience-driven adaptation. In high-income countries, migration, critical infrastructure intensity, and dam protection enhance flood resilience, but these factors are less effective in low-income countries. The disproportionate impacts and slower flood adaptation in cities in low-income countries highlight a significant protection gap.

Sahil Gandhi
The University of Manchester
sahil.gandhi@manchester.ac.uk

Matthew E. Kahn
Department of Economics
University of Southern California
3620 South Vermont Ave.
Kaprielian (KAP) Hall, 300
Los Angeles, CA 90089-0253
and NBER
kahnme@usc.edu

Rajat Kochhar
Energy and Environment Lab
University of Chicago
rajatkoc@uchicago.edu

Somik Lall
Lead Economist and Head of Climate Team
Office of the Chief Economist for
Equitable Growth, Finance,
and World Bank Institutions
1818 H ST NW
Washington DC, 20433
Slall1@worldbank.org

Vaidehi Tandel
University of Manchester
United Kingdom
vaidehi.tandel@gmail.com

1 Introduction

Flooding is the most common natural hazard across the globe, accounting for nearly half of all weather related disasters and affecting 1.6 billion people between 2000 and 2019 (CRED and UNDRR, 2020).[1] Climate change, by raising the likelihood of extreme precipitation events, is expected to increase both the frequency and intensity of flooding (IPCC, 2022; see Figure 1). This has grave implications for the productive potential of cities — source of 80 percent of the world's GDP — which are particularly vulnerable owing to rapid, mostly unplanned, urbanization in flood prone areas (Hallegatte et al., 2013; World Bank, 2024).[2] At the greatest risk are cities in low- and middle-income countries, where almost all recent urbanization has been concentrated, and which are home to 89 percent of the world's flood exposed population (UN DESA, 2019; Rentschler et al., 2022). This makes adaptation crucial, but Burke et al. (2024) conclude that for more than two-thirds of the climate change damage indicators, such as yields, mortality, incomes, *etc.*, the pace of adaptation has been too slow. Little is known about whether cities are adapting to flood risk, the magnitude and efficacy of these adaptive measures and, importantly, whether impacts of floods and adaptation progress differs across cities in high- and low-income countries.

This paper helps fill this gap by building a comprehensive database covering the universe of major floods (3,931 events) between 2000 and 2023, and measuring their impacts across 9,468 cities in 175 countries. This global, comprehensive laboratory allows us to test a number of flood adaptation hypotheses. We do this in three steps. First, we estimate the impact of urban floods on economic activity, and recovery dynamics post-floods. In addition, we test whether geographical and topographical characteristics of cities, along with their administrative importance, matter in determining the extent of impact. Second, we assess whether cities are adapting to flood risk by examining if the sensitivity of economic and mortality outcomes to flood shocks has reduced over time, and whether repeated exposure to flooding reduces the negative impact of subsequent events — the novelty factor as defined by Guiteras et al. (2015). Third, we shed light on the prevalence of private self protection efforts and efficacy of public investment in resilience by studying whether — *(i)* people are migrating away from flood-hit areas; *(ii)* high intensity of critical infrastructure helps a city mitigate the effect of floods, and; *(iii)* flood protection infrastructure, specifically dams, attenuates the effect of floods. Since flood impacts and extent of adaptation are likely to be heterogeneous across cities in high- and low-income countries on account of differences in financial constraints, institutional and state capacity, *etc.* (Kahn, 2005; Tol, 2018; 2024), we also estimate the above outcomes separately by country-income classifications.[3] An illustrative example of these differential impacts is pre-

1. With 3,254 inundation events between 2000-2019, flooding accounted for 44 percent of all weather-related disasters. This represents an increase of 130 percent from the 1,389 floods reported between 1980 and 1999. In terms of frequency of extreme weather events between 2000 and 2019, floods were followed by storms (28 percent), extreme temperature (6 percent) and landslides (5 percent) (CRED and UNDRR, 2020).

2. Roughly half of the global urban expansion between 2000 and 2030 is expected to take place in high-frequency flood zones (Güneralp et al., 2015). While urban settlements have expanded by 85 percent between 1985 and 2015, settlements exposed to high and highest flood-hazard have risen by 110 percent and 120 percent, respectively (Rentschler et al., 2023).

3. Throughout this study, we use the country classification by income levels as defined by World Bank (2020) for the year 2020-21, which is based on GNI per capita in current USD for the year 2019. The countries are classified into four income groups: Low income (<US$1,036), Lower-middle income (US$1,036 - US$4,045), Upper-middle income (US$4,046 - US$12,535) and High income (> US$12,535). For the purposes of our analysis, we classify both upper-middle- and high-income countries as high-income, and both lower-middle- and low-income countries as low-income.

Figure 1: Number of Floods Classified by Country-Level Income (1971-2023)

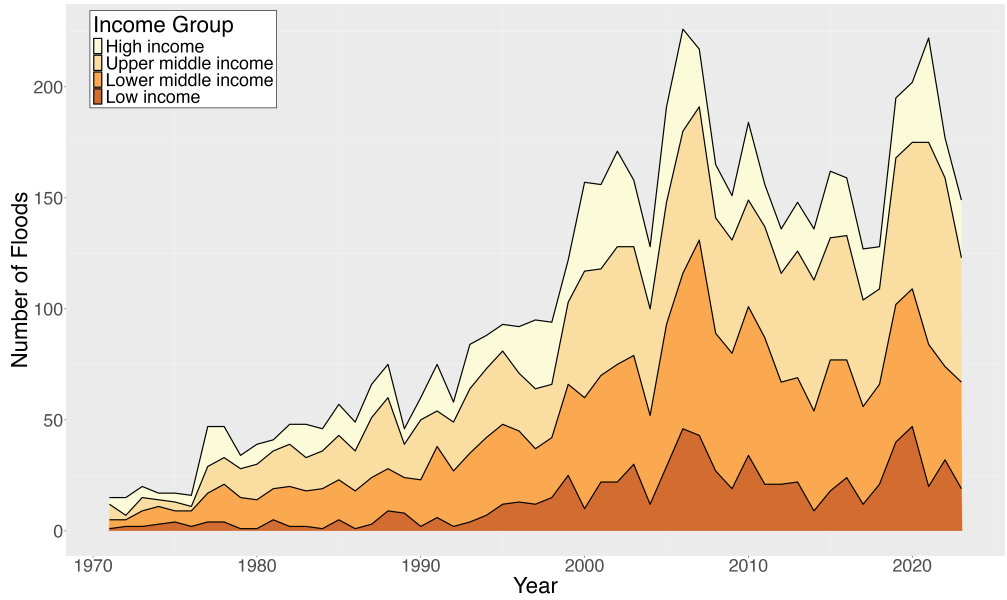

Notes: The figure is a stacked area chart illustrating the number of floods each year from 1971 to 2023, classified by income levels of the impacted country. Data on floods is sourced from the Emergency Events Database (EM-DAT). Country classification by income levels is as defined by World Bank (2020) for the year 2020-21, which is based on GNI per capita in current USD for the year 2019. The countries are classified into four income groups: Low income (<US$1,036), Lower-middle income ($1,036 - $4,045), Upper-middle income ($4,046 - $12,535) and High income (>US$12,535).

sented in Figure 2. It shows that though the percentage of flood events between 1971-2023 was equally distributed between high- and low-income countries, the proportion of deaths was much higher in poorer countries.[4]

Our paper combines a multitude of global geospatial data, available at varying temporal frequency and time spans, to analyze whether cities are adapting to flood shocks. Our novel compilation of globally comprehensive datasets provide information on *(i)* time-varying attributes such as flood events, their intensity and ensuing mortality, precipitation, economic outcomes, and population levels, and; *(ii)* time-invariant features related to the spatial extent of cities, their geography and topography, intensity of their critical infrastructure, and presence of dams upstream. We start by defining our geographic unit of observation as an "*urban center*" with a population greater than 10,000 people at the start of the millennium, which gives us a sample of 9,468 cities in 175 countries. We combine this with data on all 3,931 major flood events, and related losses thereof, between 2000 and 2023 sourced from the Emergency Events Database, and assign each flood to a city in our sample by overlaying the affected administrative layers on city spatial extents. Economic activity is proxied by monthly night-time lights from Visible Infrared Imaging Radiometer Suite (VIIRS) instrument, which has a higher spatial, temporal and radiometric resolution than its predecessors (Gibson et al., 2021). This is complemented by gridded data on monthly precipitation, yearly population, and critical infrastructure, where the latter represents the intensity of transportation, energy, water, waste,

4. For instance, Storm Daniel, which caused torrential flooding in both Libya and Greece in September 2023, led to around 2,000+ deaths in Derna, a city in Libya, but under 20 deaths in all of Greece. For more details, see https://www.reuters.com/world/europe/flooded-homes-streets-another-storm-hits-battered-central-greece-2023-09-28/.

Figure 2: Proportion of Floods and Deaths by Country-Level Income (1971-2023)

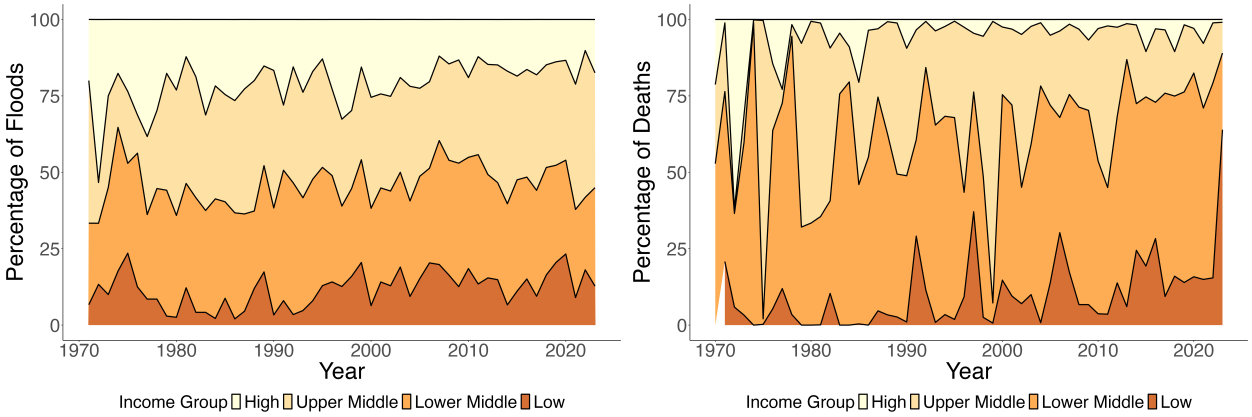

(a) Floods **(b) Deaths**

Notes: The figure is a percent stacked bar-chart illustrating the proportion of floods and resulting deaths each year from 1971 to 2023, classified by income levels of the impacted country. Figure 2a represents the percentage of floods, while Figure 2b represents the percentage of deaths from floods. Data on floods and mortality is sourced from the Emergency Events Database (EM-DAT). Country classification by income levels is as defined by World Bank (2020) for the year 2020-21, which is based on GNI per capita in current USD for the year 2019. The countries are classified into four income groups: Low income (<US$1,036), Lower-middle income ($1,036 - $4,045), Upper-middle income ($4,046 - $12,535) and High income (>US$12,535).

telecommunication, education, and health infrastructure systems in 2020. Finally, to test the effectiveness of dams in mitigating the negative impact of flood shocks, we combine the global river network data with the geolocation of dams, and overlay these two on the city spatial extents to identify which cities have a dam upstream.[5]

We have three main results related to the economic impact of floods, the changing sensitivity of economic outcomes and mortality to inundation events, and the different mechanisms driving adaptation. First, we show that floods, on average, lead to a 4.5 percent fall in urban economic activity in the month of the disaster.[6] This effect is almost 3.5 times larger in cities in low-income countries, with night lights falling by 7.4 percent post floods, as opposed to 2.1 percent in cities within high-income countries. These findings are robust to using extreme precipitation events as a proxy for floods.

Next, we use an event-study methodology to investigate how long cities take to recover from a flood shock, and whether the recovery patterns differ by country income classification. Our results indicate that the negative effect of the flood is short-lived, with the difference in economic activity between flooded and non-flooded cities not distinguishable from zero in the months immediately following a flood. This result is consistent across income groups, though the impact in low-income countries is negative but not statistically significant for two months after the flood. The event-study framework also provides a natural test of the identifying assumption that economic trends between flooded and non-flooded cities were truly parallel before the event date. Consistent with this assumption, we find that differences in the evolution of night-lights between cities which experienced and did not experience a flood in the twelve months prior

5. Detailed information on each dataset is provided in Section 2.

6. In what follows, we will round all estimates in the text to two significant digits, while all estimates in regression tables will be rounded to three decimal places

to the event were statistically indistinguishable from zero.

We also consider heterogeneity of impact by geography and show that coastal cities, which are associated with a high concentration of population and economic activity (Balboni, 2019), are the worst affected, but only within developing nations. Night lights fall by 16 percent after floods in coastal cities in low-income countries, which is more than double the post-flood damages to their inland counterparts, and seven times higher as compared to cities in high-income countries. One factor which makes floods particularly calamitous in low-income countries is that cities are fiscally constrained and, hence, unable to optimally invest in flood-protection infrastructure (UNDP, 2023). As suggestive evidence of limited financial resources hindering adaptation in low-income countries, we find that floods in their capital cities — which are politically and administratively important and, therefore, well-funded — do not, on average, have a statistically significant impact.[7]

The second main result is that cities, especially in low-income countries, are adapting to floods, with sensitivity of both economic activity and mortality to floods decreasing over time. A flood at the start of our sample in 2012 causes night lights in cities in developing nations to decrease by 22 percent, but the impact is attenuated, on average, by 2.1 percentage points (9.4 percent) with each subsequent year.[8] For cities in high-income countries, the attenuation, though positive, is not statistically significant. Given that the magnitude of post-flood losses in high-income countries was already modest to begin with, the results, rather than suggesting that there is no adaptation, instead imply that the capacity of cities to adapt may be finite (Adger et al., 2009).

Next, using data on deaths from each flood from year 2000 onwards, and employing a zero-inflated negative binomial specification to model excess zeros in the deaths data, we test if mortality from flood events is falling over time. Consistent with the adaptation hypothesis, we find that countries across the income spectrum have made progress in reducing mortality from floods. Expected deaths from floods in high- and low-income countries have decreased, year-on-year, by a significant 8.4 percent and 4.7 percent, respectively. In addition, we exploit variation in city-level income to show that urban areas with a higher per capita GDP in 2015 were less likely to experience a positive death count when a flood occurred, but conditional on death counts greater than zero, were also likely to experience lower mortality.

Our third and final result relates to the mechanisms underlying the adaptation progress. This includes the role of experience-driven adaptation in alleviating the negative impact of floods, the magnitude of private self-protection through migration, and effectiveness of public investment in resilience. We find evidence that cities with repeated exposure to floods in the past are significantly better at coping with future shocks. Specifically, each additional flood a city was exposed to between the years 2000 and 2012 reduces the impact of a post 2012 flood on economic activity by a statistically significant 4.0 percent. This

7. Some may argue that a fall in night lights post a flood may be due to power outages and not necessarily due to fall in economic activity. We address these concerns in detail in Section 3.C, citing *i)* how the impact of floods within a country differs by a city's political importance, geography and topography; *ii)* cities with higher levels of critical infrastructure, and thus a more robust electricity grid, also experience a fall in night lights, and; *iii)* the floods in our sample, at least temporarily, led to displacement of population. Therefore, it is highly unlikely that the decline in night-lights post floods are purely due to power outages.

8. The sample for all results related to night lights starts in April 2012, the month from which VIIRS nighttime lights dataset is available.

positive learning channel is robust to using different measures of past exposure and holds across different country income groups.

Next, using a 21-year panel on city level population and flood events, we find that migration does not represent an important margin of adjustment to flood shocks in the short-run, especially for people in poorer nations. For cities in low-income countries, a flood in the previous year does not have any meaningful impact on population, implying that incumbents in poorer nations tend to remain in the shocked area. On the other hand, estimates for cities in high-income countries suggest that floods in the previous year reduce population by 0.33 percent — or approximately 1,100 people — which, though small in magnitude, is statistically significant. A similar pattern emerges when we use cross-sectional variation to test if cities with a higher floods frequency experienced lower population growth. The limited potential of migration as an adaptation response in the short-run for developing countries raises climate justice concerns, as the poor are exposed to greater risks from climate but their choice set of responses may be limited.

Moving from self-protection to public investment in resilience infrastructure, we show that cities with a higher intensity of critical infrastructure are more resilient to flood shocks. Post floods, a city at the 75^{th} percentile of the critical infrastructure distribution experiences 33 percent lower economic losses as compared to a city in the 25^{th} percentile. Using city-level GDP per capita as a proxy for infrastructure investments yields similar results, with economic losses due to floods mitigated by more than a half when we traverse the divide between 25^{th} to 75^{th} percentile of GDP per capita distribution. Income based heterogeneity analysis reveals that these results are predominantly driven by cities within high-income countries, further highlighting the wealth derived protection gap.

Taking this analysis a step further, we ask if public investment in dam infrastructure aids in adaptation, *i.e.,* is the marginal effect of a flood lower in cities protected by dams. In line with most of the adaptation evidence presented above, the results suggest that dams are only effective in mitigating losses for protected cities in high-income countries. Estimates indicate that cities in developed countries without a dam upstream experience a 2.6 percent fall in night lights post a flood, but this effect is attenuated by a significant 1.3 percentage points, or 49 percent, in protected cities. In contrast, we do not find any statistically distinguishable difference in the impact of floods in cities with and without a dam upstream in low-income countries.

Collectively, our empirical work combining a rich collection of global spatial datasets and using flood incidence as an exogenous shock supports the adaptation hypotheses. Over time, the sensitivity of economic activity and mortality to floods has decreased in cities, regardless of their income levels. This adaptation progress is further underscored by evidence of learning through experience, showing that recurrent flood exposure enhances cities' resilience. However, this optimism is moderated by challenges in low-income countries, where flood impacts remain substantially higher (though gradually decreasing). Furthermore, in these regions, short-term migration is not a significant adaptation tool, and while there is some evidence that critical infrastructure can help, investments in dam infrastructure have proven ineffective in mitigating losses.

Our work is closely related to Kocornik-Mina et al. (2020), who offer an important starting point in understanding flood adaptation progress. They study the short-run effects of 53 large flood events, occurring

between 2003 to 2008, on 1,868 cities located primarily in developing countries. Using annual night lights data, they document that large floods lead to a decline in urban economic activity by 2.1 percent in the year of the flood. However, the intensity of night lights recovers to pre-flood levels in the year immediately following the flood event. Further, they show that economic activity does not relocate to safer areas in the aftermath of floods, except for newly populated areas within cities.

We build on their work by studying whether urban areas have adapted to floods, focusing on the role played by experience-driven adaptation and investments in self-protection and public-funded resilience infrastructure. Further, we highlight distributional concerns, specifically how flood impacts and adaptation progress are uneven across country income groups. We also expand the scope and extent of the analysis by including all flood events between 2000 and 2023 and measuring their economic impact on a large, globally representative sample of 9,468 cities across 175 countries. To this end, the use of monthly nighttime lights data from VIIRS allows us to study short-run recovery dynamics post floods, which is not possible with data at an annual frequency.

More generally, this paper relates to various strands of literature in climate economics. First, there is a rich literature on the economic impact of natural disasters, but studies have focused either on an isolated event, or a particular region or country, most prominently United States, China and India. This includes studies on the impact of cyclones (Strobl, 2012; Anttila-Hughes and Hsiang, 2013; Elliott et al., 2015; Deryugina et al., 2018; Pelli et al., 2023), floods (Hornbeck and Naidu, 2014; Patel, 2024), temperature shocks (Deschênes and Greenstone, 2007; Burke et al., 2015; Somanathan et al., 2021), and precipitation (Shah and Steinberg, 2017). Notable exceptions are the global analyses of the impact of cyclones, temperature shocks, and projected sea level rise by Hsiang and Jina (2014), Dell et al. (2012) and Desmet et al. (2021), respectively. Furthermore, all these studies focus on annual or long-run impacts, relying on year-to-year variation in the incidence of disasters to identify these effects. Our paper, in contrast, has a global scope, covers all major floods in the last two decades, and uses monthly variation in night-lights and flood incidence to measure short-run impacts, recovery dynamics, and resilience in urban areas.

Second, the paper contributes to a growing literature on adaptation to weather shocks.[9] Taking a broad view of adaptation by being agnostic about protection strategies, Burke et al. (2024) estimate whether the sensitivity of various societal outcomes (yields, mortality, incomes, *etc.*) to climate extremes has diminished over time. Focusing on temperature extremes and tropical cyclones, they find limited evidence of adaptation, with more than two-thirds of the outcomes showing either no change or an increasing sensitivity. Using a similar empirical design, we find more optimistic results for floods, with sensitivity of economic activity and mortality decreasing across urban areas worldwide, notwithstanding their income classification.

Next, zeroing in on the actions and behaviors that constitute adaptation, Desmet and Rossi-Hansberg (2015) use a dynamic spatial model to show that the consequences of global warming can be mitigated by allowing agents to move across space. This has been supported by various studies which extensively document that migration after natural disasters is indeed a common self-protection mechanism, whether in the aftermath of tornadoes (Boustan et al., 2012), American Dust Bowl (Hornbeck, 2012), hurricanes (Strobl,

9. See Kala et al. (2023) for a recent literature review about economics research on adaptation to climate change.

2011), or long-term temperature variation (Bohra-Mishra et al., 2014; Mullins and Bharadwaj, 2021). Hsiao (2024) highlights the distributional impact of adaptation to sea-level rise in Jakarta by showing that wealthy households are able to reduce their exposure to floods by relocating to higher, safer areas, while driving up housing prices and displacing poorer households. On the flip side, Deryugina (2011) and Kocornik-Mina et al. (2020) do not find any evidence of relocation post disasters. Our results present a nuanced picture, where at least in the short-run, migration as a margin of adjustment is only relevant for urban dwellers in high-income countries, with little evidence of out-migration from shocked areas for incumbents in poorer nations.

Migration, however, is just one instrument in the adaptation toolbox.[10] This paper focuses on floods in urban areas, and finds that place-based public investment in critical infrastructure, including dams upstream, play a crucial role in dampening the impact of floods, though these effects are more salient in high-income countries. Mård et al. (2018) find similar association between resilience and infrastructure in an analysis of 16 countries. They show that societies with high levels of flood protection do not experience any significant changes in human proximity to rivers after floods. This contrasts with Ferdous et al. (2020), who focus on the Jamuna River floodplain in Bangladesh and find evidence of lock-in of population, leading to higher flood fatalities in areas where flood protection measures were undertaken and Hsiao (2023), who highlights the moral hazard problem of building a sea wall in Jakarta, which leads to more development in risk-prone areas.[11]

To understand the factors driving both private and public investment in resilience, it's essential to note that as floods become more frequent, the marginal benefits of adaptation investments may increase, while the marginal costs — through the *learning-by-doing* effect — may decrease. Patel (2024) finds evidence of these dynamics in Bangladesh, where prior flood experience significantly alleviated the negative impacts of inundation. Similarly, Hsiang and Narita (2012) shows that countries with more intense tropical cyclone climates tend to suffer lower marginal losses from each event. Our findings build on these studies, demonstrating that experience-driven adaptation is strengthening resilience in urban areas worldwide. Cities across the income spectrum with high prior flood exposure show notably lower losses post floods.

Lastly, we contribute to the literature on climate justice which argues that disruptions from extreme weather will disproportionately affect the developing world, particularly the poor and most vulnerable (Mendelsohn et al., 2000; World Bank et al., 2003; Mendelsohn et al., 2006; Stern, 2007; Tol, 2009). IPCC (2001, 2022) estimates that poor countries will suffer the bulk of the damages from climate change, with their economic damages per capita expected to be higher as a fraction of income. Our results tend to support this discouraging hypothesis. Though the sensitivity of economic outcomes to flood shocks is falling over time in cities within low-income countries, the economic impact of floods in such cities is still large. Flood related economic losses are 3.5 times higher, on average, relative to the losses in cities

10. See Klein et al. (2015) for an extensive survey of the key adaptation opportunities available in response to climate change. Other, less disruptive options include air conditioning for households and schools (Barreca et al., 2016; Park et al., 2020); flood risk information for home owners (Fairweather et al., 2024); weather forecasts (Burlig et al., 2024), changing crop mix, input usage (Aragón et al., 2021), and credit access (Lane, 2024) for farmers, and; relocation and shifting towards suppliers in less disaster-prone areas for firms (Balboni et al., 2023).

11. Also see Bunten and Kahn (2017) who argue in favor of building less durable structures as an adaptation technique to preserve an option value to walk away from areas facing a higher climate risk.

in developed economies, with coastal cities within developing countries being worst affected (7.3 times higher losses).[12]

This heterogeneity in impact by income mainly arises because of a *protection gap* (UNISDR, 2018), whereby richer countries have a greater capacity to anticipate and respond to climate change (Kahn, 2005; Kellenberg and Mobarak, 2008). We find evidence of this gap, as reflected in three key results: *i)* capital cities in low-income countries are significantly better at mitigating losses, which suggests that fiscal constraints may dampen adaptation; *ii)* there is no out-migration from vulnerable cities in low-income countries, even though economic losses and death rates are higher, indicating self-protection options are limited, and; *iii)* upstream dams as an adaptation investment are ineffective in developing country cities, which points towards need for higher investment and operational efficiency. Thus, we do find strong evidence of disproportionate effects of floods and slower adaptation progress in low-income countries.

The remainder of the paper proceeds as follows. Section 2 provides a detailed overview of all the geospatial datasets compiled for the analysis, while Section 3 focuses on the economic impacts of floods. Short-run recovery dynamics and the heterogeneous impacts based on geography, topography, and administrative importance are also explored in this section. Section 4 presents the evidence on adaptation. Conclusions and areas for future research are discussed in Section 5.

2 Data

We compile a rich panel dataset at the city-month-year level, combining global geospatial data on city boundaries, economic activity, geographic features, infrastructure, population, river networks, and precipitation with administrative data on natural disasters. This section describes the data sources and provides details on the construction of the variables. Summary statistics on the economic and geographic characteristics of cities by country income groups are presented in Table B.2.

A ***Cities***

A spatial analysis of the impact of floods on urban economic activity requires us to first define the geographic unit of observation, *i.e.* city or *"urban center"*, and determine its spatial extent.[13] For this purpose, we use the Global Human Settlement Urban Center Database (GHS-UCDB) created by Florczyk et al. (2019), which defines spatial entities called *"urban centers"* and provides details on their location and spatial extent in 2015, as well as their geographical, socio-economic and environmental attributes at four points in time: 1975, 1990, 2000, and 2015.

The GHS-UCDB uses two key inputs for defining cities: *i)* satellite imagery from the Landsat and Sentinel missions to demarcate the physical extent of human settlements — also called "*built-up area*" — at a 1 km^2 spatial resolution, and; *ii)* national census data on population at the level of an administrative unit (*e.g.*, districts). As a first step, these two inputs are combined through spatial modeling techniques to produce global population density grids (GHS-POP) at a resolution of 1 km^2. Subsequently, the combination

12. Though not statistically significant, economic activity in cities within low-income nations takes longer to return to pre-flood levels post a disaster (three months as against one month in high-income countries).

13. The terms "*urban-centers*" and "*cities*" are used interchangeably.

of built-up area and population density grids is used to geo-locate urban centers based on the following definition:

> "*the spatially-generalized high-density clusters of contiguous grid cells of 1 km^2 with a density of at least 1,500 inhabitants per km^2 of land surface or at least 50 percent built-up surface share per km^2 of land surface, and a minimum population of 50,000.*"

The authors apply this definition to the values of built-up area and population in the year 2015 to identify 13,135 urban centers (Melchiorri et al., 2024). Furthermore, they also outline the spatial extent of the urban centers so identified, and it includes both city centres and suburban areas. Figure A.1 shows the urban spatial extent for the cities of Guangzhou, Jakarta, Los Angeles and Tokyo using this definition. The shaded region (in red) delineates the spatial domain for each urban center, which, as reflected in the map, includes the core city as well as a substantial portion of the suburban areas.

Although the geographic boundaries of the urban centers pertain to the year 2015, data on the built-up area, population and Gross Domestic Product (GDP) within the city extents is made available for three additional years: 1975, 1990 and 2000. City population and GDP (PPP in constant 2007 international USD) in the GHS-UCDB database is arrived at by aggregating the population and GDP, respectively, across all 1 km^2 grids that fall within the urban extent boundaries. The population density grids are sourced from GHS-POP, while gridded GDP data is sourced from Kummu et al. (2018), who combine national and sub-national official GDP statistics with gridded population count to provide GDP values for each 1 km^2 grid cell across the globe.

For the purpose of our analyses, we limit our sample to the 9,468 cities which had a population count of at least 10,000 people in 1990 and 2000. This includes 5,102 cities (54 percent) in 102 high or upper-middle income countries, and 4,366 cities (46 percent) in 73 lower-middle and low income countries.[14] See Figure A.2 for a map representing the spatial distribution of all 9,468 cities in our sample by country income levels. Additionally, the complete list of countries with count of cities within each is provided in Appendix Table B.1.

B ***Night-Time Lights***

Estimating the economic impact of floods and subsequent recovery dynamics at a city-level requires GDP estimates at a fine temporal and spatial scale. However, consistent and reliable GDP estimates are seldom reported at high temporal frequency, and even then, they are rarely available at the level of sub-national administrative units. To circumvent the issue of poorly measured or missing estimates of high frequency GDP data at a local level, we use night-time lights as a proxy for city-wide economic activity, our key outcome variable. Henderson et al. (2011) have shown that night luminosity is a valid proxy for national aggregate GDP, but more importantly for our context, Storeygard (2016) has also demonstrated their strong relevance as a measure of economic activity at the city level. As a result, a large literature has used night

14. Countries are classified into four income groups based on World Bank (2020) classification. These include Low income (<US$1,036), Lower-middle income (US$1,036 - US$4,045), Upper-middle income (US$4,046 - US$12,535) and High income (>US$12,535).

lights data for an empirical analysis of economic activity at varied levels of geographic aggregation (Henderson et al., 2018; Harari, 2020; for a review, see Donaldson and Storeygard, 2016).

Our main source of night lights is the Day-Night Band (DNB) data from the Visible Infrared Imaging Radiometer Suite (VIIRS) instrument onboard the Suomi National Polar-Orbiting Partnership (Suomi NPP) spacecraft, which was launched in 2011 by the National Aeronautics and Space Administration (NASA) and the National Oceanic and Atmospheric Administration (NOAA). Specifically, we use the monthly cloud-free DNB composites which exclude any data impacted by stray light, and are provided by the Earth Observation Group (EOG) of the Payne Institute for Public Policy at the Colorado School of Mines (Elvidge et al., 2013).[15]

VIIRS has several advantages over the other commonly used source of night lights — data recorded from satellites of the U.S. Air Force Defense Meteorological Satellite Program Operational Linescan System (DMSP-OLS).[16] As pointed out by Gibson et al. (2020), DMSP-OLS suffers from several drawbacks including *(i)* spatial inaccuracy caused, first, by *blurring*, whereby lights are erroneously attributed to areas outside of their source making it unsuitable to proxy for night lights in a smaller area, and second, by stray light contamination in the summer months due to the satellite's overpass time of 7:30 PM when there may still be light in non-tropical regions; *(ii) saturation* or top-coding of night lights arising from a limited dynamic range of sensors, a problem which is especially acute in urban areas which are the focus of our study (Hsu et al., 2015); *(iii)* temporal inconsistency arising from on-the-fly adjustments to the sensitivity of the sensors to better capture moonlit clouds, and; *(iv)* inter satellite differences in night lights recorded for the same place and year. In contrast, VIIRS sensors are more spatially accurate as they maintain a constant resolution across the swath, have a later overpass time of 1:30 AM, a larger dynamic range, and include in-flight calibration to establish temporal comparability (Elvidge et al., 2017). Additionally, processed VIIRS data has a higher spatial resolution of 465m × 465m (grids) at the equator and is available at a monthly frequency, as opposed to a resolution of 930m × 930m and annual periodicity, respectively, with the DMSP. The high temporal frequency of VIIRS is particularly important as it allows us to better estimate the short-run impact of floods and subsequent recovery dynamics, which may be difficult to capture with annual data — especially if recovery is rapid. Finally, while DMSP has been operational since 1970, the satellite was decommissioned in 2013, meaning researchers have to rely on VIIRS to analyse the more recent flood events.

An illustration of the spatial and temporal granularity of the VIIRS data, and its effectiveness in analysing the impact of floods and recovery dynamics forthwith, is presented in Figure 3. Chennai, the capital city of the south Indian state of Tamil Nadu, suffered from major floods between November-December 2015. Figure 3a shows the night light intensity at the grid level in October 2015 before the flood. As reflected in Figure 3b and Figure 3c, the night luminosity reduced across a majority of the grids during the flood events of November and December 2015. However, Figure 3d indicates that the intensity of lights in the city had recovered to pre-flood levels by January 2016.

VIIRS was launched in October 2011, with data post March 2012 available to researchers. Therefore,

15. Monthly nighttime lights data from VIIRS is available at https://eogdata.mines.edu/products/vnl/.
16. Kocornik-Mina et al. (2020), which our paper is closest to, use DMSP-OLS to identify the economic effects of floods.

Figure 3: Night Lights Before and After Floods in Chennai, India: 2015-16

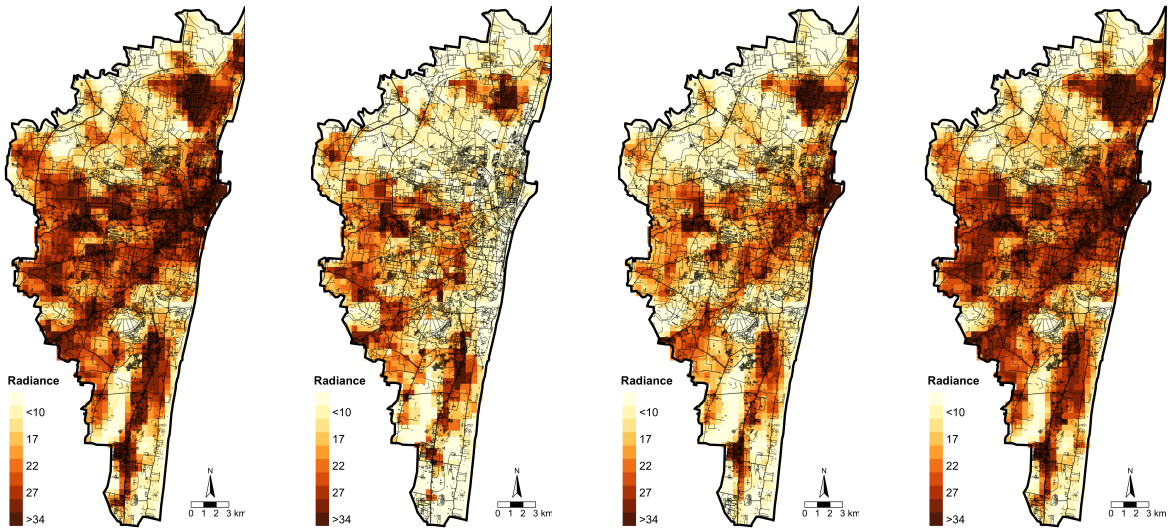

(a) October 2015 **(b) November 2015** **(c) December 2015** **(d) January 2016**

Notes: Average monthly night light intensity between October 2015 and January 2016 in Chennai, capital of the state of Tamil Nadu in India. Chennai suffered from major floods between November-December 2015, with economic losses estimated to be US$3.5bn (Vencatesan, 2021). Grid-level night lights data is sourced from VIIRS, the administrative boundary of Chennai from GHS-UCDB, and geospatial information related to Chennai from OpenStreetMap Contributors, 2017.

our monthly time series of grid level night lights data starts in April 2012, and runs up until July 2023. In order to aggregate night luminosity to the city-month-year level, we calculate the monthly weighted average of night light luminosity across all the grids that fall within each city boundary, with weights equivalent to the area of the grid cell that overlaps with the city boundary.

One limitation of the monthly VIIRS data is the lack of coverage in the mid-to-high latitude regions during certain months. This mainly arises because of solar illumination towards the south and north pole which impacts the satellites' ability to accurately measure luminosity, and causes degradation in the DNB night image quality (Chen et al., 2018). Termed as *stray light contamination*, any pixel affected by this phenomenon is dropped by NASA. Though rare, another reason for missing values is the absence of any cloud-free observations in a month, an anomaly which mostly affects tropical regions (Beyer et al., 2022). The implication is that 9.4 percent of all city-month observations in our sample have a missing value for night lights. Dropping these missing observations could bias the estimates of the impact of floods on economic activity, especially if floods are more likely in the north or southern hemisphere when the *stray light contamination* phenomenon is more prevalent or there is greater cloud cover immediately following heavy rainfall which causes a flood. To avoid such biases, we impute missing values using the multiple imputation procedure developed by Rubin (1987, 1996). This approach takes into consideration the distribution of the observed night lights data to estimate multiple possible values for the missing observations and can, importantly, account for uncertainty around the true value of night luminosity.

Some technical aspects of the imputation procedure are worth noting. We utilize the multivariate imputation by chained equations (MICE) approach (Raghunathan et al., 2001; Van Buuren, 2007) imple-

mented by the *mice* package in R statistical software (Van Buuren and Groothuis-Oudshoorn, 2011). The algorithm involves six key steps. First, we need to choose the variables to be included in the imputation process, and use them to create a dataset at the city-month-year level (our unit of analysis). Naturally, we start by including monthly night lights data, sourced from VIIRS DNB sensors, aggregated to the city level since we are interested in imputing the missing observations in this specific variable. In addition, we also include values of city-wide monthly night light luminosity from two other night light products — NASA's Black Marble product suite (Román et al., 2018) and the stray-light *corrected* version of the VIIRS monthly cloud-free DNB composites (Mills et al., 2013).[17,18] In addition, we include two lag and lead values of night lights for all the different products, as well as the standard deviation of daily night luminosity in a month averaged across all the grid cells within a city.[19] Also, given that we are interested in estimating the impact of natural disasters on economic activity in cities, we include monthly dummy variables for all flood, landslide, storm and extreme precipitation events, and two month lag dummy variables for all such disaster occurrences. These are further supplemented by a continuous measure of monthly rainfall (in inches) in the city, and total city population available at yearly temporal frequency.[20] Finally, we also add month and year fixed effects to ensure that the imputation model can flexibly account for seasonal and long-run trends in night luminosity.

The remaining steps impute missing values by implementing an iterative algorithm over a set of conditional densities, one for each variable with incomplete data (Vink et al., 2014).[21] Note that we only need to impute incomplete night luminosity data for the different night light products as no other variable in our constructed dataset has any missing values across all city-month-year observations. The second step involves estimating a linear regression model where we select one of the variable we want to impute (*var1*) and regress it on all other variables in the dataset. Only the observed values of *var1* and predictor variables are used for estimating the set of coefficients ($\hat{\beta}$). Third, we randomly draw from the posterior predictive distribution of $\hat{\beta}$, yielding a new set of coefficients β^*. In the fourth step, we use β^* and $\hat{\beta}$ to generate predicted values for the missing and observed data in *var1*, respectively. The fifth step involves taking the predicted value for the missing *var1* and identifying multiple closest predicted values of *var1* among cases where it is observed. Then, in the sixth step, we randomly select one of the closest predicted values and impute the missing *var1* by assigning to it the observed value corresponding to this randomly selected closest value. Termed *Predictive Mean Matching* (Little, 1988), this method of imputation is repeated for

17. NASA's Black Marble dataset was released in 2021 and adjusts for surface and atmospheric reflection, and seasonal vegetation. We use the All-angle version of the dataset, which is a combination of near-nadir and off-nadir luminosity data and is available from 2012 onwards. The reason we prefer VIIRS DNB over Black Marble for our main analysis is because the latter product calculates the interquartile range (IQR) of night-light luminosity for each grid cell, and drops all observations that fall outside 1.5*IQR (Román et al., 2021). This is problematic because if a disaster causes a large fall in night lights such that the monthly night lights in a grid falls below the 1.5*IQR, the same will not be captured in Black Marble and will appear as missing.

18. The stray-light corrected version of the VIIRS DNB composites has more data coverage towards the mid-to-high latitude regions. However, it is only available starting January 2014 and is considered to be of reduced quality because of the presence of extremely low or negative luminosity values arising from the stray light correction procedure (Skoufias et al., 2021).

19. NASA's Black Marble is the only night lights product which provides the standard deviation of temporal radiance composites during a month.

20. Refer to Section 2.D and Section 2.F for details on the data sources for city-wide monthly precipitation and yearly population, respectively.

21. A more general description of the chained equation process used in the MICE algorithm is provided in Azur et al. (2011).

every incomplete variable. Each cycle, starting from the first variable with missing data to the last variable with missing data, represents one iteration. The algorithm iterates 50 times, with imputed values being updated each time to increase the probability that the parameters governing the imputation ($\hat{\beta}$, β^*) converge. The final set of imputed values across all variables after 50 iterations, along with the observed data, constitutes a complete data set. As a final step, the imputation process is repeated five times to create five different completed datasets.[22]

Column [6] of Table B.2 presents summary statistics on the intensity of monthly nighttime light across cities. Cities in high-income countries have, on average, 3.5 times the luminosity of cities in low-income countries (22 versus 6.4 nW/cm^2/sr). Within each of these income groups, coastal cities have the highest night light intensity, reflecting their high economic productivity.

C *Disasters - Floods, Landslides and Storms*

The primary data for disasters is sourced from the Emergency Events Database (EM-DAT) which is a global, free-access dataset with comprehensive information on natural and man-made disasters since 1900. It was launched in 1988 by the Centre for Research on the Epidemiology of Disasters (CRED) with support from the World Health Organization (WHO) and the Belgian Government (Mazhin et al., 2021; Delforge et al., 2023). EM-DAT defines a disaster as an unforeseen and often sudden event that causes great damage, destruction and human suffering, and in the process overwhelms local capacity, necessitating a request to the national or international level for external assistance. Any such event is included as a disaster in EM-DAT if it satisfies at least one of the following three conditions: *(i)* 10 or more deaths; *(ii)* at least 100 affected, including injured or homeless; *(iii)* a call for international assistance or an emergency declaration. As of June 2024, EM-DAT contains information on 26,559 natural and man-made hazards since 1900.

EM-DAT classifies disasters triggered by natural hazards into six categories: biological, climatological, extra-terrestrial, geophysical, hydrological, and meteorological. Floods, the main disaster of interest, is categorized as a sub-type under the hydrological category and is defined by EM-DAT as an "*overflow of water from a stream channel onto normally dry land in the floodplain (riverine flooding), higher-than-normal levels along the coast (coastal flooding) and in lakes or reservoirs as well as ponding of water at or near the point where the rain fell (flash floods)*". Though we are primarily interested in the economic impact of floods, we also collect data on storm (meteorological) and landslide (hydrological) events because they are the most common subsequent or co-occurring hazards accompanying floods, necessitating their use as controls in our econometric strategy to prevent omitted variable bias.[23,24] We further restrict our sample to only include floods, landslides and storms between January 2000 and July 2023 as data pre-2000 is subject to reporting biases. This reduces our sample to 6,791 disaster events comprising of 3,931 floods, 433 landslides

22. Increasing the total number of imputations is helpful in improving precision (Bodner, 2008; White et al., 2011), but we limit the number to 5 in our case for computational feasibility.

23. EM-DAT defines landslides as "*any kind of moderate to rapid soil movement including lahars, mudslides, and debris flows (under wet conditions)*", while storms are divided into various sub-types, namely derechos, hail, lightning/thunderstorms, sand/dust storms, storm surges, tornadoes, winter storms/blizzards, extra-tropical storms, and tropical cyclones, each with their own unique standardized definition.

24. Nearly 14 percent of disaster entries in EM-DAT have an associated disaster type, with the two most common associations being floods with landslides and storms with floods (24 and 21 percent of associations, respectively).

and 2,427 storms.

EM-DAT provides information on the timing, duration, and location for all disasters, while also furnishing details, for a major proportion of them, on the total number of people affected, including deaths and injuries, and the resulting damages (in 2015 US$). This information is compiled from reports and catalogs prepared by various international, governmental and non-governmental agencies such as the United Nations organizations, humanitarian agencies, non-profit organizations, research institutes, reinsurance groups, and press agencies. With regards to information on location and areas impacted by a disaster, the database references administrative units based on the 2015 version of the Global Administrative Unit Layers (GAUL) implemented by the Food and Agriculture Organization (FAO). GAUL has compiled a standardized spatial dataset on administrative units for all countries in the world, and provides layers with a unified coding system at country, level one (*e.g.*, states, provinces, departments), and level two administrative units (*e.g.*, counties, districts). EM-DAT follows this standardized coding system to provide the code and name of the administrative unit impacted by the disaster. Among the 6,791 disasters in our dataset, we have information on the level two administrative units impacted for 3,408 events, and on level one administrative units impacted for the remaining 3,383.

Previous studies have used EM-DAT to explore the impact of natural disasters at the country level (*e.g.*, Cavallo et al., 2013; Kahn, 2005). However, we are interested in estimating the impact of floods on urban centers, and how cities can adapt. Therefore, the next critical step in our analysis is attributing the disasters and resulting losses to the 9,468 cities in our dataset. Here, we follow a three step strategy. First, we overlay the city shapefiles from GHS-UCDB on the GAUL administrative layers to determine the level one and level two administrative units that each urban center falls within. Next, we assign each disaster to all the cities that fall within the impacted administrative units. Doing this exercise for the 3,931 floods in EM-DAT results in 8,739 cities (92% of sample) in 160 countries being classified as flood affected, *i.e.,* they were hit by a flood at least once between January 2000 and July 2023.[25] The final step involves attributing the deaths, injuries and damages for each disaster among the cities affected. To this end, we divide the losses equally across all the cities that fall within the administrative divisions affected by the natural hazard. Furthermore, some disasters tend to be spread across multiple months. In such cases, given that our unit of analysis is the city-month-year, we divide the deaths attributed to a city equally over the months during which the disaster lasted. The final count of city-month-year observations between January 2000 and July 2023 with floods is 150,674 (5.6 percent of observations), 52 percent of which were concentrated in high or upper-middle income countries, while the remaining 48 percent occurred in lower-middle and low income countries.[26,27] The map in Figure A.3 provides a spatial representation of how the

25. The 15 countries out of the 175 nations in our sample which were not affected by floods between January 2000 and July 2023 include Bahrain, Barbados, Brunei, Curaçao, Cyprus, Denmark, Equatorial Guinea, Eritrea, Estonia, Finland, Iceland, Luxembourg, Malta, Sweden and Turkmenistan.

26. Summary statistics on the number of floods and extreme precipitation events across cities, and how they differ by country income groups, geography and topography are provided in Appendix Table B.3 and Table B.4. The former table focuses on the time period between January 2000 and March 2012 (before availability of night-lights data), while the latter focuses on the summary statistics after March 2012 and up until July 2023.

27. The total number of city-month-year observations between January 2000 and July 2023 with storm and landslide events is 88,758 (3.3 percent of observations) and 2,341 (0.0009 percent), respectively. 74 percent of all storms and and 58 percent of all landslides were recorded in high or upper-middle income countries.

frequency of floods differs across the cities in our sample.

D ***Precipitation***

There are two concerns with the flood measure constructed using EM-DAT. First, given that we are attributing a flood to all cities within the impacted administrative division, there is a potential for misclassification with certain urban centers wrongly identified as being flood affected. Second, EM-DAT lacks a measure of flood intensity, instead requiring us to assume that all floods are equally severe — a problematic assumption. To mitigate these concerns, we use extreme precipitation as a proxy for flooding. An analysis of the "*Origin*" variable in EM-DAT, which provides context on the factors leading to a flood event, reveals that 76 percent of all 3,931 global flood events between January 2000 to July 2023 were directly the result of heavy or torrential rainfall.[28] Therefore, using precipitation intensity as an exogenous source of variation to predict flooding allows us to test for the robustness of our results using a more consistent criteria free of misclassification error.

Monthly precipitation data is obtained from the European Centre for Medium-Range Weather Forecasts (ECMWF), an independent intergovernmental organiZation and research institute head-quartered in the United Kingdom. We use the fifth generation of ECMWF atmospheric reanalyses of the global climate dataset that provides gridded precipitation data from 1940 to 2023 at a $0.1^{\circ}\times0.1^{\circ}$(9 kilometer) horizontal resolution (Hersbach et al., 2023). As was the case with the night lights data, several weather grid cells fall within the boundaries of each city shapefile from GHS-UCDB. Therefore, we aggregate the monthly gridded precipitation data to the city level by calculating the weighted sum of monthly precipitation across all the grids that fall within each city, with weights equivalent to the proportion of the grid cell area that overlaps with the city boundary.

To create a consistent measure of extreme precipitation — one that ensures we only classify heavy rainfall shocks as natural hazards while still taking into account city-specific infrastructure investments, topography and hydrology — we use the ECMWF derived city-specific precipitation distributions. In particular, we classify a city to have experienced an extreme precipitation event in a particular month if the monthly precipitation intensity in the said city was greater than the 99^{th} percentile of the city-specific distribution created using data from January 1940 to July 2023. This methodology ensures that each precipitation shock is based on a city-specific criterion with outlier events defined using the city's empirical distribution of rainfall, not by imposing an arbitrary common monthly precipitation threshold across all cities which may ignore cities adapting to their specific weather patterns.[29] Summary statistics on the number of extreme precipitation events are provided in Appendix Table B.3 and Table B.4. The number of city-month-year observations between January 2000 and July 2023 with extreme precipitation events is 127,609 (4.7 percent of observations), 52 percent of which were concentrated in high or upper-middle income countries, while the remaining 48 percent occurred in lower-middle and low income countries.

28. The remaining 24 percent of flood events were the result of dam bursts, high tides, ice jams, melting snow, or had a missing value in the "*Origin*" column.

29. Due to the topography and hydrology of cities, and due to their investments in dam flood protection, there may not be a one to one mapping of extreme local rainfall events with local flooding as the water may accumulate in nearby geographic areas (Guiteras et al., 2015).

E ***Elevation***

Data on elevation, used for estimating the heterogeneous impact of floods across high and low altitude cities, is sourced from GTOPO30, a global digital elevation model (DEM) dataset. Developed in 1996 under the leadership of United States Geological Survey's Center for Earth Resources Observation and Science (EROS), it provides elevation (in metres) at a horizontal grid spacing of 30 arc seconds or approximately 1 kilometer (Gesch et al., 1999). We aggregate the grid-level elevation data to the city level by calculating the mean and median of elevation across all grid cells that fall within a city boundary.

F ***Population***

To estimate the role of migration as an adaptation response to floods, we use the global gridded population count data provided by *WorldPop*, a research program based in the School of Geography and Environmental Sciences at the University of Southampton (WorldPop, 2018). These datasets are available as an annual time series from 2000 to 2020 at a 1 km^2 spatial resolution.[30]

Though *WorldPop* provides a multitude of population count datasets, we use the unconstrained mosaiced 1 km resolution global version which is produced by combining the unconstrained 100m resolution datasets generated at the country level. To produce the latter, *WorldPop* combines official census population count data with various geospatial datasets that correlate with human population presence — such as land cover, elevation, night-time lights, climate, roads, settlement extents, *etc.* — and uses a *Random Forest* machine learning model to generate pixel level predictions of population density at a 100m resolution (Stevens et al., 2015; Lloyd et al., 2019). These population density prediction grids are then used as weights to redistribute census population counts, available at a coarser resolution, to grid cells that fall within the respective administrative boundaries.[31] The dataset is unconstrained in the sense that the calculation of gridded population counts is not sensitive to the presence of building footprints in the grid cell, and estimation is done over all land grid squares irrespective of whether the area is mapped as containing human settlements (constrained).

City-wide population count estimates are arrived at by overlaying the urban extent shapefiles from GHS-UCDB on the 1km *WorldPop* grids. We then calculate the weighted sum of population counts across all grid cells that fall within the city polygon, with weights corresponding to the proportion of the grid cell that overlaps with the city extent. Summary statistics in Table B.2 show that the average annual population growth rate in cities within high- and low-income countries was 1.6 and 3.5 percent, respectively. This reflects the fast pace of urbanization in developing economies.

30. Further information on *WorldPop*, including access to their open data repository, is available at www.worldpop.org.

31. This methodology is termed *top-down* modeling as it takes census population counts typically available at a large administrative unit level and disaggregates them to a finer spatial scale. It has the advantage of ensuring that the estimated population count across all grid cells that fall within an administrative boundary match the official census population count of the administrative unit.

G *Critical Infrastructure*

A strong network of infrastructure systems can potentially play a fundamental role in adaptation to climate shocks by reducing direct losses and allowing for a faster recovery. To test this hypothesis, we estimate the impact of resilient infrastructure in mitigating the negative impact of floods. For this purpose, we utilize detailed geospatial data on critical infrastructure developed by Nirandjan et al. (2022).[32]

We use the gridded Critical Infrastructure Spatial Index (CISI) dataset, available at a global scale with a resolution of $0.1^{\circ} \times 0.1^{\circ}$ (~11km), as a measure of the spatial intensity of infrastructure. Critical infrastructure encompasses seven broad infrastructure systems, namely transportation, energy, water, waste, telecommunication, education, and health. The authors extract data on all such infrastructure assets using Open Street Maps (OpenStreetMap Contributors, 2017) and rasterize the data to estimate the amount of category specific critical infrastructure in each grid cell. A final spatial composite is created by aggregating and normalizing the rasterized data per infrastructure type, with equal weighting applied for the aggregation across different infrastructure systems. The final product is a critical infrastructure index ranging from 0 to 1, with higher values representing greater infrastructure intensity.

The CISI data is time-invariant and relates to the year 2020 when geospatial data on infrastructure assets was extracted from Open Street Maps. We aggregate the grid-level CISI data to the city level by calculating the weighted average of CISI across all 11km grid cells that fall within the urban extent shapefiles provided by GHS-UCDB, with weights equal to the proportion of the grid cell that falls within the city extent. As shown in column [7] of Table B.2, cities in high-income countries have, on average, a CISI score of 0.088, as opposed to a score of 0.046 for cites in low-income countries. Figure A.4 shows the spatial distributions of CISI scores across all cities in our dataset. As expected, cities in North America and Western Europe seem to have the highest intensity of critical infrastructure, while cities in Sub-Saharan Africa have the lowest intensity.

H *Dams*

Dams are considered an important form of flood protection infrastructure as they can reduce flood risk by regulating water flow downstream. Even though they entail costly public investments, there is little consensus on their effectiveness in mitigating flood damages. For instance, Boulange et al. (2021) use flood simulation models to show that accounting for flow regulation by dams reduces number of people exposed to floods by 21 percent under an RCP2.6 scenario. On the other hand, Ma et al. (2022) use a case study of a large dam on the lower Yellow River in China to suggest that dams could increase the magnitude of moderate and large floods by altering the riverbeds' sediments. Therefore, we empirically test the hypothesis that dams can mitigate the negative impact of floods. For this purpose, we first need to identify the cities protected by dams as no such harmonized dataset exists for cities across the globe. To this end, we merge the GHS-UCDB dataset on urban extents with two other datasets: *a)* geolocation of river networks across the globe, and; *b)* geolocation of all major dams.

Spatial maps delineating the global river network have been sourced from *HydroRIVERS*, a data product

32. The dataset is available at https://zenodo.org/records/4957647.

provided by the *HydroSHEDS* (Hydrological data and maps based on SHuttle Elevation Derivatives) project which was initiated in the year 2006 by the World Wildlife Fund US (Lehner et al., 2008; Lehner and Grill, 2013).[33] Only rivers with an accumulated catchment area greater than 10 km^2 or an average natural discharge higher than 0.1 m^3/s, or both, were mapped. Every river in the dataset is represented by a network of lines consisting of individual segments called river reaches, *i.e.* river segment between two tributaries, or the stretch between the start/end of the river network and a tributary. The global coverage of *HydroRIVERS* comprises a total length of approximately 36 million kms of rivers, divided into approximately 8.5 million individual river reaches, each with an average length of 4.2 kms (Lehner, 2019). Importantly, for each river reach, the dataset also provides information on upstream and downstream connections which can be combined with geolocation of urban extents to identify cities downstream of a river reach.

For the location of dams, we rely on the Global Reservoir and Dam Database (*GRanD*), a comprehensive geocoded global database of 7,320 large dams — each with a storage capacity of more than 0.1 km^3 and built before 2016 — compiled by the Global Water System Project (Lehner et al., 2011).[34] Though there exist other dam databases, the *GRanD* dataset has been cross-validated and also provides information on the construction year, surface area, storage capacity, height, main purpose, and elevation for all dams.

The algorithm to identify the cities protected by dams involved five steps and is illustrated in Figure 4 for one particular level one administrative unit, the state of Odisha in India. First, we overlay the geocoded dams from the *GRanD* dataset on the map layer of river reaches from *HyrdoRIVERS*. Figure 4a shows the location of rivers and dams in Odisha, with line width reflecting river size. Second, for each of the 7,320 dams, we identify the river reach on which the dam resides. Third, using data on the next downstream line segment provided by *HydroRIVERS*, we construct downstream river reaches, taking the river reach with the dam as the initiation point and continuing up until the last river reach drains into the ocean or into an inland sink. These downstream segments are illustrated as blue shaded river reaches in Figure 4b. Fourth, we overlay the GHS-UCDB shapefiles of urban extents on the delineated river reaches to identify which city polygons have a river reach intersecting through them, and classifying such cities as being situated on a river bank.[35] Figure 4c represents this step, with urban extent polygons within Odisha shaded in yellow while the river banks on which the cities reside shaded as red line segments. Finally, if any such city river banks overlap with the river reach downstream of a dam as identified in the third step, we consider the city to be protected by a dam. These overlapping river reaches are shaded in red in Figure 4d, with cities containing these overlapping reaches, and hence protected by dams, shaded in green.

Column [8] of Table B.2 provides summary statistics on the number of cities protected by dams. The total number of cities protected by dams is 2,409, 74 percent of which lie in high-income countries. Only 14 percent of cities in low-income countries have a dam, while this number is 35 percent for developed economies. Refer to Figure A.5 for a spatial representation of which cities across the globe are protected

33. The two other hydrographic data products provided by HydroSHEDS include spatial polygons delineating sub-basin boundaries (*HydroBASINS*) and lake shorelines (*HydroLAKES*). Data and further information on the *HydroRivers* project is available at https://www.hydrosheds.org/products/hydrorivers.

34. The cumulative storage capacity of the 7,320 dams equals 6,864 km^3. Further information on *GRanD* is available at https://www.globaldamwatch.org/grand/, while the dataset can be accessed at https://www.globaldamwatch.org/directory.

35. We add a 500m buffer to each city's boundary to ensure cities close to a river stream are also classified as being situated on a river bank.

Figure 4: Identifying Cities Protected by Dams in Odisha, India

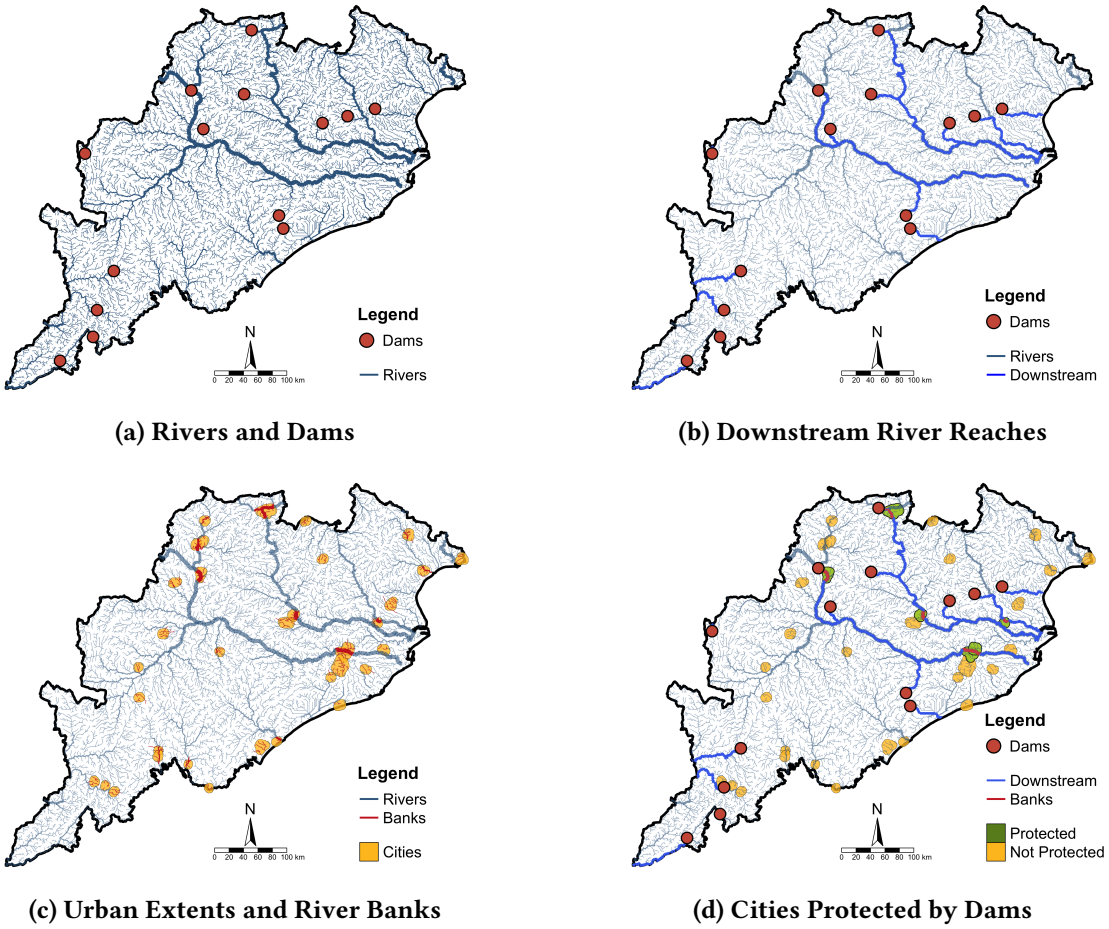

(a) Rivers and Dams

(b) Downstream River Reaches

(c) Urban Extents and River Banks

(d) Cities Protected by Dams

Notes: This figure illustrates the algorithm used to identify cities protected by dams. Figure 4a shows the location of rivers (line segments) and dams (red dots) in Odisha, India. Width of line segments is proportional to river size. Figure 4b represents, in blue, the river segments downstream of each dam in the state. Figure 4c overlays the urban extent polygons within Odisha (shaded in yellow) on the map of rivers and dams. The river banks on which the cities reside are shaded as red line segments. Figure 4d presents (in green) the cities protected by dams, identified as such if the city river banks overlap with the river reach downstream of a dam. Data on dams, rivers, and urban extents is sourced from HydroRivers, GRanD, and GHS-UCDB, respectively. This map uses the WGS84 geographic coordinate system.

by dams.

I Flood Intensity

Not all floods are created equal. Some floods are more severe than others and have a higher potential for damage. EM-DAT does not provide a measure of flood severity, only focusing on reported deaths and damages. Therefore, we rely on Dartmouth Flood Observatory (DFO), a not-for profit entity operational since 1995 and hosted at the Institute of Arctic and Alpine Research (INSTAAR) at the University of Colorado, Boulder, to obtain a measure of flood severity (Kettner et al., 2021). DFO maintains an active archive of large flood events since 1985 and provides information on flood duration, cause, location, start and end dates, socioeconomic impacts, and, importantly for our purpose, an index for flood severity. Flood severity

here is defined as a strictly hydrological occurrence without regard for actual damages, and depends on runoff volume, peak discharge, rainfall intensity and duration, drainage area, *etc.*

DFO assesses flood severity on a 1-2 scale. All floods in the active archive are divided into three classes. *Class 1* refers to large flood events which cause significant damage to structures or agriculture, fatalities, and/or have occurred after an interval of 1-2 decades since the last similar event. *Class 1.5* denotes very large events which are reported to have a greater than 2 decades but less than 100 year estimated recurrence interval. In addition, it also includes floods which have a local recurrence interval of 1-2 decades and affect a geographic region greater than 5000 sq. km. Finally, *class 2* designates extreme events with an estimated recurrence interval greater than 100 years.

All floods reported in EM-DAT do not always have a corresponding record in DFO, and vice-versa. The latter only maintains an archive of "*large*" flood events drawn from news reports, governmental sources and remote sensing.[36] DFO archives, therefore, are generally considered a curated collection of large flood events offering an incomplete picture of all floods, especially as small-scale flooding or flooding in remote areas might not be covered in the media (Munasinghe et al., 2023). Similarly, a flood reported in the DFO archives may not be documented in EM-DAT if the latter's inclusion criteria of *(i)* at least 10 deaths or; *(ii)* at least 100 affected or; *(iii)* a call for international assistance or an emergency declaration is not met.

We follow a two step process to identify severe floods in EM-DAT, our main flood events database. First, since DFO archives only include floods up until January 2022, we subset the EM-DAT flood sample to events between January 2000 and January 2022. This left us with 3,735 flood events in EM-DAT as opposed to 3,931 earlier. The number of floods in DFO for the corresponding period were 3,624. Second, for each severe (*class 2*) flood in the DFO archives (519 events, or 14.3 percent of total), we attempt to match it to an EM-DAT flood entry. The matching leads to 293 out of 3,735 (7.8 percent) EM-DAT floods being classified as severe.[37] 5,289 cities (out of 9,468) in 89 countries were impacted by severe floods between January 2000 and January 2022. The total count of city-month-year observations with severe floods during this time period is 23,322 (0.9 percent of observations), 51 percent of which were concentrated in high or upper-middle income countries, while the remaining 49 percent occurred in lower-middle and low income countries.

3 The Effects of Flood Shocks

We now turn to presenting our findings on how flood shocks affect economic activity as based on lights at night dynamics. Floods could lead to temporary power failures, disruption of essential services, damage to property, temporary closure of offices and factories, and in all cases will affect the normal functioning of economic life for sometime. The wealth of a nation may offer its cities some insurance against large

36. "*Large*" floods are loosely defined by DFO to include floods that cause fatalities, significant damage to property or agriculture, and have a long interval (decades) since events of similar magnitude and scale.

37. We classify all flood events in EM-DAT which were not matched to a severe flood in DFO archives as non-severe. Given that there are several EM-DAT floods which do not have a corresponding entry in DFO, it is seemingly erroneous to assume that all such floods are not severe. However, given that DFO maps and archives every large flood, it is highly unlikely that there exists an EM-DAT flood which does not register in DFO and was severe. Therefore, we are reasonably confident that all non matched floods in EM-DAT can be classified as non-severe.

economic devastation due to floods. Hence, cities in poorer nations may suffer greater economic losses. We test whether the effects of floods differ for cities in high-income countries compared to cities in low-income countries. Further, we use an event-study framework to analyze the pattern of recovery following a flood event, *i.e.*, the length of time it takes for cities, on average, to recover from floods. Finally, we test whether a flood's impact on a city's economic activity could vary based on topographical features (elevation), location (coastal v/s inland), and its political or administrative importance within the country (*e.g.*, capital cities).

A The Effect of Floods on Economic Activity

We examine the impact of floods on economic outcomes by running the following regression:

$$ln(Night\ Lights_{cjmy}) = \alpha + \sum_{i=-2}^{2} \left(\beta_i\ Flood_{cj\{m+i\}y}\right) + \mathbf{X}_{cjmy} + \gamma_c + \gamma_{jmy} + \epsilon_{cjmy} \quad (1)$$

where $ln(Night\ Lights_{cjmy})$ refers to the natural log of the mean night lights in city c in country j in month m and year y. $Flood_{cjmy}$ is a dummy variable that equals 1 if city c in country j experienced a flood in month m of year y. We include two month leads and lags of the flood dummy.[38] The leads help to control for activities relating to flood preparedness in response to a flood warning, or heavy rainfall prior to floods, both of which could impact economic activity in a city. The lags, on the other hand, account for recovery dynamics post floods. $\mathbf{X}_{cjmy}$ represents a vector of city-specific controls, specifically whether the city was affected by storms or landslides in month m of year y, and the corresponding two month lags and leads. γ_c and γ_{jmy} represent city, and country-month-year fixed effects, respectively. The former account for time-invariant city characteristics which could impact night lights, such as whether the city is the political or financial capital of the country, or its geographic location. The country-month-year fixed effects help to control for seasonality and economic shocks common to all the cities within a country. Standard errors are clustered at the country and month-year level to account for spatial and temporal correlation in the unobserved factors that affect economic activity. To investigate the heterogeneity by income in the impact of floods on economic activity, we also run the regression separately for cities in high- and low-income countries. Results using the imputed dataset are presented in Table 1.[39]

We find that floods have a significant negative impact on economic activity, with the magnitude of the effect being much larger for cities in low-income countries. Column [1] reports the results for all cities, while columns [3] and [5] present the estimates for cities in high- and low-income countries, respectively. On average, a flood event leads to a 4.5 percent fall in nightlights in the month of the disaster. However, this masks considerable heterogeneity in effect size by income groups. Cities in high-income countries experience a smaller, yet significant, decline of 2.1 percent in economic activity in the month of the flood, but the impact is considerably larger at 7.4 percent for cities in low-income countries.

We also investigate how extreme rainfall events — a proxy for floods — impact night lights. The re-

38. The value of the i subscript in Equation (1) represents the lead ($i \in \{-1, -2\}$), event ($i = 0$), and lag ($i \in \{1, 2\}$) months.

39. All results concerning nighttime lights use the dataset with imputed values of night luminosity, unless otherwise noted. See Section 2.B for details on the imputation procedure.

Table 1: Effect of Floods and Extreme Precipitation on Economic Activity

	Dependent Variable: *ln(Night Lights$_{cjmy}$)*					
	All		**High Income**		**Low Income**	
	(1)	(2)	(3)	(4)	(5)	(6)
Flood$_{cjmy}$	−0.045***		−0.021***		−0.074***	
	(0.014)		(0.005)		(0.015)	
Extreme Precipitation$_{cjmy}$		−0.146***		−0.092***		−0.192***
		(0.032)		(0.021)		(0.040)
Fixed Effects						
City	Yes	Yes	Yes	Yes	Yes	Yes
Country × Month × Year	Yes	Yes	Yes	Yes	Yes	Yes
Num. obs.	1,287,648	1,287,648	693,872	693,872	593,776	593,776
Adj. R^2	0.861	0.861	0.789	0.789	0.804	0.804

Notes: Two-way clustered robust standard errors are reported in parenthesis. $^{***}p < 0.01$; $^{**}p < 0.05$; $^{*}p < 0.1$.
The dependent variable in all regressions, *ln(Night Lights$_{cjmy}$)*, is the natural log of mean light intensity in city c in country j in month m of year y. We have used the cloud mask configuration of the NPP-VIIRS monthly composites, where data contaminated by stray light are removed. Missing data for *ln(Night Lights$_{cjmy}$)* was imputed using Predictive Mean Matching. *Flood$_{cjmy}$* is a dummy indicating whether city c in country j was hit by a flood in month m of year y. *Extreme Precipitation$_{cjmy}$* is a dummy indicating whether the precipitation in month m and year y in city c in country j was greater than the 99th percentile of the city-specific distribution of precipitation, which was created using data from January 1940 to August 2023. Models (3) and (4) only include observations from *High Income* and *Upper Middle Income* countries, whereas models (5) and (6) only include observations from *Low Income* and *Lower Middle Income* countries. All regressions include the controls $Storm_{cjmy}$ and $Landslide_{cjmy}$, dummies indicating whether city c in country j was hit by a storm or landslide, respectively, in month m of year y. Two month leads and lags for all three disaster types have also been included as controls. Standard errors are clustered at the country and month-year level.

gression specification is the same as in Equation (1), except that the regressor of interest changes from $Flood_{cj\{m+i\}y}$ to *Extreme Precipitation*$_{cj\{m+i\}y}$. To construct the variable, we first use monthly precipitation data from January 1940 to August 2023 to calculate the city specific distribution of rainfall for each of the 9,468 cities in our sample. Next, for each city, we classify all months with precipitation greater than the 99th percentile of the city specific distribution as an extreme precipitation event. This gives us a list of months when each city experienced precipitation that was extreme relative to its 80-year history. Results are presented in Table 1, with the average impact across all 9,468 cities reported in column [2], and the heterogeneous impact for cities in high- and low-income countries outlined in columns [4] and [6], respectively.

The direction of the effect is exactly similar to floods but the overall magnitude, regardless of income group, is much larger. On average, extreme precipitation leads to a 15 percent fall in night light intensity in the month of the event. As with floods, extreme precipitation has a much greater impact on cities in low-income countries as opposed to cities in high-income countries, with night lights falling by 19 percent in the former relative to 9.2 percent in the latter. Notably, this difference in effect sizes between floods and extreme precipitation was also reported by Kocornik-Mina et al. (2020), who found that floods lead to a 2.1 percent fall in average night light intensity in the year of the event, but extreme precipitation has a more damaging impact, with effect sizes ranging from -2.5 to -8.0 percent.[40]

Finally, we can also test if more severe floods lead to a larger negative impact on economic activity. To do so, we augment Equation (1) by adding an interaction term, $Flood_{cjmy} \times Severe_{cjmy}$, where $Severe_{cjmy}$ equals 1 if the flood that hits city c in month-year my is classified as *Class 2* based on DFO's flood severity

40. Kocornik-Mina et al. (2020) define extreme precipitation events at the grid-year level, with the extreme precipitation indicator for the grid-year equal to 1 if the aggregate rainfall within any month in the year was greater than 500mm or 1000mm. The larger damages (8.0 percent fall in night lights) are estimated with the higher threshold.

assessment (see Section 2.I). The coefficient on the interaction term represents the additional economic impact of a flood classified as severe. Results, presented in Appendix C.A, show that in high-income countries, cities hit by non-severe floods (*Class 1* and *1.5*) experience a 1.1 percent fall in night lights. This negative impact is amplified by a statistically significant 2.0 percentage points in the case of severe floods. In other words, the impact of low-intensity floods in cities in high-income countries, although significant, is not economically large, but severe floods cause almost two times more damage. However, for urban areas in low-income countries, the impact of a severe flood is not statistically different from the impact of a low-intensity flood. The latter leads to a 7.4 percent fall in nighttime lights, and the supplemental impact of a severe flood, though a negative 1.1 percent, is not significant at conventional levels. Therefore, the results signify that in low-income countries, any flood — severe or otherwise — has a large impact, as opposed to cities in high-income countries where only the most catastrophic floods cause damage. This would imply that high income countries have at least been successful in adapting to low-intensity floods. The same is not true for low-income countries, which suffer widespread damages notwithstanding the intensity of floods.

B Recovery Dynamics from Floods

How long do cities take to recover from a flood shock, and does the recovery pattern differ by income? To analyze such short-run recovery dynamics, we employ an event-study methodology to estimate the changes in economic activity before and after a flood and extreme precipitation event. Additionally, an event-study also allows us to check for differences in pre-trends in night light intensity between cities which suffered from a flood and cities which did not. We can assess the evolution of economic activity in the months prior to the shock to confirm if the trends were truly parallel before the event month — an important identifying assumption.

The estimating equation is similar to Equation (1), except that we allow i, the event-study window, to span from 30 months prior to the flood event to 30 months after. Following Cullen and Perez-Truglia (2023) and Stevenson and Wolfers (2006), we add two absorbing dummies for the extreme categories of $\leq$ -31 and $\geq$ +31 months. The identification strategy leverages the timing of floods and extreme precipitation shocks. For example, consider two cities, one of which gets flooded. We compare the night lights between the cities each month leading up to the shock and each month after the event. We should expect to see no differences in outcomes between the cities in the months leading up to the flood (no pre-trends assumption), a significant difference in outcomes in the month of the flood caused by the negative impact of the shock on economic activity in the affected city, and an attenuation in this difference in the months following the flood event as the affected city recovers.

Results from the event-study regressions are presented in Figure 5. The top panel presents event-study estimates for all 9,468 cities, while the middle and bottom panels focus on estimates for cities in high- and low-income countries, respectively. As a robustness check, we also adopt the event-study framework to estimate the evolution of economic activity in the months before and after extreme precipitation events . The results of this exercise are presented in the right panel, while the left panel exhibits the impact of floods. In all the event-study graphs, the period 0 denotes the exact month of the flood/extreme precipitation event.

Figure 5: Event Study Analysis of Impact of Floods on Night Lights Intensity

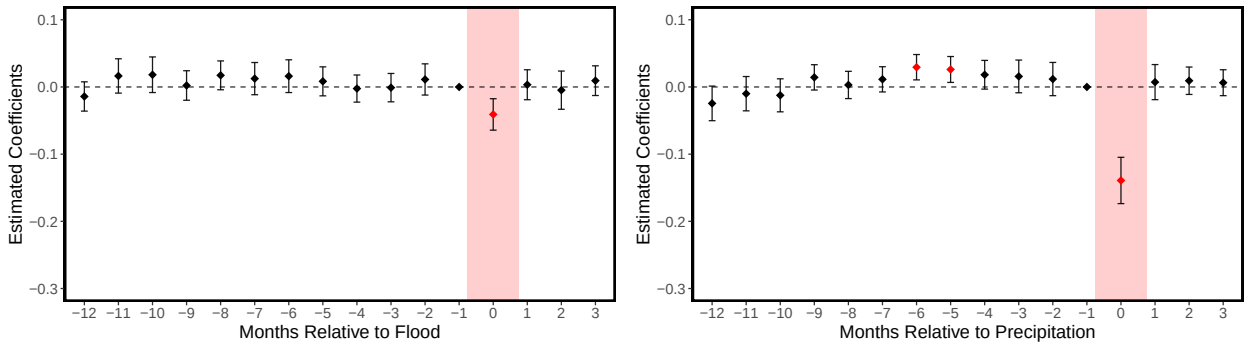

(a) All Cities — Floods

(b) All Cities — Precipitation

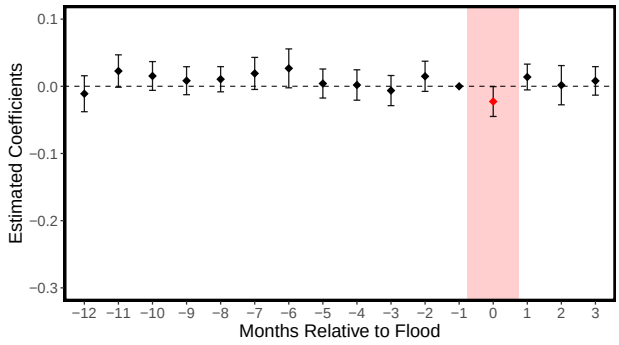

(c) High Income Cities — Floods

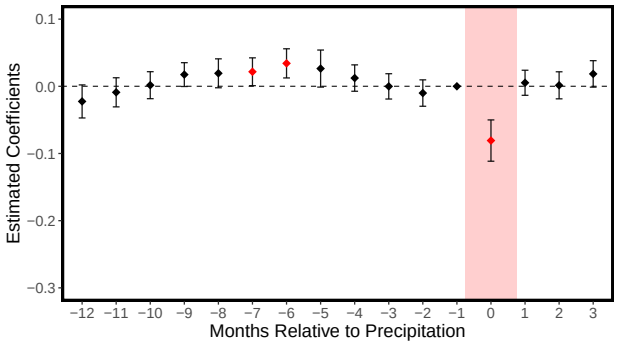

(d) High Income Cities — Precipitation

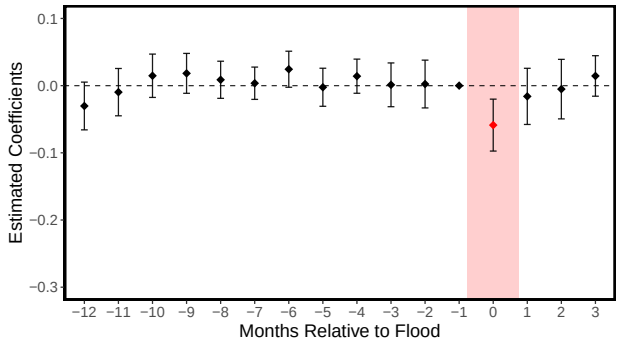

(e) Low Income Cities — Floods

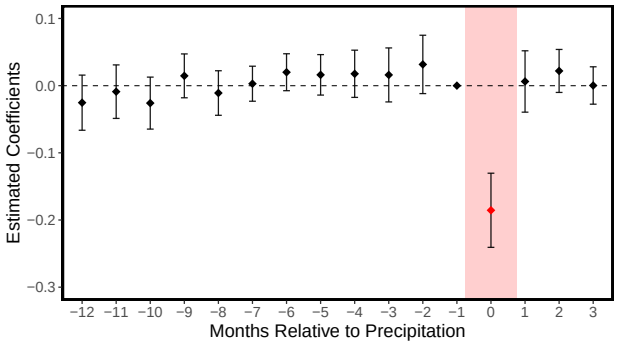

(f) Low Income Cities — Precipitation

Notes: Figure 5 presents event-study estimates of the impact of floods or extreme precipitation event on night light luminosity, spanning from 12 months prior to 3 months post a shock. Details on the regression specification are presented in Sections 3.A and 3.B. The top panel presents estimates for all 9,468 cities, while the middle and bottom panels present estimates for high- and low-income cities, respectively. The left and right panel exhibit the evolution of economic activity due to the impact of floods and extreme precipitation events, respectively. In all graphs, the period 0 denotes the exact month of the flood/extreme precipitation event, and is shaded red. The 95% confidence intervals are denoted by error bars, with two-way clustering by city and country-month-year.

In the interest of readability, we only present estimates from 12 months prior to the event to 3 month post it. The omitted category in all underlying regressions is the month immediately prior to the event month, *i.e.*, $i = -1$.

Our results indicate that there is a negative economic impact of floods but, surprisingly, it is short-

lived with the difference in economic activity between flooded and non-flooded cities not distinguishable from zero in the months immediately following a flood. This result is consistent across income groups. On average across all cities, night lights fall by 4.1 percent in the month of the flood (Figure 5a). However, the recovery is almost instantaneous, with the coefficient next month a positive but insignificant +0.33 percent. An analysis of the heterogeneity in impacts by income group reveals a similar pattern to the results in Section 3.A. The magnitude of the impact is higher in low-income countries, with night lights falling by 5.9 percent in the month of the flood (Figure 5e), as opposed to reducing by 2.3 percent in high income countries (Figure 5c). Despite the difference in magnitudes in the month of the flood, the recovery pattern across the income classes is similar. The difference in night lights between cities affected and unaffected by floods in each income class in the months following the flood is not significant, indicating that cities in both high- and low-income countries recover to their pre-flood economic levels swiftly. It is worth noting that, although not significant, the coefficient in low-income countries for the two months following the event has a negative sign (-1.5 percent in lag 1 and -0.052 percent in lag 2) and trends towards zero.

Extreme precipitation events exhibit a comparable recovery pattern to floods. They reduce night light intensity by a statistically significant 14 percent in the month of the shock, but this negative effect is entirely attenuated in the subsequent month, with the estimated coefficient a positive but not significant +0.72 percent (Figure 5b). Although cities in low-income countries are worse affected by such events — 19 percent fall in the month of the event (Figure 5f) as compared to an 8.1 percent fall in cities in high-income countries ((Figure 5d)) — the differences between cities affected and unaffected by a shock is eliminated in the month immediately following the event across both income groups. Unlike floods, we do not find suggestive evidence of a slower recovery in low-income countries with respect to extreme precipitation shocks. The coefficient one month post the event is a positive but statistically insignificant +0.62 and +0.52 percent for low- and high-income countries, respectively. Thus, both floods and its proxy, extreme precipitation, have a negative impact on economic activity which is more severe in low-income countries. However, the impact is short-lived, with cities returning to their pre-flood levels within one month irrespective of their income classification.

Finally, the evolution of night-lights prior to the flood events, *i.e.* pre-trends, merits consideration. The key assumption is that prior to any flood or extreme precipitation shock, cities that experienced such an event were on the same economic trajectory as cities that were not impacted. The event-study framework allows us to test for this identifying assumption. Consistent with this assumption, all the figures relating to floods (left panel of Figure 5) show that in the 12 months prior to the floods, the coefficients are statistically indistinguishable from zero. This implies that both flood affected as well as unaffected cities shared similar economic trends prior to the shock. In the case of extreme precipitation, a majority of the coefficients preceding the shocks are close to zero, precisely estimated, and statistically insignificant. There are, however, a few positive and significant estimates five to seven months prior for both the full sample of cities as well as for cities in high-income countries (Figures 5b and 5d), which we attribute to noise. Only in the month of the flood and extreme precipitation shock ($i = 0$) does the difference in night lights across affected and unaffected cities diverge. Therefore, on the basis of this evidence, we are reasonably confident that the

assumption about parallel trends holds.

C Heterogeneous Impact of Floods

Does the impact of floods vary with a city's geographical and topographical features, or its administrative importance? For instance, low-elevation coastal cities may experience greater economic damage from floods due to both a tendency for these areas to have a high concentration of population and economic activity (Balboni, 2019), and their increased vulnerability to sea-level rise and storm surges (Hanson et al., 2011; Hallegatte et al., 2013). Similarly, cities that are centres of political power may be more resilient to weather shocks as governments invest in climate resilient infrastructure in such areas owing to their relative administrative importance. Furthermore, geography, topography, and political significance of an urban center could also interact with income levels of the country to influence the magnitude of economic losses caused by floods. Though both Dhaka in Bangladesh and Miami in the USA may have similar exposure to coastal flood risk, the resulting damages from a flood may be higher in the former as it has limited financial capacity to invest in coastal defence infrastructure.

To test the role of elevation, coastal or inland location, or political and administrative importance — proxied by whether the city is the seat of the country's government, *i.e.* its capital city — in influencing the severity of a flood's impact on economic activity, we estimate the following regression equation:

$$ln(Night\ Lights_{cjmy}) = \alpha + \sum_{i=-2}^{2} \left(\beta_i\ Flood_{cj\{m+i\}y}\right) + \delta \left(Flood_{cjmy} \times \Omega_{cj}\right) + \mathbf{X}_{cjmy} + \gamma_c + \gamma_{jmy} + \epsilon_{cjmy} \quad (2)$$

where $\Omega_{cj} \in \{High\ Elevation_{cj}, Coastal_{cj}, Capital_{cj}\}$ represents the different geographical, topographical and political importance variables of interest. $High\ Elevation_{cj}$ is a dummy variable that equals 1 if the median elevation across all 1 km^2 grids within city c in country j is in the top 50$^{\text{th}}$ percentile of the distribution of median elevation of all 9,468 cities in the sample, *i.e.*, greater than 154 meters. $Coastal_{cj}$ is an indicator variable that takes the value 1 for cities which share their geographical boundaries, as provided by GHS-UCDB, with a coastline, while $Capital_{cj}$ is also a dummy that switches on if city c is the capital of country j. All other variables have the same interpretation as in Section 3.A. The coefficient of interest is δ which is the interaction term between the indicator for flood in the current month-year (my) and the variable of interest. Note that because Ω_{cj} is city specific and time invariant, the presence of city fixed effects (γ_c) implies that the main effect of the variable of interest is swept out and cannot be estimated. We estimate separate regression equations for each element of Ω_{cj}. Each regression is run separately for cities in high- and low-income countries. Results are presented in Table 2, with columns (1)-(3) focusing on the sub-sample of cities in high- and upper-middle-income countries, and columns (3)-(6) presenting results for cities in low- and lower-middle-income countries.

We have three main results. First, we show that the impact of floods on high elevation cities is attenuated, but only in richer countries. As shown in column (1), a flood event leads to a 3.5 percent fall in night lights in the month of the shock in low-elevation cities within high-income countries, but the coefficient

Table 2: Heterogeneity in the Effect of Floods on Economic Activity

	Dependent Variable: $ln(Night\ Lights_{cjmy})$					
	High Income			Low Income		
	(1)	(2)	(3)	(4)	(5)	(6)
$Flood_{cjmy}$	-0.035^{***}	-0.021^{***}	-0.021^{***}	-0.064^{**}	-0.075^{***}	-0.066^{***}
	(0.008)	(0.005)	(0.005)	(0.025)	(0.015)	(0.013)
$Flood_{cjmy} \times High\ Elev._{cj}$	0.031^{**}			-0.018		
	(0.012)			(0.030)		
$Flood_{cjmy} \times Capital_{cj}$		0.013			0.057^{**}	
		(0.040)			(0.028)	
$Flood_{cjmy} \times Coastal_{cj}$			0.001			-0.089^{***}
			(0.017)			(0.030)
Fixed Effects						
City	Yes	Yes	Yes	Yes	Yes	Yes
Country × Month × Year	Yes	Yes	Yes	Yes	Yes	Yes
Num. obs.	693,872	693,872	693,872	593,776	593,776	593,776
Adj. R^2	0.789	0.789	0.789	0.804	0.804	0.804

Notes: Two-way clustered robust standard errors are in parenthesis. $^{***}p < 0.01$; $^{**}p < 0.05$; $^{*}p < 0.1$.
The dependent variable in all regressions, $ln(Night\ Lights_{cjmy})$, is the natural log of mean light intensity in city c in country j in month m of year y. We have used the cloud mask configuration of the NPP-VIIRS monthly composites, where data contaminated by stray light are removed. Missing data for $ln(Night\ Lights_{cjmy})$ was imputed using Predictive Mean Matching. $Flood_{cjmy}$ is a dummy indicating whether city c in country j was hit by a flood in month m of year y. $High\ Elev._{cj}$ is a dummy indicating whether city c in country j has a median elevation that ranks in the top 50th percentile of the distribution of the median elevation across all cities, *i.e.* greater than 154 meters. $Capital_{cj}$ is a dummy that indicates whether city c is the national capital. $Coastal_{cj}$ is a dummy that indicates whether city c in country j is located on the coast. Models (1), (2) and (3) only include observations from *High Income* and *Upper Middle Income* countries, whereas models (4), (5) and (6) only include observations from *Low Income* and *Lower Middle Income* countries. All regressions include the controls $Storm_{cjmy}$ and $Landslide_{cjmy}$, dummies indicating whether city c in country j was hit by a storm or landslide, respectively, in month m of year y. Two month leads and lags for all three disaster types have also been included as controls. Standard errors are clustered at the country and month-year level.

on the interaction term is a positive and significant 3.1 percent. This implies that high elevation areas in developed countries experience a fall in economic activity by 0.42 percent after a flood, and a linear hypothesis test indicates that this effect is not significantly different from 0. On the other hand, the impact of floods in low elevation areas within low-income countries is higher in magnitude as night lights reduce by 6.4 percent post a flood (column [4]). Further, in contrast to high-income countries, this effect is worsened in high-elevation areas, with economic activity falling by an additional 1.8 percent, though this estimate is not statistically significant. Therefore, we find that low elevation areas, where most of the population and economic activity is concentrated globally, are impacted in both high- and low-income countries but at least in richer economies, this negative effect is completely mitigated for high elevation areas.

Second, we find that capital cities experience a lower reduction in economic activity post floods, but this is only true for capitals of low-income countries. In such countries, floods in non-capital cities cause their night light luminosity to decline by 7.5 percent. However, as presented in column [5], this deleterious impact is alleviated by 5.7 percentage points for capital cities. In fact, a linear hypothesis test shows that though capital cities suffer from a 1.7 percent fall in night light intensity post flood events, this effect is not statistically significant. This is in contrast to capital cities in high-income countries where we do not find any evidence of attenuation of negative impacts. The caveat, though, is that the magnitude of impact in non-capital cities in high-income countries was relatively small, but significant, to begin with, as night lights fall by 2.1 percent post a flood event (column [2]). Capital cities are able to mitigate this impact by a further 1.3 percentage points, but this is not statistically significant at conventional levels. Therefore, what our results suggest is that low-income countries, which are afflicted by financial constraints, likely only

invest in climate resilience infrastructure in cities of political and administrative importance. This enables their capital cities to withstand negative flood shocks. Since high-income countries have a larger pool of financial resources, they can channel investment in climate resilience across all their urban areas, notwithstanding their political or administrative importance. This may explain why we do not see a differential impact of floods on night lights in capital and non-capital cities in high-income countries.

Finally, we show that coastal cities in low-income countries are the urban group worst affected by floods. To see this, note that within high-income countries, floods in inland cities reduce night lights by a statistically significant 2.1 percent in the month of the disaster. Coastal cities within these countries experience similar declines in economic activity, as evidenced by the null estimate on the interaction term in column [3]. On the other hand, the interaction term in column [6] is a large and significant -0.089. This signifies that for low-income countries, the already substantial 6.6 percent fall in night lights in inland cities is amplified in coastal cities, with night lights falling by a sizable 16 percent. This result puts into focus the adaptation gap, and complements the previous finding on the impact of floods in capital cities across developed and developing nations. The impact of floods in coastal urban areas in richer countries is small and they do not suffer differentially from cities inland. This likely arises because governments in developed nations have the financial and institutional capabilities to invest in protection infrastructure, particularly in areas with high concentration of productive human capital, such as coastal cities. In contrast, the impact of floods is aggravated in coastal cities within developing nations, with economic damages up to three times higher as compared to damages to their inland counterparts. Given that developing countries are expected to account for a majority of the population in low-elevation coastal zones by the year 2100 (Barbier, 2015), and the flood risk in such cities is expected to rise five-fold by 2080 (Adger et al., 2005), it is imperative that the adaptation gap with richer countries shrinks. We study differences in adaptive capacity across time and income classifications in the next section.

One potential concern with using changes in night lights to measure the impact of floods is that a decline in night lights post floods could be attributed to power outages, and not just a loss in economic activity. However, the following four points provide suggestive evidence that lights within cities are capturing local economic activity. First, as results in this section indicate, floods have heterogeneous impacts within a country depending on the geography, topography, and political importance of the city. For instance, we find that high-elevation cities in high-income countries suffer less after a flood, or that coastal cities in low-income countries experience heavier losses. Given that our empirical specification includes country-month-year fixed effects, we are comparing flooded and non-flooded cities within a country within each particular month. Under the assumption that the strength of the electricity grid does not vary across all cities within a country at a point in time, higher damages in low-elevation areas and coastal cities seems to support the conclusion that night lights are indeed capturing economic activity. Second, we explicitly consider, in Section 4.E, how the impact of floods differs by the strength of critical infrastructure in a city. The critical infrastructure index, as defined by Nirandjan et al. (2022), includes energy infrastructure as a major component. Specifically, this relates to the city-specific infrastructure associated with production, conversion and delivery of energy, and includes the following infrastructure types: cable, line, minor line, power tower, power pole, plant, and substation. The results, presented in Section 4.E, show that cities with

relatively higher levels of critical infrastructure also suffer from a fall in night lights due to floods, though the impact is much lower compared to cities with poorer critical infrastructure. In other words, even cities with a robust electricity grid experience a decline in night lights post floods, which indicates that it is highly unlikely that the fall in night lights are purely capturing power outages. Third, we know that all the floods in our dataset either led to deaths, injuries and/or rendered at least some population homeless, following the criterion used by EM-DAT to classify a disaster as a flood (see Section 2.C). This loss of lives and displacement should have an impact on economic activity, further lending credence to our claim that we are not recording simply grid failures. Finally, in so far as floods lead to power outages, economic activity will suffer as electricity is required for operating non-agricultural firms as well as climate control, with the latter associated with an increase in worker productivity (Somanathan et al., 2021).

4 Evidence for Adaptation

Economic agents can alter their processes, practices and structures to increase resilience and mitigate potential damages arising from weather shocks, including floods. Termed adaptation, it is defined by the IPCC (2022) as:

> "*The process of adjustment to actual or expected climate and its effects in order to moderate harm or take advantage of beneficial opportunities.*"

In this section, we investigate, using various measures, whether there is evidence of adaptation to floods, and the mechanisms underlying the adaptation progress. Specifically, we examine the sensitivity of economic activity and mortality to flood shocks over time, the role of migration and experience-driven adaptation, and whether critical infrastructure and dams upstream can help in mitigating the negative impacts of floods.

We have three main findings. First, the sensitivity of economic activity and mortality to floods is decreasing over time across both high- and low-income countries. Second, recurrent flood exposure is associated with a reduction in the marginal impact of subsequent floods, underscoring the role of experience and learning-by-doing in accelerating adaptation. Third, while self-protection adaptation mechanisms (migration) and public investment in resilience infrastructure can aid adaptation, their prevalence and relevance is more prominent in richer countries — a result which highlights climate justice concerns.

A ***Effects of Floods on Economic Activity over Time***

A basic, yet fundamental, measure of adaptation is whether economic damages from floods are decreasing over time. If vulnerabilities from floods are trending downwards, it provides suggestive evidence of cities responding to increasing flood occurrences and intensity by adjusting their ecological, economic and social systems. To examine this hypothesis in our sample period, we augment Equation (1) to include a month time trend and interact it with the dummy for flood events, *i.e.* $Flood_{cjmy} \times Month\ Trend_{my}$. A discrete variable, $Month\ Trend_{my}$ sequentially takes the value from 1 to 136, with the variable equal to 1 for every city in April 2012, the first month of our sample, and equal to 136 in July 2023, the latest time period in

the dataset. As a robustness check, we run a separate regression where the time-trend variable equals $Year\ Trend_y$. This variable is at an annual temporal frequency and takes values from 1 to 12, corresponding sequentially to each year in the period 2012 to 2023. If cities are adapting over time, we expect the coefficient on the trend variables to be positive, indicating the damages from flood events are diminishing over time. Because we include country-month-year fixed effects (γ_{jmy}), the level effects of the time-trend is swept out and the coefficient on the time-trend variables cannot be estimated. Results are presented in Table 3.

Table 3: Effect of Floods on Economic Activity over Time

	Dependent Variable: *ln(Night Lights*$_{cjmy}$*)*					
	All		**High Income**		**Low Income**	
	(1)	(2)	(3)	(4)	(5)	(6)
$Flood_{cjmy}$	−0.091**	−0.097**	−0.037***	−0.038***	−0.209***	−0.223***
	(0.044)	(0.048)	(0.012)	(0.014)	(0.046)	(0.050)
$Flood_{cjmy} \times Month\ Trend_{my}$	0.001		0.000		0.002***	
	(0.000)		(0.000)		(0.001)	
$Flood_{cjmy} \times Year\ Trend_y$		0.008		0.003		0.021***
		(0.006)		(0.003)		(0.007)
Fixed Effects						
City	Yes	Yes	Yes	Yes	Yes	Yes
Country × Month × Year	Yes	Yes	Yes	Yes	Yes	Yes
Num. obs.	1,287,648	1,287,648	693,872	693,872	593,776	593,776
Adj. R^2	0.861	0.861	0.789	0.789	0.804	0.804

Notes: Two-way clustered robust standard errors are in parenthesis. $^{***}p < 0.01$; $^{**}p < 0.05$; $^{*}p < 0.1$.
The dependent variable in all regressions, $ln(Night\ Lights_{cjmy})$, is the natural log of mean light intensity in city c in country j in month m of year y. We have used the cloud mask configuration of the NPP-VIIRS monthly composites, where data contaminated by stray light are removed. Missing data for $ln(Night\ Lights_{cjmy})$ was imputed using Predictive Mean Matching. $Flood_{cjmy}$ is a dummy indicating whether city c in country j was hit by a flood in month m of year y. $Month\ Trend_{my}$ is a discrete variable that sequentially takes the value from 1 to 136, with 1 representing the first month of the sample (April 2012), and 136 representing the last month (July 2023). $Year\ Trend_y$ is a discrete variable that sequentially takes the value from 1 to 12, with 1 representing the first year of the sample (2012), and 12 representing the last year (2023). Models (3) and (4) only include observations from *High Income* and *Upper Middle Income* countries, whereas models (5) and (6) only include observations from *Low Income* and *Lower Middle Income* countries. All regressions include the controls $Storm_{cjmy}$ and $Landslide_{cjmy}$, dummies indicating whether city c in country j was hit by a storm or landslide, respectively, in month m of year y. Two month leads and lags for all three disaster types have also been included as controls. Standard errors are clustered at the country and month-year level.

Our results demonstrate that the impact of floods on night lights is falling over time, but only for cities within low-income countries is this effect statistically significant. We first estimate regressions for the entire sample of 9,468 cities, with results presented in columns [1] and [2]. The coefficients on the interaction terms are positive, and equal 0.068 and 0.82 percentage points for month and year trends, respectively. This suggests that the negative impact of a flood on economic activity diminished, on average, with each subsequent time period between April 2012 to July 2023. The estimates, though, are not statistically significant (*p-value* between 0.15 and 0.16) and we cannot reject the null hypothesis that the reduction in losses over time are not statistically different from zero. However, the full sample masks crucial heterogeneity, as becomes evident when we divide the sample between cities in high- and low-income countries. We find that the attenuation towards zero of the coefficients on the interaction terms is being driven by cities in high-income countries, as the estimates for this subgroup equal a positive, but statistically insignificant, 0.026 and 0.29 percentage points for month and year trends, respectively (columns [3]-[4]). In contrast, the corresponding estimates for the interaction term for cities in low-income countries are a statistically significant 0.18 and 2.1 percentage points (columns [5]-[6]). These estimates suggest that though a flood in April 2012 led to night lights falling by an average of 21 percent in cities in low-income countries, this

effect is mitigated by 0.2 percentage points for every subsequent month in the dataset. Similar evidence of adaptation is exhibited with year trends. A flood in 2012 causes night lights to decrease, on average, by 20 percent, but the impact is attenuated by 2.1 percentage points, or approximately 10 percent, with each subsequent year.

The lack of adaptation to floods over time in cities within high-income countries needs to be understood in conjunction with the evidence that the magnitude of economic losses in such countries due to disasters is small to begin with. Rather than suggesting that there is no adaptation in high-income countries, the results provide evidence that the capacity of cities to adapt is finite and there may be limits to adaptation (Adger et al., 2009).[41] However, cities in low-income countries are, as yet, far from these restrictive adaptation limits, as evident by their progress on the adaptation front over time. To what extent, and why, may adaptation thresholds impede resilience in low-income countries is an empirical question that future research should tackle.

B Effects of Floods on Deaths over Time

An important natural disaster adaptation metric is the death count. If death tolls attributable to floods are declining over time despite climate change exacerbating both the frequency and intensity of extreme flood events (Brunner et al., 2021), it would point towards improved resilience. Not only can we quantify this temporal dynamic, we can also analyze the socio-economic and geographic determinants of fatalities arising from floods to understand the factors which can be influenced to further decrease deaths.

To test whether fatalities due to floods are trending downwards, we use data on the total number of deaths reported for each flood in the EM-DAT database.[42] Since deaths from floods is a non-negative count variable which is highly skewed with many zero counts and some truly destructive disasters with mass casualties, we model the data using a zero-inflated negative binomial (ZINB) regression.[43,44] The advantage of a ZINB model is that it assumes that zero outcomes can arise due to two different processes. First, there may be zero deaths because there was no flood in a city during a month-year and, therefore, the only plausible value for deaths from floods under this scenario is zero. These are termed *certain* or *excess* zeros. The second reason a zero can arise in the death count is if the flood did not lead to any casualties. These are the *true* zeros. The number of zeroes, therefore, are inflated by the *excess* zeros, which implies that the

41. Adaptation limits in a climate change setting can be defined as a threshold beyond which an economic agent cannot adjust from climate risks through adaptive actions (Moser and Ekstrom, 2010; Dow et al., 2013). This can arise either because no adaptation options exist or the adaptive effort required is inordinate so as to render it prohibitive. Furthermore, adaptation limits can be considered *hard* or *soft*. *Hard* adaptation limits refer to a situation where no adaptive action exists to mitigate the risk, even in the foreseeable future. *Soft* adaptation limits refer to a state where although no adaptive adjustments currently exist, there is a possibility innovation could enable such options to become available in the future. For more information on adaptation limits, refer to Klein et al. (2015).

42. Total deaths in EM-DAT include confirmed fatalities in addition to people missing since the disaster and, hence, presumed dead according to official figures.

43. We do not use a Poisson model because of the overdispersion of the deaths data. To test this, we compare the log-likelihoods of a negative binomial regression model and a Poisson regression model. Specifically, we use a likelihood ratio test to test the null hypothesis that the restriction implicit in the Poisson model — conditional variance equals the conditional mean — is true. We reject the null of the Poisson restriction in favour of the negative binomial regression at the 1 percent significance level.

44. See Heim et al. (2022) for an application of the ZINB approach to study the anti-competitive impact of minority share holdings in rival firms. Also, Kahn (2005) has used this model to study the role of income, geography, and institutions in mitigating deaths from disasters.

number of zero deaths cannot be modeled in the same manner as non-zero positive count of deaths. ZINB models account for this complication by generating and combining two separate models. First, a logit model is generated for the *certain zero* deaths, predicting whether or not a city-month-year observation (our unit of analysis) would fall in this group. Subsequently, a negative binomial model is used to predict the count of deaths for those city-month-year observations which have strictly positive fatalities. Finally, the two models are combined such that the expected count of deaths arising from floods is expressed as a combination of the two processes.

$$\mathbb{E}(deaths = k) = [Pr(No\ Flood) \times 0] + [Pr(Flood) \times \mathbb{E}(deaths = k \mid Flood)] \tag{3}$$

We start by modeling the zero-death counts, estimating a logit model where the dependent variable equals 1 if there were no fatalities from a flood in city c in nation j in month m of year y.[45] The explanatory variables in the logistic regression include a dummy for whether there was a flood in the city during the month-year, and the interaction of this indicator with a host of variables related to the socio-economic, geographic and administrative importance of the city and country. These include continuous variables such as the city's population, income and built-up area, along with dummy variables indicating whether it is a coastal city, has high median elevation, has capital city status, and is located within a high-income country.[46] Finally, we also interact the flood indicator with the monthly precipitation in the city during the corresponding month, which acts as a proxy for the severity of the flood. The logic for including these variables is as follows: a city population can only suffer deaths due to flood if such an inundation event takes place. Further, interacting this indicator with different characteristics of the city allows for the possibility that cities with smaller populations and higher incomes are less likely to experience fatalities from a flood, or a city with a large population and low income will suffer no deaths if the flood severity was minimal or was well fortified on account of being a capital city.

Next, the likelihood of a non-zero death count for city c in month m of year y conditional on a flood is modeled as a function of the socio-economic, geographic and administrative importance variables, along with the proxy for flood severity — all of which were also included in the logistic regression. In addition,

45. One caveat related to the death toll results is the measurement error in the dependent variable. As discussed in Section 2.C, EM-DAT provides deaths and injuries for each disaster, and not the affected cities therein. This is not a concern if the administrative unit affected by the disaster comprises a single city. However, when the death toll is provided for an administrative unit larger than the city, we have made the assumption that total deaths were divided equally between all the cities in our sample that are located within the disaster zone. This implies a certain degree of measurement error in the regressand, as there is bound to be variation in deaths between cities in the same region due to the flood. However, it is important to note that this only makes the estimates less precise, but the coefficients would still remain unbiased. It is also important to note that we round down the number of imputed deaths to the nearest integer because the number of deaths need to be a count variable for the ZINB model. This is required since we have divided the total deaths across a region equally among the cities in that region, and the fatalities may not always be perfectly divisible by the number of cities confined within the region. This rounding down has the added benefit that we reduce the measurement error in deaths count, especially in the case of low deaths. As an example, consider a region consisting of 5 cities. If the total number of deaths in the region after a flood was 1, and this death was divided among all cities in the region, the imputed mortality count in each city would be 0.2. Rounding to the higher integer would imply 5 deaths in total, with each city recording one death. However, 4 of these observations would clearly be inaccurate. On the other hand, by rounding down, we record the number of deaths in each city as 0, and the measurement error is only limited to the one city which experienced the death.

46. Population data from WorldPop (2018) is available at a yearly level from the year 2000 to 2020, while income and built-up area, sourced from GHS-UCDB, is available for the year 2015.

to test our hypothesis that the number of deaths from floods is trending downward over time, we add a year trend, which is similar to the $Year\ Trend_y$ variable in Section 4.A, except for a minor difference. Specifically, we expand the time period of our analysis to 21 years, including all floods in the EM-DAT dataset between January 2000 to December 2020.[47] Therefore, the $Year\ Trend_y$ variable can take the value from 1 to 21, corresponding sequentially to each year in the period 2000 to 2020.

As a robustness check, we also employ a fixed effects panel regression specification to examine whether flood related mortality is falling over time. However, this uses an unbalanced panel as we drop all city-month-year observations which do not experience a flood. In other words, if a city in a given month-year does not suffer from a flood, it is not in the data set. The regression specification takes the following form:

$$\log(1 + Deaths_{cjmy}) = \alpha + \beta_1\ Year\ Trend_y + \beta_2\ ln(Population)_{cjy} + \beta_3\ Precipitation_{cjmy} + \gamma_c + \gamma_m + \epsilon_{cjmy} \quad (4)$$

where γ_c and γ_m are city and month fixed effects, respectively.[48] $ln(Population)_{cjy}$ refers to the natural log of the population of city c in year y. $Precipitation_{cjmy}$ is the monthly precipitation experienced by city c in month m of year y and proxies for the severity of the flood. A positive coefficient indicates that a more severe flood is associated with higher deaths. Standard errors for the ZINB specification as well as the unbalanced panel regressions are clustered at the country and month-year level. Results from both models are presented in Table 4. For the two models, we first present average estimates across all cities, and subsequently check for heterogeneity in time-trend by income groups, reporting estimates separately for cities in high-income (columns [2] and [5]) and low-income countries (columns [3] and [6]).

We find strong evidence consistent with our hypothesis that deaths from floods are falling over time, and this is true across both high- and low-income countries. Focusing on the ZINB model and the sample for all cities in column [1], the coefficient on the time trend is a significant -0.07. This can be interpreted as expected deaths from floods decreasing by 6.8 percent with each passing year, given that other variables in the model are held constant.[49] The corresponding ZINB estimate for cities in high- and low-income countries is a negative and significant 8.4 and 4.7 percent, respectively, indicating that countries across the income spectrum have made progress in reducing mortality from floods. This falling time trend in deaths is also reflected in the estimates of Equation (4), which uses an unbalanced panel. With each additional year, the impact of a flood on deaths is lower by a statistically significant 0.4 percent. Put differently, a flood in the year 2020 was expected to have an 8 percent lower mortality as opposed to a flood in the year 2000, after controlling for time-invariant city specific characteristics and the severity of the flood. The coefficient

47. Starting the analysis in the year 2000 is feasible for the current exercise because unlike previous empirical specifications, this one does not involve using night lights as the outcome variable, data for which was available only post March 2012. We limit the analysis to the year 2020 as yearly data on population was only available up until 2020.

48. We use $\log(1 + Deaths_{cjmy})$ as the dependent variable to account for cities that experienced a flood event, but did not suffer from any loss of human lives. Also, we do not include month-year fixed effects because they would absorb our main regressor of interest, $Year\ Trend_y$.

49. To interpret, note that the coefficient on the $Year\ Trend_y$ represents the difference in the logs of expected deaths for a one unit increase in year, holding all other variables constant. This is equivalent to $\log \frac{deaths_{y+1}}{deaths_y} = -0.07$, which implies that percent change in deaths, $\frac{deaths_{y+1} - deaths_y}{deaths_y}$, equals $\exp(-0.07) - 1$, or 6.8 percent.

for high-income countries (-0.005) is relatively higher than the estimate for low-income countries (-0.003), though the latter is not statistically significant (*p-value*=0.19).

The ZINB model also allows us to shed light on the role of geography, income, population, and flood severity in determining the death count from floods. First, the expected number of deaths post floods in coastal cities across all countries is 2.8 times the expected number of deaths in inland cities (column [1]). Results in Panel B of Table 4, which presents estimates from the zero inflated logit model and predicts membership in the *certain zero* group, are similar. If the flooded city is on the coast, there is a 69 percent lower chance that the deaths would be in the *certain zero* group. The heightened mortality impact of floods in coastal cities is consistent with the results presented in Section 3.C, where we show that coastal cities are highly vulnerable as the negative economic impact of floods was more severe in such cities. Second, higher population is associated with a higher death count after floods, though this is only significant for cities in low-income countries. In such cities, a one standard deviation increase in population, equivalent to approximately 1 million people, is associated with a 44 percent increase in deaths after a flood event (column [3]). Third, richer cities adapt better, though, as before, this also only holds true for cities within low-income countries. The coefficient on $ln(GDP/capita_{cj})$ for this subgroup is a negative and significant 0.45, which implies that a one standard deviation increase in income leads to a 36 percent fall in the count of deaths (column [3]).[50] This result, when read in conjunction with the statistically insignificant estimate of income in high income countries (column [2]), supports the hypothesis that the relationship between income and damage caused by flooding is non-linear and depends on the stage of economic development (see Kellenberg and Mobarak, 2008). Additionally, in results shown in column [3] of Panel B, we find that a higher population in cities within low-income countries attenuates the probability of being in the *certain zero* group (-0.32), while higher income increases the same probability (+0.83). Finally, flood severity, as proxied by monthly precipitation, is a strong predictor of the count of deaths, a finding consistent across all income groups. A one inch increase in rainfall during the month of the flood in a city within a high-income country is expected to increase death counts by 10 percent (column [2]), while the corresponding magnitude, at 22 percent, is higher in cities within low-income countries (column [3]).

In conclusion, our results across different specifications and income groups suggest that deaths from floods have been falling over the last two decades. Further, cities with a higher GDP per capita are less likely to experience a positive death count when a flood occurs, but conditional on death counts greater than zero, are likely to experience lower mortality. Many Integrated Assessment Models assume that the climate damage function is stationary over time (Pindyck, 2013). We reject this pessimistic hypothesis as we find that richer cities suffer less death and the death gradient with respect to flood events flattens over time.

C Does Repeated Exposure to Flooding Reduce the Marginal Impact of the Next Flood?

The impact of a flood could depend crucially on whether it was an unanticipated, one-off event, or a recurrent and expected occurrence that people had been exposed to in the past. Additionally, repeated

50. A one standard deviation change in GDP per capita across cities in low-income countries is equivalent to a change of US$3,000 in PPP constant 2007 international USD.

Table 4: Effect of Floods on Deaths over Time

	Zero-Inflated Negative Binomial			Unbalanced Panel		
	All	High Income	Low Income	All	High Income	Low Income
	(1)	(2)	(3)	(4)	(5)	(6)
Panel A: Zero-Inflated Count Model						
Year Trend$_y$	−0.070***	−0.088***	−0.048***	−0.004**	−0.005***	−0.003
	(0.022)	(0.030)	(0.018)	(0.002)	(0.001)	(0.002)
ln(Population$_{cjy}$*)*	0.128	0.084	0.237*	0.043***	−0.034	0.042**
	(0.102)	(0.071)	(0.127)	(0.014)	(0.045)	(0.021)
ln(GDP/capita$_{cj}$*)*	−0.238**	0.196	−0.447***			
	(0.118)	(0.137)	(0.134)			
ln(Builtup/km$^2_{cj}$*)*	−0.616**	−0.873***	−0.307			
	(0.267)	(0.243)	(0.222)			
High Income$_j$	0.282					
	(0.379)					
Precipitation$_{cjmy}$	0.167***	0.099***	0.200***	0.003***	0.003***	0.003**
	(0.038)	(0.030)	(0.051)	(0.001)	(0.001)	(0.002)
High Elev.$_{cj}$	0.489*	1.190***	−0.100			
	(0.267)	(0.242)	(0.185)			
Capital$_{cj}$	1.218*	1.764	0.748			
	(0.700)	(1.141)	(0.697)			
Coastal$_{cj}$	1.041***	1.307***	0.830**			
	(0.249)	(0.207)	(0.337)			
Intercept	−2.092	−5.896	−1.324			
	(2.241)	(3.766)	(2.292)			
Panel B: Zero-Inflated Logit Model						
Flood$_{cjmy}$	−5.235***	−2.985	−6.761*			
	(1.812)	(2.836)	(3.525)			
Flood$_{cjmy}$ × *ln(Population*$_{cjy}$*)*	−0.221***	0.080	−0.319**			
	(0.085)	(0.264)	(0.153)			
Flood$_{cjmy}$ × *ln(GDP/capita*$_{cj}$*)*	0.473***	−0.193	0.831*			
	(0.164)	(0.444)	(0.446)			
Flood$_{cjmy}$ × *ln(Builtup/km*$^2_{cj}$*)*	−0.191	−0.696	−0.001			
	(0.255)	(0.974)	(0.217)			
Flood$_{cjmy}$ × *High Income*$_j$	0.445					
	(0.912)					
Flood$_{cjmy}$ × *Precipitation*$_{cjmy}$	0.018	0.019	0.023			
	(0.025)	(0.042)	(0.027)			
Flood$_{cjmy}$ × *High Elev.*$_{cj}$	−0.186	−0.695	0.250			
	(0.476)	(1.069)	(0.310)			
Flood$_{cjmy}$ × *Capital*$_{cj}$	−14.732***	−16.124***	−15.311***			
	(5.025)	(0.902)	(0.889)			
Flood$_{cjmy}$ × *Coastal*$_{cj}$	−1.174*	−1.101	−1.284			
	(0.663)	(1.593)	(0.913)			
Intercept	4.109***	3.711	4.117***			
	(1.403)	(2.326)	(1.562)			
Fixed Effects						
City				Yes	Yes	Yes
Month				Yes	Yes	Yes
Log θ	−3.264	−3.660	−3.127			
	(0.046)	(0.096)	(0.051)			
Log Likelihood	−51,718	−22,204	−28,934			
Num. obs.	2,385,936	1,285,704	1,100,232	134,134	72,832	61,302
Adj. R^2				0.236	0.193	0.247

Notes: Two-way clustered robust standard errors are in parenthesis. $^{***}p < 0.01$; $^{**}p < 0.05$; $^{*}p < 0.1$.
Columns (1) to (3) report estimates from a zero-inflated negative binomial (ZINB) model. As the ZINB model includes two equations, the *Panel B* reports the logit model estimates of the probability that nobody in city c in a given month-year died from a flood. *Panel A* reports the results from the negative binomial regression which predicts the counts of deaths for those city-month-year observations which are not *certain* zeros. The dependent variable in all ZINB regressions is the *Total Deaths*$_{cjmy}$, which is the total deaths due to floods in city c in country j in month m of year y. Columns (4) to (6) report estimates from a fixed-effects panel regression model which drops all city-month-year observations which do not experience a flood. The dependent variable in all unbalanced panel regressions is the log(1 + *Total Deaths*$_{cjmy}$), which is the total deaths due to floods in a city during a given month, but increased by 1 so as to allow us to take the natural log of the count variable in case the number of deaths due to floods were 0. All floods in the EM-DAT dataset between January 2000 to July 2023 were included in the sample. The regressions in columns (1) and (4) include all 9,468 cities in the sample, while columns (2) and (5) only include observations from *High Income* and *Upper Middle Income* countries, and columns (3) and (6) only include observations from *Low Income* and *Lower Middle Income* countries. Logged values of *GDP/capita* and *Builtup area per square km.* pertain to the year 2015. *High Elev*$_{cj}$ is a dummy indicating whether city c in country j has a median elevation that ranks in the top 50th percentile of the distribution of the median elevation across all cities. $Coastal_{cj}$ and $Capital_{cj}$ are dummies that indicate whether city c in country j is a coastal or capital city, respectively. *High Income*$_j$ is a dummy that equals 1 if the country j is a *High Income* or *Upper Middle Income* country based on the World Bank income classification. $Log\theta$ refers to the natural log of the inverse of the dispersion parameter, where high values of the dispersion parameter imply the negative binomial converges to a Poisson distribution. Standard errors are clustered at the country and month-year level.

exposure to flooding can have two countervailing effects. On the one hand, it can foster experience-driven adaptation by incentivizing investment in protective infrastructure which increases resilience, thus reducing the marginal cost of weathering an inundation event. Alternatively, frequent flooding could lead to disinvestment, as the repeat events act as a tax on capital investment, leading to productivity losses (Guiteras et al., 2015). Which effect dominates is an empirical question that we tackle in this section.

To test whether cities that have faced repeated floods are more resilient, we construct two measures of past flood exposure. We use EM-DAT's data on flood occurrences between the period January 2000 to March 2012, *i.e.*, over a 12-year period.[51] First, for each city, we construct a discrete variable, $Exposure_{cj}$, which equals the number of flood events which have impacted city c in nation j between January 2000 and March 2012.[52] Second, we create a dummy variable, $High\ Exposure_{cj}$, that takes the value 1 if city c had above median number of flood events across our sample of 9,468 cities between 2000-2012. We modify Equation (1) and estimate two separate regressions by adding interaction terms $Flood_{cjmy} \times Exposure_{cj}$ and $Flood_{cjmy} \times High\ Exposure_{cj}$ respectively. If repeated flooding drives authorities and citizens to learn from such events and better prepare for future disasters, we would expect the coefficient on the interaction terms to be positive. This would imply that the experience-driven adaptation effect is stronger, resulting in attenuation of the negative effect of floods. Conversely, if recurrent shocks cause a substantial and persistent decline in the productive potential of the city, we expect the interaction terms to be negative. Results are presented in Table 5.

Table 5: Impact of Floods by Past Exposure

	Dependent Variable: $ln(Night\ Lights_{cjmy})$					
	All		**High Income**		**Low Income**	
	(1)	(2)	(3)	(4)	(5)	(6)
$Flood_{cjmy}$	−0.085***	−0.093***	−0.045***	−0.051***	−0.137***	−0.137***
	(0.020)	(0.023)	(0.016)	(0.019)	(0.032)	(0.036)
$Flood_{cjmy} \times Exposure_{cj}$	0.003***		0.002*		0.005***	
	(0.001)		(0.001)		(0.002)	
$Flood_{cjmy} \times High\ Exposure_{cj}$		0.066***		0.041**		0.087***
		(0.023)		(0.019)		(0.033)
Fixed Effects						
City	Yes	Yes	Yes	Yes	Yes	Yes
Country × Month × Year	Yes	Yes	Yes	Yes	Yes	Yes
Num. obs.	1,287,648	1,287,648	693,872	693,872	593,776	593,776
Adj. R^2	0.861	0.861	0.789	0.789	0.804	0.804

Notes: Two-way clustered robust standard errors are in parenthesis. $^{***}p < 0.01$; $^{**}p < 0.05$; $^{*}p < 0.1$.
The dependent variable in all regressions, $ln(Night\ Lights_{cjmy})$, is the natural log of mean light intensity in city c in country j in month m of year y. We have used the cloud mask configuration of the NPP-VIIRS monthly composites, where data contaminated by stray light are removed. Missing data for $ln(Night\ Lights_{cjmy})$ was imputed using Predictive Mean Matching. $Flood_{cjmy}$ is a dummy indicating whether city c in country j was hit by a flood in month m of year y. $Exposure_{cj}$ is a discrete variable that represents the number of floods city c in country j experienced between January 2000 and March 2012. $High\ Exposure_{cj}$ is a dummy variable that equals 1 if the number of flood events in city c in country j between January 2000 and March 2012, were greater than the median number of flood events across all 9,468 cities during this time-frame. Columns (3) and (4) only include observations from *High Income* and *Upper Middle Income* countries, whereas columns (5) and (6) only include observations from *Low Income* and *Lower Middle Income* countries. All regressions include the controls $Storm_{cjmy}$ and $Landslide_{cjmy}$, dummies indicating whether city c in country j was hit by a storm or landslide, respectively, in month m of year y. Two month leads and lags for all three disaster types have also been included as controls. Standard errors are clustered at the country and month-year level.

51. This start date of January 2000 is determined based on EM-DAT's caveat that flood data pre-2000 is subject to reporting biases. The end date of March 2012 is determined based on the availability of VIIRS night lights data — our main outcome of interest — which is available at a monthly level from April 2012.

52. $Exposure_{cj}$ ranges from 0 to 61, with a mean of 7.3 floods per city between January 2000 to March 2012, median of 5 floods per city, and a standard deviation of 7.9.

We find that, on average, cities with a higher prior exposure to floods are significantly better at coping with future shocks. Columns [1] and [2] present results for all 9,468 cities. Estimate of $Flood_{cjmy}$ in column [1] suggests that a city which did not suffer from even a single such event between January 2000 to March 2012 (*i.e.*, $Exposure_{cj}$ equals 0) experiences an 8.5 percent reduction in night lights in the month of a flood. However, the interaction term, $Flood_{cjmy} \times Exposure_{cj}$, is positive and statistically significant with a coefficient equal to 0.0034. The magnitude implies that for a city which was exposed to the median number of floods in the past, the impact is moderated by 1.7 percentage points, or 20 percent. The results in column [2], where we define exposure through a dummy variable, $High\ Exposure_{cj}$, indicate that, on average, cities with below median exposure to floods in the past suffer from a 9.3 percent fall in economic activity. Nevertheless, this deleterious impact is mitigated by 6.6 percentage points, or 71 percent, for cities with above median exposure.

The positive learning channel also dominates when we analyze heterogeneity in the role of past exposure across different income groups. Column [3] focuses on cities in high-income countries. Even though the magnitude of the impact of a flood on cities with no past exposure is lower (-4.5 percent), which is consistent with previous results, the positive effect of past experience with floods is still salient. Economic losses are attenuated by 22 percent for cities exposed to the median number of floods prior to 2012. Cities in low-income countries with no prior familiarity to flooding sustain a 14 percent fall in economic activity after a shock, but the same is reduced by 18 percent in cities with median exposure (column [5]). In a similar vein, estimates using a dummy variable to define high exposure (columns [4] and [6]) indicate that cities in high- and low-income countries that have above median prior experience with flood shocks suffer damages that are 80 percent and 64 percent less, respectively, during an inundation event.

Overall, we find strong evidence, consistent with the *learning-by-doing* channel (Arrow, 1962; Lucas Jr, 1988), that cities faced with repeated flooding cope better with future shocks. This could arise because such cities update their beliefs regarding future flood risk, which increases the perceived marginal benefit of protective infrastructure, leading to any productive capital destroyed in floods rebuilt to withstand future disasters (Patel, 2024). It could also be the case that experience leads to more coordinated disaster management in the future. Either way, we reject the negative hypothesis that recurrent flooding acts as a tax on capital investment. Instead, our results reveal that experience-driven adaptation can increase resilience and reduce the marginal impact of successive floods across cities in both high- and low-income countries.

D ***Migration as an Adaptation Response to Flooding***

Floods act as a negative amenity, forcing the affected population to migrate to safer areas. A large literature has analyzed the role of rural to urban migration as an adaptation response, focusing on agricultural productivity shocks caused by negative weather events in rural areas as a push factor (Gröger and Zylberberg, 2016; Minale, 2018; Albert et al., 2021). Their results show that following inclement weather, rural incomes fall, and households adapt by migrating out. However, the choice set of destination cities may be limited to urban areas with industries (Henderson et al., 2017), and migration may even reduce in low-income countries as people get caught in a poverty trap (Cattaneo and Peri, 2016). A related literature uses

dynamic general equilibrium models to endogenize migration and understand how climate change will impact migration (Burzyński et al., 2022; Kleemans, 2023). Model projections suggest that climate-induced permanent and seasonal migration is likely to increase, though only a small proportion of the affected populace may be able to migrate given the high migration costs (Bryan et al., 2014). In this section, we investigate how flood shocks in urban areas impact migration, and whether flood risk affects population growth rate.

Ex-ante, the direction of the response of migration to flood risk is not clear. Positive migration costs, potential loss of local social capital, and expectations of post-disaster government relief could temper a migration response to floods. Similarly, even though coastal cities are more susceptible to fall in economic activity due to flood shocks (see Section 3.C), they have historically been more productive, and access to the coast acts as a positive amenity. This could induce net in-migration to flood-prone regions, especially if the city also invests in flood protection infrastructure (Boustan et al., 2012).

We start by examining whether cities affected by flood shocks experience out-migration and estimate the following regression equation:

$$ln(Population_{cjy}) = \alpha + \beta_1 Flood_{cj\{y-1\}} + \mathbf{X}_{cj\{y-1\}} + \delta_c + \delta_{jy} + \epsilon_{cjy} \tag{5}$$

where, the dependent variable, $ln(Population)_{cjy}$, is the natural log of population in city c in country j in year y, constructed by aggregating the yearly 1km grid-level population numbers from WorldPop (2018) to the city-year level using shapefiles from GHS-UCDB. $Flood_{cj\{y-1\}}$ is a dummy variable that takes the value 1 if city c in country j was hit by a flood in the previous year. $\mathbf{X}_{cj\{y-1\}}$ represents a vector of city-specific controls, specifically whether the city was affected by storms or landslides in the previous year, and the one period time lag of population. δ_c and δ_{jy} represent city and country-year fixed effects, respectively. The former accounts for time-invariant city level characteristics such as geography, while the latter helps to control for time-varying factors at the country-level, such as GDP growth, which may influence population levels across all cities in the country. Standard errors are clustered at the country and year level. Since population estimates are available only for the years 2000 to 2020, we limit the time period of our analysis to these 21 years. Results are presented in columns [1]-[3] of Table 6.

Our results indicate that migration as an adaptation response to floods is only pertinent among cities in high-income countries. Column [1] reports the results for all 9,468 cities in our sample. Cities exposed to floods in the previous year do not experience, on average, any change in their population, with the estimate on $Flood_{cj\{y-1\}}$ a precisely estimated 0. Next, we estimate Equation (5) separately for cities in high- and low-income countries, with results presented in columns [2] and [3], respectively. A flood in the previous year reduces population in cities in high-income countries by 0.33 percent which, though small in magnitude, is statistically significant.[53] However, for cities in low-income countries, floods do not have any meaningful impact on population, with the estimate a positive but statistically insignificant 0.24 percent (p-$value$ = 0.12).

Next, we use cross-sectional variation in population growth rates to test if cities that have suffered from

53. For a city with the same number of people as the year 2020 mean population across all 5,102 cities in high-income countries, this amounts to an out-migration of approximately 1,100 people.

Table 6: Effect of Floods on Population

Dependent Variable →	$ln(Population_{cjy})$			$\Delta Population_{cj\{2000,2015\}}$		
	All	**High Income**	**Low Income**	**All**	**High Income**	**Low Income**
	(1)	(2)	(3)	(4)	(5)	(6)
$Flood_{cj\{y-1\}}$	0.000	−0.003**	0.002			
	(0.002)	(0.002)	(0.001)			
$No.\ of\ Floods_{cj,\{2000,2015\}}$				−0.004***	−0.006***	−0.001
				(0.001)	(0.001)	(0.003)
Fixed Effects						
City	Yes	Yes	Yes			
Country				Yes	Yes	Yes
Country × Year	Yes	Yes	Yes			
Num. obs.	189,360	102,040	87,320	9,468	5,102	4,366
Adj. R^2	0.994	0.995	0.992	0.291	0.346	0.241

Notes: Clustered robust standard errors are in parenthesis. *** $p < 0.01$; ** $p < 0.05$; * $p < 0.1$.
The dependent variable in columns (1)-(3) is $ln(Population_{cjy})$, which is the natural log of the population of city c in country j in year y. The dependent variable in columns (4)-(6) is $\Delta Population_{cj\{2000,2015\}}$, a continuous variable that represents the growth rate of population in city c in country j between years 2015 and 2000. $Flood_{cj\{y-1\}}$ is a dummy indicating whether city c in country j was hit by a flood in any month of the previous year. $No.\ of\ Floods_{cj}$ is a discrete variable indicating the number of floods that city c in country j was exposed to between 2000 and 2015. Models (2) and (5) only includes observations from *High Income* and *Upper Middle Income* countries, whereas models (3) and (6) only includes observations from *Low Income* and *Lower Middle Income* countries. Models (1)-(3) include as controls the one year lag of population in city c in country j, as well as $Storm_{cj\{y-1\}}$ and $Landslide_{cj\{y-1\}}$, dummies indicating whether city c was hit by a storm or landslide, respectively, in the previous year. Controls in models (4)-(6) include the year 2000 values of GDP per capita, Builtup Area (per sq. km) and population, and the growth rate between the years 2000 and 2015 of GDP per capita and Builtup Area. Also included as controls are $High\ Elev_{cj}$, which is a dummy indicating whether city c in country j has a median elevation that ranks in the top 50th percentile of the distribution of the median elevation across all cities, *i.e.*, greater than 154 meters, and $Coastal_{cj}$ and $Capital_{cj}$, which are dummies that indicate whether city c in country j is a coastal or capital city, respectively. Standard errors are clustered at the country and year level in models (1)-(3) and at the country level in models (4)-(6).

more floods experienced lower population growth. Using data from 2000 to 2015, we run the following regression specification:[54]

$$\Delta Population_{cj,\{2000,2015\}} = \alpha + \beta\ (No.\ of\ Floods_{cj,\{2000,2015\}}) + \mathbf{X}_{cj} + \delta_j + \epsilon_{cj} \tag{6}$$

where, the dependent variable, $\Delta Population_{cj,\{2000,2015\}}$, is the growth rate of population in city c in country j between years 2000 and 2015, while the regressor of interest is $No.\ of\ Floods_{cj,\{2000,2015\}}$, which equals the total number of floods that affected city c in the same 15 year period. We control for the year 2000 values of GDP per capita, built-up area (per square km.) and population, the growth rate of GDP per capita and built-up area between 2000 and 2015, geographic and topographic characteristics of the city as well as its administrative importance. Finally, we add country fixed effects (δ_c) to account for time-invariant factors common to all cities in a country. Columns [4]-[6] of Table 6 presents the results, first at the aggregate level, and then divided by income groups.

The pattern of the findings is similar to the migration results: only in high-income countries is the population growth rate significantly lower for cities that experienced a higher frequency of floods. As reflected in column [5], one additional flood between 2000 and 2015 in a city within a high-income country reduces the population growth rate during this period by a statistically significant 0.62 percentage points.

54. This specification uses city-wide data on population, GDP, and built-up area from GHS-UCDB. The latest year for which information on all these three variables is available for our sample cities is 2015. While the earliest year available is 1975, we are constrained by the fact that pre-2000 data on floods reported by EM-DAT is subject to reporting biases. Both these factors require us to limit the time period of our analysis between 2000 and 2015.

Given that the median number of floods between 2000 and 2015 in such cities was 5, this represents a 3.1 percentage points lower growth rate for a city experiencing the median flood frequency. For context, the median growth rate of population in cities within developed nations during this time period was 8.9 percent. Therefore, a city growing at the median growth rate and suffering from the median number of floods would see its growth rate fall by more than a third. Unlike the migration results, we find evidence for the negative correlation between growth rate of population and number of floods even for cities in low-income countries. However, the effect (-0.089 percentage points, *p-value*=0.73) is small in magnitude and statistically insignificant.[55]

Migration, thus, represents an important margin of adjustment, but only for households in richer nations. Given the large economic losses due to floods in developing countries, it is surprising that our results, as well as recent empirical work on disasters, show that incumbents in poorer nations tend to remain in the shocked area (Kocornik-Mina et al., 2020).[56] Potential explanations include positive migration costs and built up local social capital (Glaeser et al., 2002). Moreover, natural disasters can trigger huge federal transfer payments. The expectation of such ex-post relief can create a moral hazard effect that acts to anchor people to risky places. Finally, existing residents, especially the poor, may find it difficult to finance the migration costs to move to a safer city. Our results, therefore, shed light on the unequal impacts of climate change, as the poor are exposed to greater risks from climate but their choice set of responses may be limited.

E Do High Levels of GDP/Capita and Critical Infrastructure Improve Resilience?

Economically productive cities are more likely to cope better when climate disasters strike. This increased resilience could arise due to various factors strongly correlated with a high GDP per capita such as higher levels of human capital, better compliance with and effective enforcement of building codes and flood-risk zones, and high quality of critical infrastructure such as roads and hospitals, among others. To test this hypothesis empirically, we can use city-level GDP and population in 2015, provided by GHS-UCDB, to construct estimates of GDP per capita at the city level, and analyze whether more productive cities experience a smaller decline in economic activity post a flood.[57] Depending on the specification, we augment Equation (1) by including one of two interaction terms: $Flood_{cjmy} \times ln(GDP/capita)_{cj}$ or $Flood_{cjmy} \times High\ GDP/capita_{cj}$. The variable $ln(GDP/capita)_{cj}$ is a continuous and time-invariant variable measuring the natural log of per capita GDP in 2015 (in PPP constant 2007 US$) in city c in country j, while $High\ GDP/capita_{cj}$ is a dummy variable that equals 1 if the per capita income of city c in country j is in the top 50^{th} percentile of the distribution of per capita GDP across all the 9,468 cities in our sample.[58]

55. As a robustness check, we run the same specification as Equation (6) using the yearly population and flood numbers from 2000 to 2020, available from WorldPop (2018) and EM-DAT, respectively, but without controlling for the growth rate of GDP per capita and built-up area as the same were not available post 2015. The results are similar both in direction and magnitude.

56. Recent empirical research studying localized shocks, such as bombings, generally does not find strong evidence of population decline in affected areas (Davis and Weinstein, 2002; Miguel and Roland, 2011). However, unlike bombed territories, flood prone areas are likely to be repeatedly shocked.

57. Note that this empirical exercise is different from the heterogeneity analysis by income reported in previous sections (cities in high- and low-income countries), because there exist cities with a high GDP per capita even in low-income countries.

58. One could be concerned about the limited overlap between a World Bank income classification of Lower-Middle income and Low income, and being above the median of the distribution of GDP per capita across all 9,468 cities. However, 14 percent of

A positive coefficient on the interaction term would indicate that more productive cities are resilient, and are able to mitigate flood related losses.

We are also able to directly test whether cities with a higher intensity of critical infrastructure are more resilient to flood shocks. To this end, we use the Critical Infrastructure Spatial Index (CISI) developed by Nirandjan et al. (2022), which is a continuous measure ranging between 0 and 1 available at a resolution of 0.10×0.10 degrees. Higher values of the index indicate greater spatial intensity of 39 different infrastructure types pertaining to energy, water, waste, transportation, telecommunications, education, and health as of November 2020 (see Section 2.G for additional details). Similar to the empirical exercise before with GDP per capita, we include, depending on specification, interaction terms $Flood_{cjmy} \times CISI_{cj}$ or $Flood_{cjmy} \times High\ CISI_{cj}$ in Equation (1). $CISI_{cj}$ is a weighted average of the CISI of all grids that lie within a city boundary, with weights equal to the area of the grid that is within the city boundary. $High\ CISI_{cj}$ is a dummy variable that takes the value 1 if the weighted CISI of city c in country j is in the top 50th percentile of the distribution of weighted CISI across all cities.[59] Results are presented in Table 7, with columns [1] and [2] reporting estimates from the GDP per capita regressions, and columns [3] and [4] detailing the critical infrastructure results.[60]

The results across all specifications consistently suggest that economically productive cities with good critical infrastructure are more resilient to flood shocks, with the impact on night lights attenuated by a significant proportion in such urban areas. The coefficient on the interaction term, $Flood_{cjmy} \times ln(GDP/capita)_{cj}$, in column [1] is a positive and statistically significant 0.22. This indicates that for every 10 percent increase in GDP per capita, the impact of a flood shock on night luminosity decreases by about 0.21 percent. Stated differently, a city in the 25th percentile of GDP per capita will experience a 5.5 percent fall in economic activity after a flood, as opposed to a 2.6 percent fall for a city in the 75th percentile of income.[61] The result is near identical when we change the interaction term to $Flood_{cjmy} \times High\ GDP/capita_{cj}$ in column [2], with the coefficient a positive and statistically significant 0.041. This indicates that although a city in the bottom 50th percentile of GDP per capita suffers, on average, from a 6.6 percent fall in night lights post a flood, this negative impact is attenuated by 4.1 percentage points for cities with a per capita income greater than the median, or US$5,600.

Critical infrastructure also plays a crucial role in improving resilience. This is evidenced by the positive and significant coefficient on the interaction term, $Flood_{cjmy} \times CISI_{cj}$, in column [3].[62] To interpret the estimate, note that CISI among our sample of cities ranges from 0 to 0.49. Therefore, a city at the 25th percentile of the CISI distribution will suffer from a 5.2 percent fall in night lights. This negative effect is

cities in Lower-Middle income and Low income countries (621 out of 4,366 cities) have a higher per capita GDP than the median. Similarly, 19 percent of the cities in Upper-Middle and High income countries (989 out of 5,102 cities) have a per capita GDP that is below the median.

59. Approximately 34 percent of cities in Lower-Middle income and Low income countries (1,499 out of 4,366 cities) have a higher weighted CISI value than the median of the weighted CISI distribution across all 9,468 cities in our sample. Correspondingly, 36 percent of the cities in Upper-Middle and High income countries (1,868 out of 5,102 cities) have a weighted CISI that is below the median.

60. Because we include city fixed effects (γ_c), the level effects of GDP per capita and CISI variables are swept out and the coefficient on these variables cannot be estimated.

61. This is equivalent to an increase in per capita GDP from US$2,700 to US$10,000.

62. CISI data was unavailable for Diu, a coastal town in the union territory of Dadra and Nagar Haveli and Daman and Diu in north-western India. This is why the number of observations drop in columns [3] and [4] of Table 7.

Table 7: Adaptation Through Productivity and Critical Infrastructure

	Dependent Variable: $ln(Night\ Lights_{cjmy})$			
	(1)	(2)	(3)	(4)
$Flood_{cjmy}$	−0.229***	−0.066***	−0.058***	−0.053***
	(0.086)	(0.013)	(0.015)	(0.014)
$Flood_{cjmy} \times ln(GDP/capita_{cj})$	0.022**			
	(0.010)			
$Flood_{cjmy} \times High\ GDP/capita_{cj}$		0.041***		
		(0.012)		
$Flood_{cjmy} \times CISI_{cj}$			0.232**	
			(0.114)	
$Flood_{cjmy} \times High\ CISI_{cj}$				0.021**
				(0.010)
Fixed Effects				
City	Yes	Yes	Yes	Yes
Country × Month × Year	Yes	Yes	Yes	Yes
Num. obs.	1,287,648	1,287,648	1,287,512	1,287,512
Adj. R^2	0.861	0.861	0.861	0.861

Notes: Two-way clustered robust standard errors are in parenthesis. *** $p < 0.01$; ** $p < 0.05$; * $p < 0.1$.
The dependent variable in all regressions, $ln(Night\ Lights_{cjmy})$, is the natural log of mean light intensity in city c in country j in month m of year y. We have used the cloud mask configuration of the NPP-VIIRS monthly composites, where data contaminated by stray light are removed. Missing data for $ln(Night\ Lights_{cjmy})$ was imputed using Predictive Mean Matching. $Flood_{cjmy}$ is a dummy indicating whether city c in country j was hit by a flood in month m of year y. $ln(GDP/capita_{cj})$ refers to the natural log of city c's GDP per capita, which is measured in PPP US$ (2007) and pertains to the year 2015. $High\ GDP/capita_{cj}$ is a dummy indicating whether city c has a GDP per capita that ranks in the top 50th percentile of the distribution of GDP per capita across all cities *i.e.* cities with a GDP per capita above US$5,567. $CISI_{cj}$ refers to the weighted average of the Critical Infrastructure Spatial Index (between 0 and 1) across all grid cells that fall within a city boundary, with weights equal to the area of the grid that falls within the city boundary. $High\ CISI_{cj}$ is a dummy indicating whether city c has a weighted CISI that ranks in the top 50th percentile of the distribution of CISI across all cities *i.e.* cities with a weighted CISI above 0.051. All regressions include the controls $Storm_{cjmy}$ and $Landslide_{cjmy}$, dummies indicating whether city c was hit by a storm or landslide, respectively, in month m of year y. Two month leads and lags for all three disaster types have also been included as controls. Standard errors are clustered at the country and month-year level.

mitigated by 33 percent for cities in the 75th percentile of the distribution, with night lights falling by 3.6 percent for such cities.[63] Results from changing the interaction term to $Flood_{cjmy} \times High\ CISI_{cj}$ in column [4] lend further credence to our hypothesis. The estimated coefficient is a positive and significant 0.021. This signifies that the 5.3 percent reduction in economic activity in the aftermath of a flood in cities in the bottom 50th percentile of the CISI distribution ($\leq$ 0.051) is alleviated, on average, by 2.1 percentage points, or 40 percent, for cities with CISI in the top half of the distribution. Heterogeneous impacts by country income groups for GDP per capita and CISI measures are presented in Appendix D in Table D.1 and Table D.2, respectively. Although the results go in the hypothesized direction (a positive coefficient on the interaction terms) for cities in both high- and low-income countries, they are only significant for the former sub-group.

In summary, our results document that economically productive cities are more resilient to flood shocks, with critical infrastructure assets fundamental in aiding this adaptation. Economic development not only helps to finance the construction and maintenance of high-quality infrastructure, but also im-

63. The 25th and 75th percentile of CISI distribution equals 0.024 and 0.095, respectively.

proves a governments' ability to enforce regulations and target disaster relief which, in turn, provides implicit insurance against floods.

F *Do Dams Protect Cities?*

Dams have long played a predominant role in river water management, and their flood mitigation potential is considered to be sufficient justification for large investments in their construction. This has resulted in approximately half of the world's rivers being regulated by dams, with less than a quarter flowing uninterrupted to the oceans (World Commission on Dams, 2000; Grill et al., 2019). However, dams could have unintended consequences for cities downstream, hampering their effectiveness in alleviating the impact of floods. For instance, the implicit insurance provided by them could crowd out private investment in adaptation, or could induce greater development and lock-in capital and people in flood-prone areas, thus exacerbating the impact of floods. In this section, we examine several hypothesis related to dams and floods, including whether cities protected by dams experience *i)* more flood events; *ii)* higher population growth, and *iii)* lower reductions in economic activity post floods. We classify a city as being protected by a dam if it has a river segment within a 500m buffer of its boundaries, and if that river segment has a dam upstream.[64] As the summary statistics in Table B.2 show, 35 percent of cities in high-income countries are protected by dams, while the number is 14 percent for cities in low-income nations.

We start by examining whether the likelihood of flood events and investment in dams are related, and estimate the following linear regression to analyze this formally:

$$Floods_{cjmy} = \alpha + \beta Dams_{cj} + \mathbf{X}_{cj} + \delta_{jmy} + \epsilon_{cjmy} \tag{7}$$

where $Floods_{cjmy}$ is a dummy variable that equals 1 if city c in country j experienced a flood in month m of year y, and $Dams_{cj}$ is a time-invariant dummy that equals 1 if city c in country j is protected by a dam.[65] $\mathbf{X}_{cj}$ is a vector of city-specific controls and includes the year 2015 values for built-up area and GDP per capita, as well as dummies for high-elevation, coastal location, and political importance, *i.e.*, whether city c is the administrative capital of country j. δ_{jmy} represents country-month-year fixed effects and accounts for time-varying country-level factors such as seasonality in floods. Note that we do not add city fixed effects as including the same would lead to the estimate on dams, our main coefficient of interest, being swept out. Standard errors are clustered at the country and month-year level. Results are presented in columns [1]-[3] of Table 8, with the first column presenting results for all 9,468 cities, and columns [2] and [3] detailing estimates for cities in high- and low-income countries, respectively.

On average across all countries, cities with dams face a 1.1 percentage points higher probability of floods as opposed to cities without dams. Heterogeneity analysis by income points towards effects being larger for high-income countries, with cities with dams in such countries experiencing a 1.3 percentage points (0.74 for cities in low-income countries) higher likelihood of floods as compared to cities without dams. These results are not surprising given that dams are more likely to be placed in areas at greater risk. Furthermore, if dams also prevent some floods from occurring, the coefficient is likely an underestimate.

64. Further details on the data sources and algorithm used to classify a city as protected by dams are detailed in Section 2.H.
65. *GRanD*, the dams dataset used in this paper, does not provide information on the year of construction of the dam.

Table 8: Dams and Adaptation

Dependent Variable →	$Flood_{cjmy}$			$\Delta Population_{cj\{2000,2015\}}$			$ln(Night\ Lights_{cjmy})$		
	All	**High Income**	**Low Income**	**All**	**High Income**	**Low Income**	**All**	**High Income**	**Low Income**
	(1)	(2)	(3)	(4)	(5)	(6)	(7)	(8)	(9)
$Dams_{cj}$	0.011^{**}	0.013^{**}	0.007^{***}	-0.004	-0.032^{***}	0.043			
	(0.005)	(0.005)	(0.002)	(0.013)	(0.012)	(0.028)			
$Flood_{cjmy}$							-0.050^{***}	-0.026^{***}	-0.071^{***}
							(0.012)	(0.006)	(0.017)
$Flood_{cjmy} \times Dams_{cj}$							0.018	0.013^{***}	-0.019
							(0.013)	(0.004)	(0.023)
Fixed Effects									
City							Yes	Yes	Yes
Country × Year				Yes	Yes	Yes			
Country × Month × Year	Yes	Yes	Yes				Yes	Yes	Yes
Num. obs.	2,679,444	1,443,866	1,235,578	9,468	5,102	4,366	1,287,648	693,872	593,776
Adj. R^2	0.385	0.388	0.383	0.287	0.329	0.242	0.861	0.789	0.804

Notes: Clustered robust standard errors are in parenthesis. $^{***}p < 0.01$; $^{**}p < 0.05$; $^{*}p < 0.1$.
The independent variable $Dams_{cj}$ is a dummy that equals 1 if city c in country j: *(i)* has a river segment either within or around a 500m buffer of its boundaries, and; *(ii)* the river segment has a dam upstream. The dependent variable in column (1) is $Flood_{cjmy}$, a dummy indicating whether city c in country j was hit by a flood in month m of year y. The dependent variable in columns [4]-[6] is $\Delta Population_{cj\{2000,2015\}}$, a continuous variable that represents the growth rate of population in city c in country j between years 2015 and 2000. The regressions in columns [1]-[3] include the year 2015 values of $ln(GDP/capita)_{cj}$ and $Builtup\ Area_{cj}$ (per sq. km) as controls. Controls in models (4)-(6) include the year 2000 values of GDP per capita, Builtup Area (per sq. km) and population, and the growth rate between the years 2000 and 2015 of GDP per capita and Builtup Area. Additional controls in models [1]-[6] include the dummy variables for whether city c in country j is either a coastal city, the capital of the country, or is at a high elevation (median elevation that ranks in the top 50^{th} percentile of the distribution of the median elevation across all cities, *i.e.*, greater than 154 meters). The dependent variable in columns [7]-[9], $ln(Night\ Lights_{cjmy})$, is the natural log of mean light intensity in city c in country j in month m of year y. We have used the cloud mask configuration of the NPP-VIIRS monthly composites, where data contaminated by stray light are removed. Missing data for $ln(Night\ Lights_{cjmy})$ was imputed using Predictive Mean Matching. Standard errors are clustered at the country and month-year level in columns [1]-[3] and columns [7]-[9], and at the country level in columns [4]-[6].

Next, we analyze if the population growth rate is different in cities downstream of a dam as opposed to cities not protected by dams. To test this, we use cross-sectional variation in population growth rates to run the following regression specification:

$$\Delta Population_{cj,\{2000,2015\}} = \alpha + \beta Dams_{cj} + \mathbf{X}_{cj} + \delta_j + \epsilon_{cj} \tag{8}$$

where, $\Delta Population_{cj,\{2000,2015\}}$ is the growth rate of population in city c in country j between years 2000 and 2015. We include the same controls as in Equation (7) except that the values for built-up area and GDP per capita are from the base year 2000, we add the base year values for population, and also include the growth rate of GDP per capita and built-up area between 2000 and 2015. We include country fixed effects (δ_j) and cluster standard errors at the country level. Results are presented in columns [4]-[6] of Table 8.

We find that in high-income countries, cities protected by dams have a significantly lower population growth rate as compared to cities without dams, but no such differences across protected and unprotected cities exist in low-income countries. Estimates in column [4] include all 9,468 urban extents, and indicate that, on average, cities protected by dams do not have a statistically significant difference in population growth rate. However, heterogeneity analysis by income reveals that for cities downstream of dams in developed economies, the population growth rate is lower by a significant 3.2 percentage points as compared to growth rates in unprotected urban areas within this income subgroup (column [5]). This amounts to a 31 percent lower growth rate when compared to the median population growth of 10 percent between 2000 and 2015 in cities without dams within high-income nations. In contrast to protected cities in rich countries, their low-income country counterparts witnessed a 4.3 percent higher population growth rate, but the estimates are noisy and not statistically significant (p-$value$=0.12, column [6]).

The final part of our analysis tests the adaptation hypothesis by examining whether dams are able to mitigate the economic losses from floods. To estimate this, we add the interaction term $Dams_{cj} \times Flood_{cjmy}$ in Equation (1). The coefficient on this term signifies the magnitude by which the presence of a dam upstream attenuates the impact of the floods on economic activity in cities. Results are presented in columns [7]-[9] of Table 8.

We find that the effectiveness of dams as an adaptation investment is limited to only cities in high-income countries. Column [7] presents results for all cities. A flood leads to a significant 5.0 percent fall in night lights in cities not protected by dams, but this negative impact is mitigated by 1.8 percentage points, or 36 percent, in cities downstream of a dam. This effect, though, is not statistically significant at conventional levels with the p-$value$ on the interaction term equal to 0.17. However, heterogeneity analysis by income suggests that the null result may be driven by the fact that estimates of adaptation effectiveness go in opposite direction in high- and low-income countries. As column [8] shows, in unprotected cities in high-income countries, a flood causes economic activity to reduce by 2.6 percent, but the effect is attenuated by a significant 1.3 percentage points, or 49 percent, in protected cities.[66] On the other hand, estimates in column [9] suggest that cities downstream of a dam in low-income countries are worse off in a flood, with damages amplified by an additional 1.9 percentage point over and above the 7.1 percent negative

66. Using a linear hypothesis test, we fail to reject the null hypothesis that the 1.3 percent fall in night lights post floods in cities protected by dams in high-income countries is not statistically different from 0.

impact detected in unprotected cities. However, the estimate on the interaction term is not statistically significant (*p-value*=0.41). Thus, we find mixed evidence on the potential of dams to mitigate losses, with the attenuation effect only observed for high-income countries.

In summary, our results suggest that cities protected by dams suffer from higher number of floods, and dams offer protection from flood related economic losses but only in cities within high-income countries. In spite of this implicit protection offered by dams to downstream cities in developed countries, such urban areas have experienced a lower population growth rate. However, given that the presence of a dam upstream may be endogenous to the city's wealth, our results only provide suggestive evidence of the effectiveness of dams.

5 Conclusion

In his Nobel Prize winning research on the economics of climate change, William Nordhaus emphasized the feedback loop between how economic growth raises the concentration of global greenhouse gas emissions and how the rise of this stock externality has a causal effect on global consumption (Nordhaus, 2019). In his core research model, the climate damage function is assumed to be a stationary equation. As the world's average temperature increases, consumption declines by a deterministic amount. To simplify the analysis, his approach did not allow for adaptation progress over time or for resilience productivity differentials between rich and poor nations at a point in time.

We have created a unique global city-level panel data set covering 3,931 flood events from 2000 to 2023, and have tested and rejected this key modelling assumption. This paper documents heterogeneous effects of floods on urban economic activity across 9,468 cities in high- and low-income countries, and provides reduced-form evidence of adaptation to flood risks at a global scale. We find that a flood event is associated with a 4.5 percent decline, on average, in mean night lights of cities during the month of the disaster; cities in low-income countries see a decline of 7.5 percent whereas cities in high-income countries experience a much smaller decline of 2.1 percent. Furthermore, non-capital cities and coastal cities in developing countries are worse off after a flood shock, pointing to resource constraints, weak state capacity, and unresponsive private capital as conceivable reasons for the outsized impacts suffered by these places against floods. Conversely, effective zoning of flood-risk areas and implementation of building codes, well-functioning critical infrastructure, and higher demand and private capacity for protection against floods may be some reasons why cities in high-income countries see lower impact of floods on economic activity. Interestingly, we find that the negative impact of floods is short-lived as the economic activity in cities across both high- and low-income countries recovers to pre-flood levels almost immediately.

Moving forward, as flood events become more frequent, the extent of flood damage in urban areas will depend on whether the climate damage function is flattening over time owing to successful public and private adaptation. We document that the sensitivity of floods on economic activity and mortality is declining over time. The paper then tests several place-based adaptation hypotheses, specifically the role of migration, prior experience with flooding, income, critical infrastructure, and flood-protection in mitigating damage from floods in cities. We note three important findings in this regard. First, we find

evidence of experience-driven adaptation, with cities in both high- and low-income countries which were exposed to recurrent inundation events in the past sustaining lower economic damages from subsequent floods. Repeated shocks could lead to building back better — allowing productive assets to withstand future shocks — as well as to increased government investments in early warning systems, flood mapping, and post-disaster relief.

Second, our results indicate that migration is an adaptation response for populace residing in cities in high-income countries but not in low-income countries. The decision to migrate to a safer location is a function of place-based amenities at the origin, losses from and risk of floods at the origin, cost of moving (including social cost), and employment opportunities, wages and rents in the safer location. The lack of evidence on migration in low-income countries suggests either that households value the amenities in risky places highly, the cost of migrating is prohibitive relative to incomes, or safer locations have lower employment opportunities and wages. Further, governments need to consider the unintended consequences of post-disaster transfers, which could induce people to stay put in risky places.

Third, public investment in critical infrastructure and flood-protection in the form of dams is effective in attenuating the effect of floods, but as with migration, this is only true for cities in richer countries. In low-income countries, cities with a higher intensity of critical infrastructure do experience a lower impact of floods, and cities downstream from a dam are worse off post-floods, but neither effect is statistically significantly different from zero. This suggests that critical infrastructure, though available, may be of lower quality or poorly maintained due to funding constraints, and that dams may be crowding out private investment in self-protection.

Our results have important implications for climate justice as we show that poorer places suffer disproportionately more and are slower to adapt, with certain menu of adaptation options either unavailable or ineffective. The reasons driving these differences merits further research. Shi et al. (2015) point out that strong political leadership, high municipal expenditures, and awareness about climate change are associated with adaptation planning among environmentally progressive cities. Poorer nations suffer from poor urban planning and lack of investment in infrastructure. A large proportion of the urban population in such nations lives in slum settlements, which feature low-quality buildings and are primarily located in flood-risk areas. Despite this, much of the urban population growth in developing countries over the last two decades has been in slums (Marx et al., 2013). We conjecture that all these factors could potentially contribute to the large income-based heterogeneity in the impact of floods and adaptation that we document. Detailed flood maps coupled with knowledge of high- and low-income areas within each city could help to shed light on the mechanisms behind the differences.

Finally, a fruitful area of further research involves analyzing the interplay between how private and public decisions jointly determines disaster resilience. In this regard, the Ehrlich and Becker (1972) framework offers a model for improving our understanding of producing resilience. In cases where governments anticipate that resilience infrastructure investments could actually discourage private adaptation efforts — the crowding out effect induced by "climate proofing" an area — the government must consider introducing complementary policies to limit this substitution effect.

References

Adger, W Neil, Suraje Dessai, Marisa Goulden, Mike Hulme, Irene Lorenzoni, Donald R Nelson, Lars Otto Naess, Johanna Wolf, and Anita Wreford. 2009. "Are There Social Limits to Adaptation to Climate Change?" *Climatic Change* 93:335–354. (Cited on pages 4, 31).

Adger, W Neil, Terry P Hughes, Carl Folke, Stephen R Carpenter, and Johan Rockstrom. 2005. "Social-Ecological Resilience to Coastal Disasters." *Science* 309 (5737): 1036–1039. (Cited on page 28).

Albert, Christoph, Paula Bustos, and Jacopo Ponticelli. 2021. *The Effects of Climate Change on Labor and Capital Reallocation.* Technical report. National Bureau of Economic Research. (Cited on page 37).

Anttila-Hughes, Jesse, and Solomon Hsiang. 2013. "Destruction, Disinvestment, and Death: Economic and Human Losses Following Environmental Disaster." *Available at SSRN 2220501,* (cited on page 6).

Aragón, Fernando M, Francisco Oteiza, and Juan Pablo Rud. 2021. "Climate change and agriculture: subsistence farmers' response to extreme heat." *American Economic Journal: Economic Policy* 13 (1): 1–35. (Cited on page 7).

Arrow, Kenneth J. 1962. "The Economic Implications of Learning by Doing." *The Review of Economic Studies* 29 (3): 155–173. (Cited on page 37).

Azur, Melissa J, Elizabeth A Stuart, Constantine Frangakis, and Philip J Leaf. 2011. "Multiple Imputation by Chained Equations: What is it and How Does it Work?" *International Journal of Methods in Psychiatric Research* 20 (1): 40–49. (Cited on page 12).

Balboni, Clare, Johannes Boehm, and Mazhar Waseem. 2023. *Firm Adaptation and Production Networks: Structural Evidence from Extreme Weather Events in Pakistan.* Technical report. Center for Economic and Policy Research. (Cited on page 7).

Balboni, Clare Alexandra. 2019. "In Harm's Way? Infrastructure Investments and the Persistence of Coastal Cities." PhD diss., London School of Economics and Political Science. (Cited on pages 4, 26).

Barbier, Edward B. 2015. "Climate Change Impacts on Rural Poverty in Low-Elevation Coastal Zones." *Estuarine, Coastal and Shelf Science* 165:A1–A13. (Cited on page 28).

Barreca, Alan, Karen Clay, Olivier Deschenes, Michael Greenstone, and Joseph S Shapiro. 2016. "Adapting to climate change: The remarkable decline in the US temperature-mortality relationship over the twentieth century." *Journal of Political Economy* 124 (1): 105–159. (Cited on page 7).

Beyer, Robert, Yingyao Hu, and Jiaxiong Yao. 2022. "Measuring Quarterly Economic Growth from Outer Space," (cited on page 11).

Bodner, Todd E. 2008. "What Improves with Increased Missing Data Imputations?" *Structural Equation Modeling: A Multidisciplinary Journal* 15 (4): 651–675. (Cited on page 13).

Bohra-Mishra, Pratikshya, Michael Oppenheimer, and Solomon M Hsiang. 2014. "Nonlinear Permanent Migration Response to Climatic Variations but Minimal Response to Disasters." *Proceedings of the National Academy of Sciences* 111 (27): 9780–9785. (Cited on page 7).

Boulange, Julien, Naota Hanasaki, Dai Yamazaki, and Yadu Pokhrel. 2021. "Role of Dams in Reducing Global Flood Exposure Under Climate Change." *Nature Communications* 12 (1): 417. (Cited on page 17).

Boustan, Leah Platt, Matthew E Kahn, and Paul W Rhode. 2012. "Moving to Higher Ground: Migration Response to Natural Disasters in the Early Twentieth Century." *American Economic Review* 102 (3): 238–44. (Cited on pages 6, 38).

Brunner, Manuela I, Daniel L Swain, Raul R Wood, Florian Willkofer, James M Done, Eric Gilleland, and Ralf Ludwig. 2021. "An Extremeness Threshold Determines the Regional Response of Floods to Changes in Rainfall Extremes." *Communications Earth & Environment* 2 (1): 173. (Cited on page 31).

Bryan, Gharad, Shyamal Chowdhury, and Ahmed Mushfiq Mobarak. 2014. "Underinvestment in a Profitable Technology: The Case of Seasonal Migration in Bangladesh." *Econometrica* 82 (5): 1671–1748. (Cited on page 38).

Bunten, Devin Michelle, and Matthew E Kahn. 2017. "Optimal Real Estate Capital Durability and Localized Climate Change Disaster Risk." *Journal of Housing Economics* 36:1–7. (Cited on page 7).

Burke, Marshall, Solomon M Hsiang, and Edward Miguel. 2015. "Global Non-Linear Effect of Temperature on Economic Production." *Nature* 527 (7577): 235–239. (Cited on page 6).

Burke, Marshall, Mustafa Zahid, Mariana CM Martins, Christopher W Callahan, Richard Lee, Tumenkhusel Avirmed, Sam Heft-Neal, Mathew Kiang, Solomon M Hsiang, and David Lobell. 2024. *Are We Adapting to Climate Change?* Technical report. National Bureau of Economic Research. (Cited on pages 1, 6).

Burlig, Fiona, Amir Jina, Erin M Kelley, Gregory V Lane, and Harshil Sahai. 2024. *Long-Range Forecasts as Climate Adaptation: Experimental Evidence from Developing-Country Agriculture.* Technical report. National Bureau of Economic Research. (Cited on page 7).

Burzyński, Michał, Christoph Deuster, Frédéric Docquier, and Jaime De Melo. 2022. "Climate Change, Inequality, and Human Migration." *Journal of the European Economic Association* 20 (3): 1145–1197. (Cited on page 38).

Cattaneo, Cristina, and Giovanni Peri. 2016. "The migration response to increasing temperatures." *Journal of development economics* 122:127–146. (Cited on page 37).

Cavallo, Eduardo, Sebastian Galiani, Ilan Noy, and Juan Pantano. 2013. "Catastrophic natural disasters and economic growth." *Review of Economics and Statistics* 95 (5): 1549–1561. (Cited on page 14).

Chen, H, H Oudrari, C Sun, T Schwarting, and X Xiong. 2018. "Preliminary Study of JPSS-1/NOAA-20 VIIRS Day-Night Band Straylight Characterization and Correction Methods." In *Image and Signal Processing for Remote Sensing XXIV,* 10789:68–76. SPIE. (Cited on page 11).

CRED, and UNDRR. 2020. "Human Cost of Disasters: An Overview of the Last 20 Years (2000-2019)." *Technical Report,* (cited on page 1).

Cullen, Zoë, and Ricardo Perez-Truglia. 2023. "The Old Boys' Club: Schmoozing and the Gender Gap." *American Economic Review* 113 (7): 1703–1740. (Cited on page 23).

Davis, Donald R, and David E Weinstein. 2002. "Bones, Bombs, and Break Points: The Geography of Economic Activity." *American Economic Review* 92 (5): 1269–1289. (Cited on page 40).

Delforge, Damien, Valentin Wathelet, Regina Below, Cinzia Lanfredi Sofia, Margo Tonnelier, Joris van Loenhout, and Niko Speybroeck. 2023. "EM-DAT: The Emergency Events Database," (cited on page 13).

Dell, Melissa, Benjamin F Jones, and Benjamin A Olken. 2012. "Temperature shocks and economic growth: Evidence from the last half century." *American Economic Journal: Macroeconomics* 4 (3): 66–95. (Cited on page 6).

Deryugina, Tatyana. 2011. *The dynamic effects of hurricanes in the US: The role of non-disaster transfer payments.* JSTOR. (Cited on page 7).

Deryugina, Tatyana, Laura Kawano, and Steven Levitt. 2018. "The Economic Impact of Hurricane Katrina on its Victims: Evidence from Individual Tax Returns." *American Economic Journal: Applied Economics* 10 (2): 202–233. (Cited on page 6).

Deschênes, Olivier, and Michael Greenstone. 2007. "The Economic Impacts of Climate Change: Evidence from Agricultural Output and Random Fluctuations in Weather." *American Economic Review* 97 (1): 354–385. (Cited on page 6).

Desmet, Klaus, Robert E Kopp, Scott A Kulp, Dávid Krisztián Nagy, Michael Oppenheimer, Esteban Rossi-Hansberg, and Benjamin H Strauss. 2021. "Evaluating the Economic Cost of Coastal Flooding." *American Economic Journal: Macroeconomics* 13 (2): 444–486. (Cited on page 6).

Desmet, Klaus, and Esteban Rossi-Hansberg. 2015. "On the Spatial Economic Impact of Global Warming." *Journal of Urban Economics* 88:16–37. (Cited on page 6).

Donaldson, Dave, and Adam Storeygard. 2016. "The View from Above: Applications of Satellite Data in Economics." *Journal of Economic Perspectives* 30 (4): 171–98. (Cited on page 10).

Dow, Kirstin, Frans Berkhout, Benjamin L Preston, Richard JT Klein, Guy Midgley, and M Rebecca Shaw. 2013. "Limits to Adaptation." *Nature Climate Change* 3 (4): 305–307. (Cited on page 31).

Ehrlich, Isaac, and Gary S Becker. 1972. "Market insurance, self-insurance, and self-protection." *Journal of Political Economy* 80 (4): 623–648. (Cited on page 47).

Elliott, Robert JR, Eric Strobl, and Puyang Sun. 2015. "The local impact of typhoons on economic activity in China: A view from outer space." *Journal of Urban Economics* 88:50–66. (Cited on page 6).

Elvidge, Christopher D, Kimberly Baugh, Mikhail Zhizhin, Feng Chi Hsu, and Tilottama Ghosh. 2017. "VIIRS Night-Time Lights." *International Journal of Remote Sensing* 38 (21): 5860–5879. (Cited on page 10).

Elvidge, Christopher D, Kimberly E Baugh, Mikhail Zhizhin, and Feng-Chi Hsu. 2013. "Why VIIRS Data are Superior to DMSP for Mapping Nighttime Lights." *Proceedings of the Asia-Pacific Advanced Network* 35 (0): 62. (Cited on page 10).

Fairweather, Daryl, Matthew E Kahn, Robert D Metcalfe, and Sebastian Sandoval Olascoaga. 2024. *Expecting Climate Change: A Nationwide Field Experiment in the Housing Market.* Technical report. National Bureau of Economic Research. (Cited on page 7).

Ferdous, Md Ruknul, Giuliano Di Baldassarre, Luigia Brandimarte, and Anna Wesselink. 2020. "The Interplay Between Structural Flood Protection, Population Density, and Flood Mortality Along the Jamuna River, Bangladesh." *Regional Environmental Change* 20 (1): 1–9. (Cited on page 7).

Florczyk, Aneta J, Christina Corbane, Marcello Schiavina, Martino Pesaresi, Luca Maffenini, Michele Melchiorri, Panagiotis Politis, Filip Sabo, Sergio Freire, Daniele Ehrlich, et al. 2019. "GHS Urban Centre Database 2015, Multitemporal and Multidimensional Attributes, R2019A." *European Commission, Joint Research Centre (JRC),* (cited on pages 8, 66).

Gesch, Dean B, Kristine L Verdin, and Susan K Greenlee. 1999. "New Land Surface Digital Elevation Model Covers the Earth." *Eos, Transactions American Geophysical Union* 80 (6): 69–70. (Cited on page 16).

Gibson, John, Susan Olivia, and Geua Boe-Gibson. 2020. "Night Lights in Economics: Sources and Uses." *Journal of Economic Surveys* 34 (5): 955–980. (Cited on page 10).

Gibson, John, Susan Olivia, Geua Boe-Gibson, and Chao Li. 2021. "Which Night Lights Data Should We Use in Economics, and Where?" *Journal of Development Economics* 149:102602. (Cited on page 2).

Glaeser, Edward L, David Laibson, and Bruce Sacerdote. 2002. "An economic approach to social capital." *The Economic Journal* 112 (483): F437–F458. (Cited on page 40).

Grill, Günther, Bernhard Lehner, Michele Thieme, Bart Geenen, David Tickner, Francesca Antonelli, Suresh Babu, Pasquale Borrelli, L Cheng, H Crochetiere, et al. 2019. "Mapping the World's Free-Flowing Rivers." *Nature* 569 (7755): 215–221. (Cited on page 43).

Gröger, André, and Yanos Zylberberg. 2016. "Internal Labor Migration as a Shock Coping Strategy: Evidence from a Typhoon." *American Economic Journal: Applied Economics* 8 (2): 123–153. (Cited on page 37).

Guiteras, Raymond, Amir Jina, and A Mushfiq Mobarak. 2015. "Satellites, Self-Reports, and Submersion: Exposure to Floods in Bangladesh." *American Economic Review* 105 (5): 232–36. (Cited on pages 1, 15, 36).

Güneralp, Burak, İnci Güneralp, and Ying Liu. 2015. "Changing Global Patterns of Urban Exposure to Flood and Drought Hazards." *Global environmental change* 31:217–225. (Cited on page 1).

Hallegatte, Stephane, Colin Green, Robert J Nicholls, and Jan Corfee-Morlot. 2013. "Future Flood Losses in Major Coastal Cities." *Nature Climate Change* 3 (9): 802–806. (Cited on pages 1, 26).

Hanson, Susan, Robert Nicholls, Nicola Ranger, Stéphane Hallegatte, Jan Corfee-Morlot, Celine Herweijer, and Jean Chateau. 2011. "A Global Ranking of Port Cities with High Exposure to Climate Extremes." *Climatic Change* 104:89–111. (Cited on page 26).

Harari, Mariaflavia. 2020. "Cities in Bad Shape: Urban Geometry in India." *American Economic Review* 110 (8): 2377–2421. (Cited on page 10).

Heim, Sven, Kai Hüschelrath, Ulrich Laitenberger, and Yossi Spiegel. 2022. "The Anticompetitive Effect of Minority Share Acquisitions: Evidence from the Introduction of National Leniency Programs." *American Economic Journal: Microeconomics* 14 (1): 366–410. (Cited on page 31).

Henderson, J Vernon, Tim Squires, Adam Storeygard, and David Weil. 2018. "The Global Distribution of Economic Activity: Nature, History, and the Role of Trade." *The Quarterly Journal of Economics* 133 (1): 357–406. (Cited on page 10).

Henderson, J Vernon, Adam Storeygard, and Uwe Deichmann. 2017. "Has Climate Change Driven Urbanization in Africa?" *Journal of Development Economics* 124:60–82. (Cited on page 37).

Henderson, Vernon, Adam Storeygard, and David N Weil. 2011. "A Bright Idea for Measuring Economic Growth." *American Economic Review* 101 (3): 194–99. (Cited on page 9).

Hersbach, H, B Bell, P Berrisford, G Biavati, A Horányi, J Muñoz Sabater, J Nicolas, et al. 2023. "ERA5 Monthly Averaged Data on Single Levels from 1940 to Present." *Copernicus Climate Change Service (C3S) Climate Data Store (CDS)* 10:252–266. (Cited on page 15).

Hornbeck, Richard. 2012. "The Enduring Impact of the American Dust Bowl: Short-and Long-Run Adjustments to Environmental Catastrophe." *American Economic Review* 102 (4): 1477–1507. (Cited on page 6).

Hornbeck, Richard, and Suresh Naidu. 2014. "When the Levee Breaks: Black Migration and Economic Development in the American South." *American Economic Review* 104 (3): 963–990. (Cited on page 6).

Hsiang, Solomon M, and Amir S Jina. 2014. *The Causal Effect of Environmental Catastrophe on Long-Run Economic Growth: Evidence from 6,700 Cyclones.* Technical report. National Bureau of Economic Research. (Cited on page 6).

Hsiang, Solomon M, and Daiju Narita. 2012. "Adaptation to Cyclone Risk: Evidence from the Global Cross-Section." *Climate Change Economics* 3 (02): 1250011. (Cited on page 7).

Hsiao, Allan. 2023. "Sea level rise and urban adaptation in Jakarta." *Working Paper,* (cited on page 7).

———. 2024. "Sea level rise and urban inequality." In *AEA Papers and Proceedings,* 114:47–51. American Economic Association 2014 Broadway, Suite 305, Nashville, TN 37203. (Cited on page 7).

Hsu, Feng-Chi, Kimberly E Baugh, Tilottama Ghosh, Mikhail Zhizhin, and Christopher D Elvidge. 2015. "DMSP-OLS Radiance Calibrated Nighttime Lights Time Series with Intercalibration." *Remote Sensing* 7 (2): 1855–1876. (Cited on page 10).

IPCC. 2001. *Climate Change 2001: The Scientific Basis: Contribution of Working Group I to the Third Assessment Report of the Intergovernmental Panel on Climate Change.* Cambridge University Press. (Cited on page 7).

———. 2022. "Climate Change 2022: Impacts, Adaptation, and Vulnerability." *Contribution of Working Group II to the Sixth Assessment Report of the Intergovernmental Panel on Climate Change,* (cited on pages 1, 7, 29).

Kahn, Matthew E. 2005. "The Death Toll from Natural Disasters: The Role of Income, Geography, and Institutions." *Review of Economics and Statistics* 87 (2): 271–284. (Cited on pages 1, 8, 14, 31).

Kala, Namrata, Clare Balboni, and Shweta Bhogale. 2023. "Climate Adaptation." *VoxDevLit* 7:3. (Cited on page 6).

Kellenberg, Derek K, and Ahmed Mushfiq Mobarak. 2008. "Does Rising Income Increase or Decrease Damage Risk from Natural Disasters?" *Journal of Urban Economics* 63 (3): 788–802. (Cited on pages 8, 34).

Kettner, AJ, G Robert Brakenridge, Guy JP Schumann, and X Shen. 2021. "DFO—Flood Observatory." *Earth Observation for Flood Applications,* 147–164. (Cited on page 19).

Kleemans, Marieke. 2023. "Migration Choice under Risk and Liquidity Constraints." *Working Paper,* (cited on page 38).

Klein, Richard JT, Guy Midgley, Benjamin L Preston, Mozaharul Alam, Frans Berkhout, Kirstin Dow, and M Rebecca Shaw. 2015. "Adaptation Opportunities, Constraints, and Limits." In *Climate Change 2014: Impacts, Adaptation, and Vulnerability. Part A: Global and Sectoral Aspects. Contribution of Working Group II to the Fifth Assessment Report of the Intergovernmental Panel on Climate Change,* 899. Cambridge: Cambridge University Press. (Cited on pages 7, 31).

Kocornik-Mina, Adriana, Thomas KJ McDermott, Guy Michaels, and Ferdinand Rauch. 2020. "Flooded Cities." *American Economic Journal: Applied Economics* 12 (2): 35–66. (Cited on pages 5, 7, 10, 22, 40).

Kummu, Matti, Maija Taka, and Joseph HA Guillaume. 2018. "Gridded Global Datasets for Gross Domestic Product and Human Development Index over 1990–2015." *Scientific Data* 5 (1): 1–15. (Cited on page 9).

Lane, Gregory. 2024. "Adapting to Climate Risk with Guaranteed Credit: Evidence from Bangladesh." *Econometrica* 92 (2): 355–386. (Cited on page 7).

Lehner, B. 2019. "HydroRIVERS Global River Network Delineation Derived from HydroSHEDS Data at 15 Arc-Second Resolution." *Technical Documentation* 1:1–7. (Cited on page 18).

Lehner, Bernhard, and Günther Grill. 2013. "Global River Hydrography and Network Routing: Baseline Data and New Approaches to Study the World's Large River Systems." *Hydrological Processes* 27 (15): 2171–2186. (Cited on page 18).

Lehner, Bernhard, Catherine Reidy Liermann, Carmen Revenga, Charles Vörösmarty, Balazs Fekete, Philippe Crouzet, Petra Döll, Marcel Endejan, Karen Frenken, Jun Magome, et al. 2011. "High-Resolution Mapping of the World's Reservoirs and Dams for Sustainable River-Flow Management." *Frontiers in Ecology and the Environment* 9 (9): 494–502. (Cited on page 18).

Lehner, Bernhard, Kristine Verdin, and Andy Jarvis. 2008. "New Global Hydrography Derived from Spaceborne Elevation Data." *Eos, Transactions American Geophysical Union* 89 (10): 93–94. (Cited on page 18).

Little, Roderick JA. 1988. "Missing-Data Adjustments in Large Surveys." *Journal of Business & Economic Statistics* 6 (3): 287–296. (Cited on page 12).

Lloyd, Christopher T, Heather Chamberlain, David Kerr, Greg Yetman, Linda Pistolesi, Forrest R Stevens, Andrea E Gaughan, Jeremiah J Nieves, Graeme Hornby, Kytt MacManus, et al. 2019. "Global Spatio-Temporally Harmonised Datasets for Producing High-Resolution Gridded Population Distribution Datasets." *Big Earth Data* 3 (2): 108–139. (Cited on page 16).

Lucas Jr, Robert E. 1988. "On the Mechanics of Economic Development." *Journal of monetary economics* 22 (1): 3–42. (Cited on page 37).

Ma, Hongbo, Jeffrey A Nittrouer, Xudong Fu, Gary Parker, Yuanfeng Zhang, Yuanjian Wang, Yanjun Wang, Michael P Lamb, Julia Cisneros, Jim Best, et al. 2022. "Amplification of Downstream Flood Stage Due to Damming of Fine-Grained Rivers." *Nature Communications* 13 (1): 3054. (Cited on page 17).

Mård, Johanna, Giuliano Di Baldassarre, and Maurizio Mazzoleni. 2018. "Nighttime Light Data Reveal How Flood Protection Shapes Human Proximity to Rivers." *Science Advances* 4 (8): eaar5779. (Cited on page 7).

Marx, Benjamin, Thomas Stoker, and Tavneet Suri. 2013. "The economics of slums in the developing world." *Journal of Economic Perspectives* 27 (4): 187–210. (Cited on page 47).

Mazhin, Sadegh Ahmadi, Mehrdad Farrokhi, Mehdi Noroozi, Juliet Roudini, Seyed Ali Hosseini, Mohammad Esmaeil Motlagh, Pirhossein Kolivand, and Hamidreza Khankeh. 2021. "World-wide Disaster Loss and Damage Databases: A Systematic Review." *Journal of Education and Health Promotion* 10 (1). (Cited on page 13).

Melchiorri, Michele, Sergio Freire, Marcello Schiavina, Aneta Florczyk, Christina Corbane, Luca Maffenini, Martino Pesaresi, Panagiotis Politis, Filip Szabo, Daniele Ehrlich, et al. 2024. "The Multi-Temporal and Multi-Dimensional Global Urban Centre Database to Delineate and Analyse World Cities." *Scientific Data* 11 (1): 82. (Cited on page 9).

Mendelsohn, Robert, Ariel Dinar, and Larry Williams. 2006. "The Distributional Impact of Climate Change on Rich and Poor Countries." *Environment and Development Economics* 11 (2): 159–178. (Cited on page 7).

Mendelsohn, Robert, Wendy Morrison, Michael E Schlesinger, and Natalia G Andronova. 2000. "Country-Specific Market Impacts of Climate Change." *Climatic Change* 45 (3): 553–569. (Cited on page 7).

Miguel, Edward, and Gerard Roland. 2011. "The Long-Run Impact of Bombing Vietnam." *Journal of Development Economics* 96 (1): 1–15. (Cited on page 40).

Mills, Stephen, Stephanie Weiss, and Calvin Liang. 2013. "VIIRS day/night band (DNB) stray light characterization and correction." In *Earth observing systems XVIII,* 8866:549–566. SPIE. (Cited on page 12).

Minale, Luigi. 2018. "Agricultural Productivity Shocks, Labour Reallocation and Rural–Urban Migration in China." *Journal of Economic Geography* 18 (4): 795–821. (Cited on page 37).

Moser, Susanne C, and Julia A Ekstrom. 2010. "A Framework to Diagnose Barriers to Climate Change Adaptation." *Proceedings of the National Academy of Sciences* 107 (51): 22026–22031. (Cited on page 31).

Mullins, Jamie T, and Prashant Bharadwaj. 2021. *Weather, Climate, and Migration in the United States.* Technical report. National Bureau of Economic Research. (Cited on page 7).

Munasinghe, Dinuke, Renato Prata de Moraes Frasson, Cédric H David, Matthew Bonnema, Guy Schumann, and G Robert Brakenridge. 2023. "A Multi-Sensor Approach for Increased Measurements of Floods and their Societal Impacts from Space." *Communications Earth & Environment* 4 (1): 462. (Cited on page 20).

Nirandjan, Sadhana, Elco E Koks, Philip J Ward, and Jeroen CJH Aerts. 2022. "A spatially-explicit harmonized global dataset of critical infrastructure." *Scientific Data* 9 (1): 150. (Cited on pages 17, 28, 41, 63).

Nordhaus, William. 2019. "Climate change: The Ultimate Challenge for Economics." *American Economic Review* 109 (6): 1991–2014. (Cited on page 46).

OpenStreetMap Contributors. 2017. "Planet Dump, retrieved from https://planet.osm.org." Available at https://www.openstreetmap.org, Last Accessed: 2023-12-23, (cited on pages 11, 17, 60).

Park, R Jisung, Joshua Goodman, Michael Hurwitz, and Jonathan Smith. 2020. "Heat and Learning." *American Economic Journal: Economic Policy* 12 (2): 306–39. (Cited on page 7).

Patel, Dev. 2024. "Floods." *Available at SSRN 4636828,* (cited on pages 6, 7, 37).

Pelli, Martino, Jeanne Tschopp, Natalia Bezmaternykh, and Kodjovi M Eklou. 2023. "In the Eye of the Storm: Firms and Capital Destruction in India." *Journal of Urban Economics* 134:103529. (Cited on page 6).

Pindyck, Robert S. 2013. "Climate Change Policy: What Do the Models Tell Us?" *Journal of Economic Literature* 51 (3): 860–72. (Cited on page 34).

Raghunathan, Trivellore E, James M Lepkowski, John Van Hoewyk, Peter Solenberger, et al. 2001. "A Multivariate Technique for Multiply Imputing Missing Values Using a Sequence of Regression Models." *Survey Methodology* 27 (1): 85–96. (Cited on page 11).

Rentschler, Jun, Paolo Avner, Mattia Marconcini, Rui Su, Emanuele Strano, Michalis Vousdoukas, and Stéphane Hallegatte. 2023. "Global Evidence of Rapid Urban Growth in Flood Zones Since 1985." *Nature* 622 (7981): 87–92. (Cited on page 1).

Rentschler, Jun, Melda Salhab, and Bramka Arga Jafino. 2022. "Flood Exposure and Poverty in 188 Countries." *Nature Communications* 13 (1): 3527. (Cited on page 1).

Román, Miguel O, Zhuosen Wang, Ranjay Shrestha, Tian Yao, and Virginia Kalb. 2021. "Black Marble User Guide Version 1.2." *NASA: Washington, DC, USA,* 66. (Cited on page 12).

Román, Miguel O, Zhuosen Wang, Qingsong Sun, Virginia Kalb, Steven D Miller, Andrew Molthan, Lori Schultz, Jordan Bell, Eleanor C Stokes, Bhartendu Pandey, et al. 2018. "NASA's Black Marble Nighttime Lights Product Suite." *Remote Sensing of Environment* 210:113–143. (Cited on page 12).

Rubin, Donald B. 1987. "Multiple Imputation for Survey Nonresponse," (cited on page 11).

———. 1996. "Multiple Imputation After 18+ Years." *Journal of the American Statistical Association* 91 (434): 473–489. (Cited on page 11).

Shah, Manisha, and Bryce Millett Steinberg. 2017. "Drought of Opportunities: Contemporaneous and Long-Term Impacts of Rainfall Shocks on Human Capital." *Journal of Political Economy* 125 (2): 527–561. (Cited on page 6).

Shi, Linda, Eric Chu, and Jessica Debats. 2015. "Explaining progress in climate adaptation planning across 156 US municipalities." *Journal of the American Planning Association* 81 (3): 191–202. (Cited on page 47).

Skoufias, Emmanuel, Eric Strobl, and Thomas Tveit. 2021. "Can We Rely on VIIRS Nightlights to Estimate the Short-Term Impacts of Natural Hazards? Evidence from Five South East Asian Countries." *Geomatics, Natural Hazards and Risk* 12 (1): 381–404. (Cited on page 12).

Somanathan, Eswaran, Rohini Somanathan, Anant Sudarshan, and Meenu Tewari. 2021. "The Impact of Temperature on Productivity and Labor Supply: Evidence from Indian Manufacturing." *Journal of Political Economy* 129 (6): 1797–1827. (Cited on pages 6, 29).

Stern, Nicholas. 2007. *The Economics of Climate Change: The Stern Review.* Cambridge University Press. (Cited on page 7).

Stevens, Forrest R, Andrea E Gaughan, Catherine Linard, and Andrew J Tatem. 2015. "Disaggregating Census Data for Population Mapping Using Random Forests with Remotely-Sensed and Ancillary Data." *PloS One* 10 (2): e0107042. (Cited on page 16).

Stevenson, Betsey, and Justin Wolfers. 2006. "Bargaining in the Shadow of the Law: Divorce Laws and Family Distress." *The Quarterly Journal of Economics* 121 (1): 267–288. (Cited on page 23).

Storeygard, Adam. 2016. "Farther on Down the Road: Transport Costs, Trade and Urban Growth in Sub-Saharan Africa." *The Review of Economic Studies* 83 (3): 1263–1295. (Cited on page 9).

Strobl, Eric. 2011. "The Economic Growth Impact of Hurricanes: Evidence from US Coastal Counties." *Review of Economics and Statistics* 93 (2): 575–589. (Cited on page 6).

———. 2012. "The Economic Growth Impact of Natural Disasters in Developing Countries: Evidence from Hurricane Strikes in the Central American and Caribbean Regions." *Journal of Development Economics* 97 (1): 130–141. (Cited on page 6).

Tol, Richard SJ. 2009. "The Economic Effects of Climate Change." *Journal of Economic Perspectives* 23 (2): 29–51. (Cited on page 7).

———. 2018. "The Economic Impacts of Climate Change." *Review of Environmental Economics and Policy,* (cited on page 1).

———. 2024. "A Meta-Analysis of the Total Economic Impact of Climate Change." *Energy Policy* 185:113922. (Cited on page 1).

UN DESA. 2019. "World Urbanization Prospects: The 2018 Revision." *Department of Economic and Social Affairs, Population Division, United Nations,* (cited on page 1).

UNDP. 2023. *SDG Insights.* Technical report. Available at: https://sdgpush.undp.org/, Last Accessed: 2024-10-24. United Nations Development Programme. (Cited on page 4).

UNISDR. 2018. *Economic Losses, Poverty & Disasters: 1998-2017.* United Nations Office for Disaster Risk Reduction. (Cited on page 8).

Van Buuren, Stef. 2007. "Multiple Imputation of Discrete and Continuous Data by Fully Conditional Specification." *Statistical Methods in Medical Research* 16 (3): 219–242. (Cited on page 11).

Van Buuren, Stef, and Karin Groothuis-Oudshoorn. 2011. "*mice*: Multivariate Imputation by Chained Equations in R." *Journal of Statistical Software* 45:1–67. (Cited on page 12).

Vencatesan, Anjana. 2021. "From Rains to Floods: A Case of Chennai in 2015." Available at https://www.environmentandsociety.org/arcadia/rains-floods-case-chennai-2015, Last Accessed: 2024-06-08, *Environment Society Portal, Arcadia (Summer 2021), no. 23. Rachel Carson Center for Environment and Society,* (cited on page 11).

Vink, Gerko, Laurence E Frank, Jeroen Pannekoek, and Stef Van Buuren. 2014. "Predictive Mean Matching Imputation of Semicontinuous Variables." *Statistica Neerlandica* 68 (1): 61–90. (Cited on page 12).

White, Ian R, Patrick Royston, and Angela M Wood. 2011. "Multiple Imputation Using Chained Equations: Issues and Guidance for Practice." *Statistics in Medicine* 30 (4): 377–399. (Cited on page 13).

World Bank. 2020. "New World Bank Country Classifications by Income Level: 2020-2021." Available at https://blogs.worldbank.org/en/opendata/new-world-bank-country-classifications-income-level-2020-2021, Last Accessed: 2024-04-30, *World Bank Blogs,* (cited on pages 1–3, 9, 61).

———. 2024. "A Story of Urban Development in Korea: From Overconcentration toward Balanced Territorial Development and Urban Regeneration," (cited on page 1).

World Bank, ADB, AfDB, BMZ, DFID, DGIS, EC, et al. 2003. *Poverty and Climate Change: Reducing the Vulnerability of the Poor through Adaptation.* Technical report. OECD. (Cited on page 7).

World Commission on Dams. 2000. *Dams and Development: A New Framework for Decision-Making: The Report of the World Commission on Dams.* Earthscan. (Cited on page 43).

WorldPop. 2018. "Global High Resolution Population Denominators Project." *Funded by The Bill Melinda Gates Foundation (OPP1134076) School of Geography and Environmental Science, University of Southampton; Department of Geography and Geosciences, University of Louisville; Departement de Geographie, Universite de Namur) and Center for International Earth Science Information Network (CIESIN), Columbia University,* (cited on pages 16, 32, 38, 40).

Appendix

Table of Contents

A Data Appendix

A Urban Boundaries

Figure A.1: Urban Spatial Extent

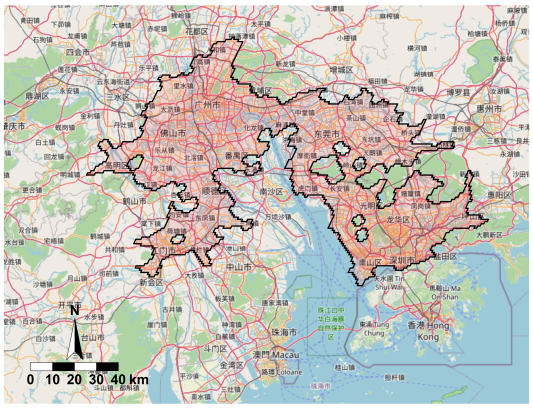

(a) Guangzhou (China)

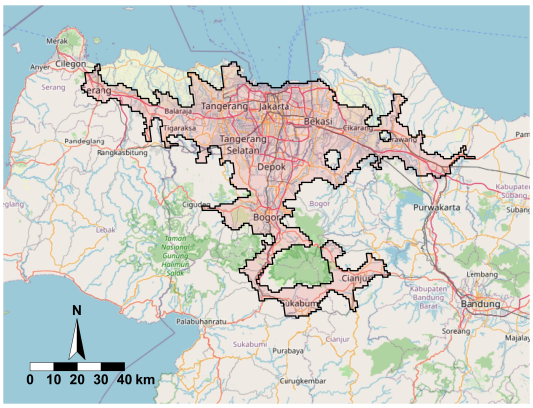

(b) Jakarta (Indonesia)

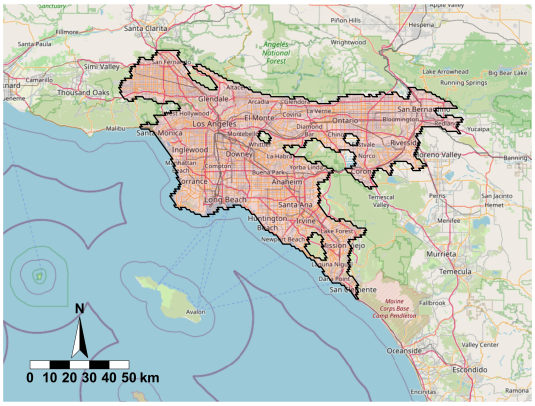

(c) Los Angeles (USA)

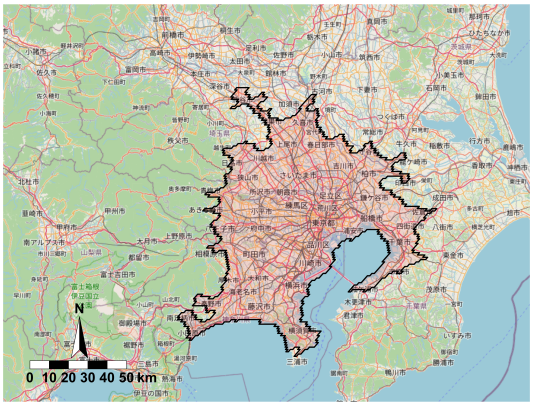

(d) Tokyo (Japan)

Notes: This figure overlays the urban spatial extents, sourced from GHS-UCDB, on the geospatial maps, sourced from OpenStreetMap Contributors, 2017, for four major cities. The shaded region (red) shows the polygons used to define the urban boundaries of these cities in our analysis. Hence, our geographic coverage includes the core city and also covers a large part of the suburban areas.

B *Spatial distribution of cities and country classification by income levels*

Figure A.2: Spatial Distribution of Cities and Country Classification by Income Levels

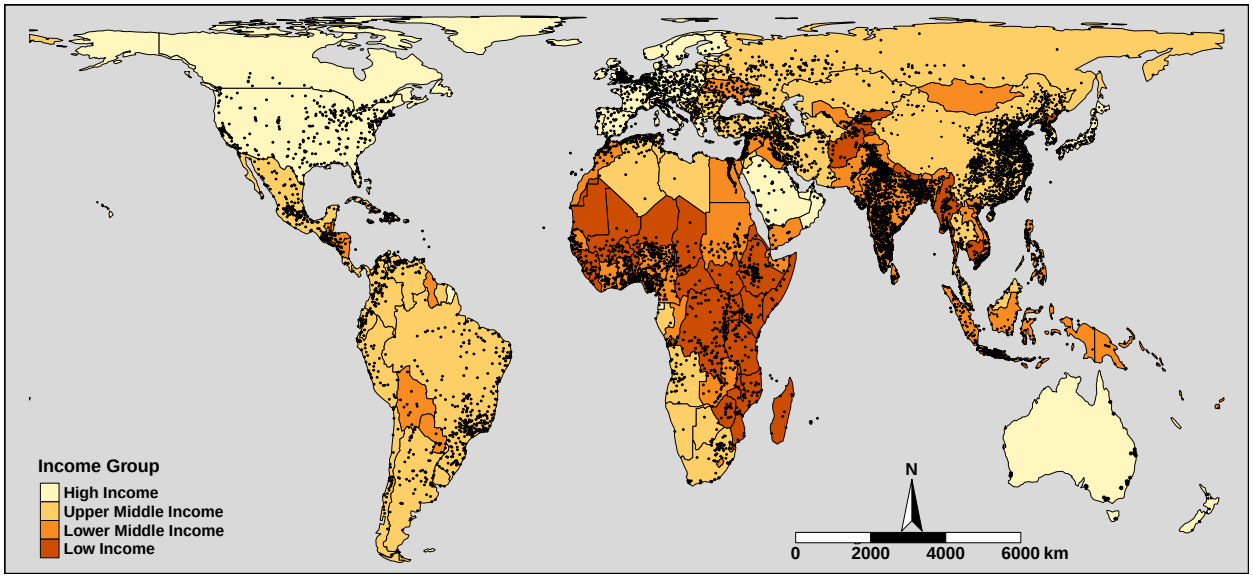

Notes: The map shows the spatial distribution of the 9,468 cities in our sample, with each city represented as a dot. Each dot represents the centroid of the urban spatial extent, which was sourced from GHS-UCDB. The background colors represent the income classification of the country as defined by the World Bank (2020), and are based on GNI per capita in current USD for the year 2019. This map uses the Hobo-Dyer Equal Area projection.

Figure A.3: Frequency of Flood between January 2000 - July 2023

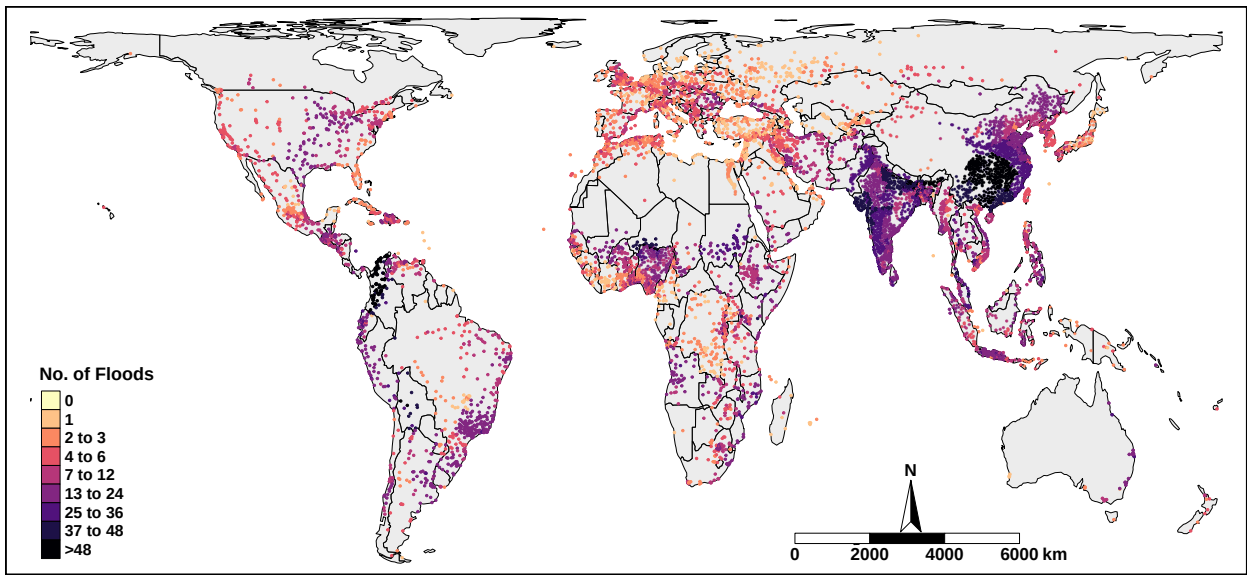

Notes: The map shows the spatial distribution of the frequency of floods across all 9,468 cities in our sample between January 2000 and July 2023. Each city is represented as a dot, and represents the centroid of the urban spatial extent, which was sourced from GHS-UCDB. The data on city-wide flood frequency was constructed using information on date and location of floods from EM-DAT. This map uses the Hobo-Dyer Equal Area projection.

C Frequency of Flood between January 2000 - July 20230 2000 4000 6000 km

Figure A.4: Spatial Distribution of Critical Infrastructure Spatial Index (CISI)

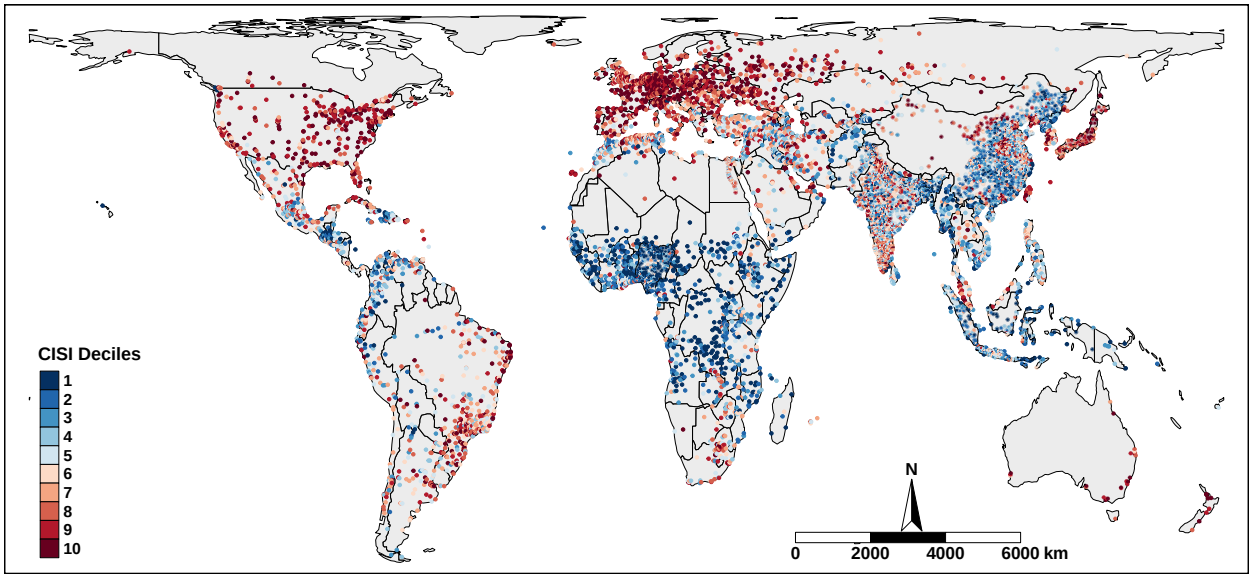

Notes: The map shows the spatial distribution of CISI as of November 2020 across all 9,468 cities in our sample. Each city is represented as a dot, and represents the centroid of the urban spatial extent, which was sourced from GHS-UCDB. The data on city-wide CISI was constructed using information on the spatial intensity of infrastructure available at a resolution of $0.1^{\circ} \times 0.1^{\circ}$ (~11km) and provided by Nirandjan et al. (2022). We aggregate the grid-level CISI data to the city level by calculating the weighted average of CISI across all 11km grid cells that fall within the urban extent shape-files, with weights equal to the proportion of the grid cell that falls within the city extent. This map uses the Hobo-Dyer Equal Area projection.

D Spatial Distribution of Critical Infrastructure Spatial Index (CISI)

E Cities protected by dams

Figure A.5: Cities Protected by Dams

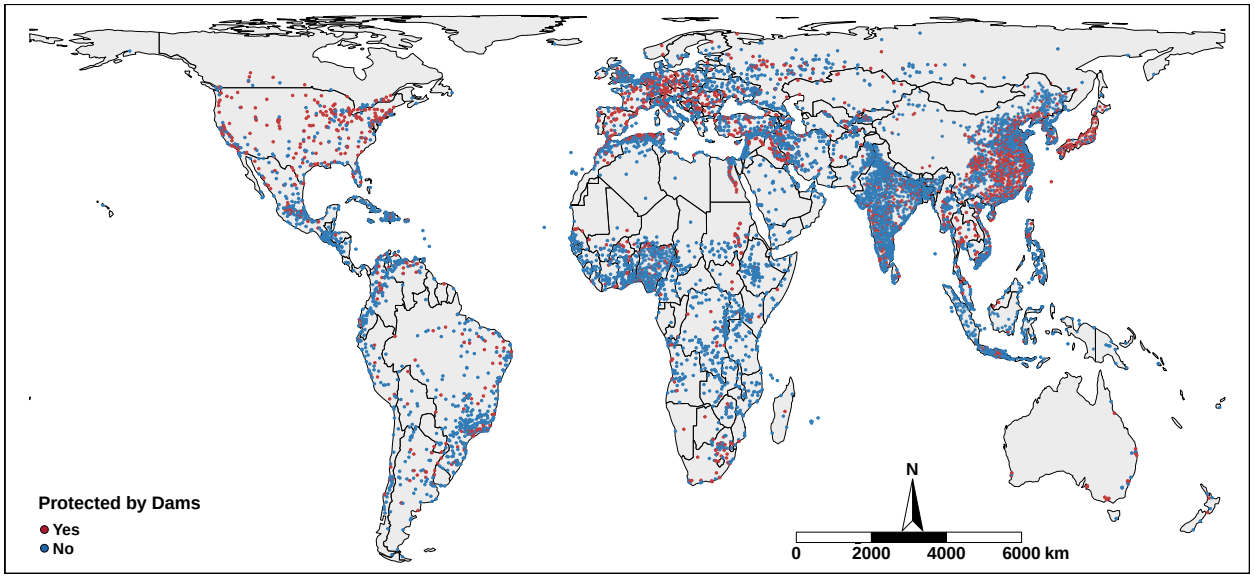

Notes: The map shows which of the 9,468 cities in our sample were protected by dams. Each city is represented as a dot, and represents the centroid of the urban spatial extent, which was sourced from GHS-UCDB. The algorithm and data sources used to identify whether a city was protected by a dam are detailed in Section 2.H. This map uses the Hobo-Dyer Equal Area projection.

B Summary Statistics

A List of Countries and Share of Cities

B Economic and geographic characteristics

C Floods and Extreme Precipitation Events between January 2000 - March 2012

D Floods and Extreme Precipitation Events between April 2012 - July 2023

Table B.1: List of Countries and Share of Cities

Country Name	Cities	%	Country Name	Cities	%	Country Name	Cities	%
Afghanistan	25	0.26	Gambia	4	0.04	North Macedonia	7	0.07
Albania	6	0.06	Georgia	5	0.05	Norway	4	0.04
Algeria	92	0.97	Germany	87	0.92	Oman	11	0.12
Angola	42	0.44	Ghana	48	0.51	Pakistan	168	1.77
Argentina	70	0.74	Greece	10	0.11	Palestine, State of	7	0.07
Armenia	3	0.03	Guatemala	39	0.41	Panama	6	0.06
Australia	27	0.29	Guinea	17	0.18	Papua New Guinea	8	0.08
Austria	6	0.06	Guinea-Bissau	3	0.03	Paraguay	8	0.08
Azerbaijan	15	0.16	Guyana	2	0.02	Peru	41	0.43
Bahamas	1	0.01	Haiti	21	0.22	Philippines	90	0.95
Bahrain	1	0.01	Honduras	13	0.14	Poland	46	0.49
Bangladesh	80	0.84	Hungary	11	0.12	Portugal	9	0.10
Barbados	1	0.01	Iceland	1	0.01	Puerto Rico	3	0.03
Belarus	14	0.15	India	1,563	16.51	Qatar	3	0.03
Belgium	12	0.13	Indonesia	311	3.28	Romania	27	0.29
Belize	1	0.01	Iran	172	1.82	Russian Federation	204	2.15
Benin	20	0.21	Iraq	69	0.73	Rwanda	7	0.07
Bolivia	12	0.13	Ireland	5	0.05	Saudi Arabia	43	0.45
Bosnia & Herzegovina	5	0.05	Israel	9	0.1	Senegal	29	0.31
Botswana	7	0.07	Italy	91	0.96	Serbia	13	0.14
Brazil	347	3.66	Jamaica	4	0.04	Sierra Leone	9	0.10
Brunei Darussalam	1	0.01	Japan	109	1.15	Singapore	1	0.01
Bulgaria	7	0.07	Jordan	9	0.10	Slovakia	6	0.06
Burkina Faso	27	0.29	Kazakhstan	27	0.29	Slovenia	2	0.02
Burundi	10	0.11	Kenya	38	0.40	Solomon Islands	1	0.01
Cabo Verde	1	0.01	Korea DPR	76	0.80	Somalia	18	0.19
Cambodia	8	0.08	Korea, Republic of	39	0.41	South Africa	77	0.81
Cameroon	45	0.48	Kosovo	7	0.07	South Sudan	13	0.14
Canada	48	0.51	Kuwait	4	0.04	Spain	72	0.76
Central African Republic	6	0.06	Kyrgyzstan	9	0.10	Sri Lanka	20	0.21
Chad	23	0.24	Lao	4	0.04	Sudan	52	0.55
Chile	33	0.35	Latvia	3	0.03	Suriname	1	0.01
China	1,776	18.76	Lebanon	7	0.07	Sweden	12	0.13
Colombia	87	0.92	Lesotho	1	0.01	Switzerland	16	0.17
Comoros	2	0.02	Liberia	5	0.05	Syrian Arab Republic	24	0.25
Congo	114	1.20	Libya	15	0.16	Taiwan	21	0.22
Congo	4	0.04	Lithuania	6	0.06	Tajikistan	14	0.15
Costa Rica	3	0.03	Luxembourg	1	0.01	Tanzania	38	0.40
Côte d'Ivoire	35	0.37	Madagascar	6	0.06	Thailand	41	0.43
Croatia	6	0.06	Malawi	8	0.08	Timor-Leste	1	0.01
Cuba	19	0.20	Malaysia	36	0.38	Togo	13	0.14
Curaçao	1	0.01	Mali	16	0.17	Trinidad and Tobago	4	0.04
Cyprus	3	0.03	Malta	1	0.01	Tunisia	26	0.27
Czechia	12	0.13	Mauritania	4	0.04	Turkey	129	1.36
Denmark	4	0.04	Mauritius	1	0.01	Turkmenistan	10	0.11
Djibouti	1	0.01	Mexico	157	1.66	Uganda	23	0.24
Dominican Republic	16	0.17	Moldova	5	0.05	Ukraine	78	0.82
Ecuador	30	0.32	Mongolia	1	0.01	United Arab Emirates	5	0.05
Egypt	182	1.92	Montenegro	1	0.01	United Kingdom	138	1.46
El Salvador	9	0.10	Morocco	59	0.62	Uruguay	6	0.06
Equatorial Guinea	2	0.02	Mozambique	38	0.40	USA	324	3.42
Eritrea	2	0.02	Myanmar	86	0.91	Uzbekistan	56	0.59
Estonia	2	0.02	Namibia	2	0.02	Venezuela	73	0.77
Eswatini	2	0.02	Nepal	9	0.10	Viet Nam	128	1.35
Ethiopia	86	0.91	Netherlands	37	0.39	Yemen	15	0.16
Fiji	1	0.01	New Zealand	8	0.08	Zambia	35	0.37
Finland	6	0.06	Nicaragua	14	0.15	Zimbabwe	19	0.20
France	76	0.80	Niger	23	0.24			
Gabon	3	0.03	Nigeria	376	3.97	**Total**	**9,468**	**100**

Notes: The table provides details on the cities within each country, both as a number and the percentage of total cities. These 9,468 cities form the entire sample for our analysis. Details on these urban centers have been sourced from Global Human Settlement Urban Center Database (GHS-UCDB) created by Florczyk et al. (2019).

Table B.2: Summary Statistics of Economic and Geographic Characteristics

	No. of Cities	Mean Elevation (meters)	GDP/capita (2015 US$)	Avg. Annual Pop. Growth b/w 2000-20 (%)	Built-up Area in 2015 (% of Total Area)	Avg. Monthly NTL b/w 2012-23 (in nW/cm2/sr)	Area Weighted CISI in 2020 (Index b/w 0-1)	No. of Cities Protected by Dams
	(1)	(2)	(3)	(4)	(5)	(6)	(7)	(8)
Panel A: Aggregate								
All Cities	9,468	360 (500)	8.2 (9.2)	2.5 (2.6)	35 (18)	15 (16)	0.069 (0.06)	2,409 [25]
High Income	5,102 [54]	370 (540)	12 (10)	1.6 (2.0)	45 (16)	22 (18)	0.088 (0.066)	1,779 [35]
Low Income	4,366 [46]	350 (460)	3.3 (3.0)	3.5 (3.0)	23 (13)	6.4 (7.7)	0.046 (0.042)	630 [14]
Panel B: High Income Cities								
Coastal	777 [8.2]	39 (45)	18 (14)	1.6 (1.9)	46 (14)	28 (23)	0.097 (0.062)	212 [27]
Inland	4,325 [46]	430 (560)	11 (9.2)	1.6 (2.0)	44 (16)	21 (17)	0.086 (0.067)	1,567 [36]
Low Elevation	2,820 [30]	54 (43)	14 (11)	1.4 (1.8)	46 (15)	22 (19)	0.092 (0.066)	1,119 [40]
High Elevation	2,282 [24]	760 (610)	11 (9.1)	1.9 (2.1)	42 (16)	23 (18)	0.083 (0.066)	660 [29]
Panel C: Low Income Cities								
Coastal	437 [4.6]	35 (47)	4.3 (4.3)	2.7 (2.7)	25 (14)	9.3 (12)	0.044 (0.041)	42 [10]
Inland	3,929 [42]	390 (470)	3.2 (2.8)	3.6 (3.0)	23 (13)	6.1 (7.0)	0.047 (0.042)	588 [15]
Low Elevation	1,914 [20]	53 (45)	3.9 (3.3)	2.7 (2.3)	23 (13)	7.0 (8.1)	0.049 (0.041)	345 [18]
High Elevation	2,452 [26]	590 (500)	2.8 (2.5)	4.1 (3.3)	23 (13)	6.0 (7.3)	0.044 (0.042)	285 [12]

Notes: *Panel A* provides summary statistics for all 9,468 cities and also separately for *High Income* and *Low Income* cities, where income classification is based on the World Bank country classifications by income level (GNI per capita) in calendar year 2020. All cities in *Low Income* (<= US$1,045) and *Lower Middle Income* (US$1,046 - US$4,095) countries were classified as *Low Income* cities, while all cities in *Upper Middle Income* (US$4,096 - US$12,695) and *High Income* (> US$12,695) countries were classified as *High Income* cities. *Panel B* (*Panel C*) provides summary statistics for *High* (*Low*) *Income* cities after further classifying them into *Coastal* or *Inland* cities, and *Low Elevation* or *High Elevation* cities. A city is defined to be at a *high elevation* if it has a median elevation that ranks in the top 50^{th} percentile of the distribution of the median elevation across all cities, *i.e.* greater than 154 meters. The sum of *Coastal* and *Inland* cities equals the total number of cities in the respective income group, as do the sum of *Low* and *High Elevation* cities. Column (1) lists the number of cities in each of the categories, while the figures in brackets report the number of cities in the category as a percentage of total cities in our sample (9,468). *GDP per capita* in column (3) is measured in PPP 2015 US$ and is sourced from GHS-UCDB. *Average Annual Population Growth* in column (4) is computed as the average of the annual population change across all cities in the group. Note that population data from WorldPop was only available between 2000 and 2020 and, therefore, annual population change was calculated for all years between 2001 and 2020. *Built-up Area* in column (5) is defined as the percentage of the total area of the city (km^2) that contains built-up structures (sourced from GHS-UCDB). *Average Monthly NTL* in column (6) was calculated as the average across all months, from April 2012 to July 2023, of the mean night light intensity in all cities in the group. We have used the cloud mask configuration of the NPP-VIIRS monthly composites, where data contaminated by stray light are removed. Missing data for mean light intensity was dropped for the purpose of calculating summary statistics. *Area Weighted CISI* in column (7) was calculated as the average of the weighted Critical Infrastructure Spatial Index (between 0 and 1) across all cities in the group. Weighted CISI for each city was calculated by taking the weighted average of CISI across all grid cells that fall within the city boundary, with weights equal to the area of the grid that falls within the city boundary. Standard deviation for all variables are reported in parenthesis. All estimates in columns (2) to (7) have been rounded to two significant digits. Column (8) lists the number of cities in each category which have a dam upstream (geolocation of dams obtained from GRanD database) and are, hence, assumed to be protected by a dam. The figures in brackets reports the number of cities protected by a dam in the category as a percentage of total cities in the respective category.

Table B.3: Summary Statistics on Floods and Extreme Precipitation Events b/w January 2000 - March 2012

	Months with Floods (1)	Avg. Months with Floods (2)	Months with Extreme Precip. (3)	Avg. Months with Extreme Precip. (4)	Months with Floods in Cities Protected by Dams (5)	Avg. Months with Floods in Cities Protected by Dams (6)	Deaths Due to Floods (7)	Avg. Deaths Due to Flood Event (per 1mn Pop.) (8)
Panel A: Aggregate								
All Cities	69,665	7.4 (7.9)	62,749	6.6 (3.1)	19,091 [27]	7.9 (8.1)	19,440	17 (190)
High Income	34,273 [49]	6.7 (8.4)	33,378 [53]	6.5 (2.9)	13,608 [40]	7.6 (8.2)	8,540 [44]	8.6 (140)
Low Income	35,392 [51]	8.1 (7.3)	29,371 [47]	6.7 (3.2)	5,483 [15]	8.7 (7.7)	10,900 [56]	25 (240)
Panel B: High Income Cities								
Coastal	3,059 [4.4]	3.9 (5.9)	5,740 [9.1]	7.4 (2.8)	880 [29]	4.2 (6.2)	1,038 [5.3]	6.2 (92)
Inland	31,214 [45]	7.2 (8.7)	27,638 [44]	6.4 (2.9)	12,728 [41]	8.1 (8.4)	7,502 [39]	8.9 (140)
Low Elevation	18,674 [27]	6.6 (8.1)	19,097 [30]	6.8 (3.0)	8,656 [46]	7.7 (8.4)	2,545 [13]	3.9 (52)
High Elevation	15,599 [22]	6.8 (8.8)	14,281 [23]	6.3 (2.7)	4,952 [32]	7.5 (8.0)	5,994 [31]	14 (200)
Panel C: Low Income Cities								
Coastal	2,356 [3.4]	5.4 (5.8)	3,179 [5.1]	7.3 (3.1)	332 [14]	7.9 (6.4)	2,619 [13]	40 (320)
Inland	33,036 [47]	8.4 (7.3)	26,192 [42]	6.7 (3.2)	5,151 [16]	8.8 (7.8)	8,281 [43]	24 (230)
Low Elevation	16,431 [24]	8.6 (8.3)	14,594 [23]	7.6 (3.1)	2,892 [18]	8.4 (8.6)	6,316 [32]	21 (160)
High Elevation	18,961 [27]	7.7 (6.3)	14,777 [24]	6.0 (3.2)	2,591 [14]	9.1 (6.6)	4,584 [24]	29 (290)

Notes: *Panel A* provides summary statistics for all 9,468 cities and also separately for *High Income* and *Low Income* cities, where income classification is based on the World Bank country classifications by income level (GNI per capita) in calendar year 2020. All cities in *Low Income* (<= US$1,045) and *Lower Middle Income* (US$1,046 - US$4,095) countries were classified as *Low Income* cities, while all cities in *Upper Middle Income* (US$4,096 - US$12,695) and *High Income* (> US$12,695) countries were classified as *High Income* cities. *Panel B* (*Panel C*) provides summary statistics for *High* (*Low*) *Income* cities after further classifying them into *Coastal* or *Inland* cities, and *Low Elevation* or *High Elevation* cities. A city is defined to be at a *high elevation* if it has a median elevation (across all grid cells within the city boundary) that ranks in the top 50^{th} percentile of the distribution of the median elevation across all cities, *i.e.* greater than 154 meters. The sum of *Coastal* and *Inland* cities equals the total number of cities in the respective income group, as do the sum of *Low* and *High Elevation* cities. Column (1) lists the aggregate number of months across all city-month-year observations when the cities within the group suffered from a flood. The figures in brackets report the number of flood affected city-month-year observations in the group as a percentage of total flood affected city-month-year observations in our sample. Column (2), titled *Average Months with Floods*, is the average number of months that a city within the group was flooded between January 2000 and March 2012 (169 months). Column (3) lists the aggregate number of months across all city-month-year observations when the cities within the group suffered from an *extreme precipitation* event. A city is said to have suffered from an *extreme precipitation* event whenever the precipitation in month m and year y in city c was greater than the 95^{th} percentile of the city-specific distribution of monthly precipitation, which was created using data from January 1940 to August 2023. The figures in brackets report the number of city-month-year observations which experienced an *extreme precipitation* event in the respective group as a percentage of total city-month-year observations which experienced an *extreme precipitation* event in our sample. Column (4), titled *Average Months with Extreme Precipitation*, is the average number of months that a city within the group suffered from an *extreme precipitation* event between January 2000 and March 2012 (169 months). Columns (5) and (6) provide the same information as columns (1) and (2), *i.e.* aggregate months with floods, and average months with floods, but focus on the subset of cities protected by dams. The figures in brackets in column (5) report, for the subset of cities protected by dams, the number of flood affected city-month-year observations in the group as a percentage of total flood affected city-month-year observations in the respective category. Column (7) reports the total deaths from floods across all city-month-year observations when the cities within the group were flooded. Column (8), titled *Average Deaths Due to Flood Event (per 1 mn Population)*, is the average number of deaths per 1 mn population per every flood affected city-month-year observation in the group. Figures in parenthesis in columns (2), (4), (6) and (8) report the standard deviation for the respective variable in each group. All estimates in columns (2), (4), (6) and (8), and all figures in parenthesis have been rounded to two significant digits.

Table B.4: Summary Statistics on Floods and Extreme Precipitation Events b/w April 2012 - July 2023

	Months with Floods	Avg. Months with Floods	Months with Extreme Precip.	Avg. Months with Extreme Precip.	Months with Floods in Cities Protected by Dams	Avg. Months with Floods in Cities Protected by Dams	Deaths Due to Floods	Avg. Deaths Due to Flood Event (per 1mn Pop.)
	(1)	(2)	(3)	(4)	(5)	(6)	(7)	(8)
Panel A: Aggregate								
All Cities	81,009	8.6 (8.8)	64,860	6.9 (3.3)	25,091 [31]	10 (11)	15,550	14 (440)
High Income	44,780 [55]	8.8 (10)	32,341 [50]	6.3 (3.2)	19,322 [43]	11 (12)	4,765 [31]	2.3 (26)
Low Income	36,229 [45]	8.3 (7.2)	32,519 [50]	7.4 (3.3)	5,769 [16]	9.2 (8)	10,785 [69]	28 (660)
Panel B: High Income Cities								
Coastal	3,739 [4.6]	4.8 (6.5)	5,891 [9.1]	7.6 (3.3)	1,083 [29]	5.1 (6.7)	1,032 [6.6]	3.2 (25)
Inland	41,041 [51]	9.5 (10)	26,450 [41]	6.1 (3.1)	18,239 [44]	12 (12)	3,733 [24]	2.2 (26)
Low Elevation	24,252 [30]	8.6 (9.6)	18,881 [29]	6.7 (3.3)	12,074 [50]	11 (11)	2,269 [15]	1.6 (16)
High Elevation	20,528 [25]	9 (11)	13,460 [21]	5.9 (3.0)	7,248 [35]	11 (12)	2,496 [16]	3.2 (35)
Panel C: Low Income Cities								
Coastal	2,504 [3.1]	5.7 (4.9)	3,728 [5.7]	8.5 (4.0)	317 [13]	7.5 (7.1)	1,553 [10]	22 (210)
Inland	33,725 [42]	8.6 (7.3)	28,791 [44]	7.3 (3.2)	5,452 [16]	9.3 (8.1)	9,232 [59]	28 (680)
Low Elevation	15,051 [19]	7.9 (7.0)	14,921 [23]	7.8 (3.3)	2,613 [17]	7.6 (7.3)	4,719 [30]	21 (630)
High Elevation	21,178 [26]	8.6 (7.3)	17,598 [27]	7.2 (3.4)	3,156 [15]	11 (8.5)	6,065 [39]	33 (680)

Notes: *Panel A* provides summary statistics for all 9,468 cities and also separately for *High Income* and *Low Income* cities, where income classification is based on the World Bank country classifications by income level (GNI per capita) in calendar year 2020. All cities in *Low Income* (<= US$1,045) and *Lower Middle Income* (US$1,046 - US$4,095) countries were classified as *Low Income* cities, while all cities in *Upper Middle Income* (US$4,096 - US$12,695) and *High Income* (> US$12,695) countries were classified as *High Income* cities. *Panel B* (*Panel C*) provides summary statistics for *High* (*Low*) *Income* cities after further classifying them into *Coastal* or *Inland* cities, and *Low Elevation* or *High Elevation* cities. A city is defined to be at a *high elevation* if it has a median elevation (across all grid cells within the city boundary) that ranks in the top 50^{th} percentile of the distribution of the median elevation across all cities, *i.e.* greater than 154 meters. The sum of *Coastal* and *Inland* cities equals the total number of cities in the respective income group, as do the sum of *Low* and *High Elevation* cities. Column (1) lists the aggregate number of months across all city-month-year observations when the cities within the group suffered from a flood. The figures in brackets report the number of flood affected city-month-year observations in the group as a percentage of total flood affected city-month-year observations in our sample. Column (2), titled *Average Months with Floods*, is the average number of months that a city within the group was flooded between April 2012 and July 2023 (136 months). Column (3) lists the aggregate number of months across all city-month-year observations when the cities within the group suffered from an *extreme precipitation* event. A city is said to have suffered from an *extreme precipitation* event whenever the precipitation in month m and year y in city c was greater than the 95^{th} percentile of the city-specific distribution of monthly precipitation, which was created using data from January 1940 to August 2023. The figures in brackets report the number of city-month-year observations which experienced an *extreme precipitation* event in the respective group as a percentage of total city-month-year observations which experienced an *extreme precipitation* event in our sample. Column (4), titled *Average Months with Extreme Precipitation*, is the average number of months that a city within the group suffered from an *extreme precipitation* event between April 2012 and July 2023 (136 months). Columns (5) and (6) provide the same information as columns (1) and (2), *i.e.* aggregate months with floods, and average months with floods, but focus on the subset of cities protected by dams. The figures in brackets in column (5) report, for the subset of cities protected by dams, the number of flood affected city-month-year observations in the group as a percentage of total flood affected city-month-year observations in the respective category. Column (7) reports the total deaths from floods across all city-month-year observations when the cities within the group were flooded. Column (8), titled *Average Deaths Due to Flood Event (per 1 mn Population)*, is the average number of deaths per 1 mn population per every flood affected city-month-year observation in the group. Note that population data from WorldPop was only available between 2000 and 2020. Therefore, to calculate average number of deaths per 1 mn population for each city for years beyond 2020, we have assumed the lagged value of the population of each city (*i.e.* 2020 values) for each subsequent year (*i.e.* 2021-2023). Figures in parenthesis in columns (2), (4), (6) and (8) report the standard deviation for the respective variable in each group. All estimates in columns (2), (4), (6) and (8), and all figures in parenthesis have been rounded to two significant digits.

C The Effect of Flood Shocks

A Heterogeneous Impact by Flood Severity

Table C.1: Effect of Severe Floods on Economic Activity

	Dependent Variable: $ln(Night\ Lights_{cjmy})$		
	All	**High Income**	**Low Income**
	(1)	(2)	(3)
$Flood_{cjmy}$	-0.041^{**}	-0.011^{*}	-0.074^{***}
	(0.018)	(0.005)	(0.025)
$Flood_{cjmy} \times Severe_{cjmy}$	-0.009	-0.020^{**}	-0.011
	(0.019)	(0.009)	(0.038)
Fixed Effects			
City	Yes	Yes	Yes
Country × Month × Year	Yes	Yes	Yes
Num obs.	1,126,692	607,138	519,554
Adj. R^2	0.867	0.801	0.809

Notes: Two-way clustered robust standard errors are in parenthesis. $^{***}p < 0.01$; $^{**}p < 0.05$; $^{*}p < 0.1$.
The dependent variable in all regressions, $ln(Night\ Lights_{cjmy})$, is the natural log of mean light intensity in city c in country j in month m of year y. We have used the cloud mask configuration of the NPP-VIIRS monthly composites, where data contaminated by stray light are removed. Missing data for $ln(Night\ Lights_{cjmy})$ was imputed using Predictive Mean Matching. $Flood_{cjmy}$ is a dummy indicating whether city c in country j was hit by a flood in month m of year y. $Severe_{cjmy}$ is a dummy indicating whether the flood that hit city c in month m and year y was *Severe*, *i.e.*, classified as *Class 2* based on a flood severity assessment by Dartmouth Flood Observatory. See Section 2.I for more information on the measure of flood severity. Model (2) only includes observations from *High Income* and *Upper Middle Income* countries, whereas model (3) only includes observations from *Low Income* and *Lower Middle Income* countries. All regressions include the controls $Storm_{cjmy}$ and $Landslide_{cjmy}$, dummies indicating whether city c in country j was hit by a storm or landslide, respectively, in month m of year y. Two month leads and lags for all three disaster types have also been included as controls. Standard errors are clustered at the country and month-year level.

D Adaptation Results Across High- and Low-Income Countries

A GDP and Resilience to Floods

B Critical Infrastructure and Resilience to Floods

Table D.1: Adaptation Through Productivity Across High- and Low-Income Countries

	Dependent Variable: $ln(Night\ Lights_{cjmy})$			
	High Income		Low Income	
	(1)	(2)	(3)	(4)
$Flood_{cjmy}$	−0.071	−0.034***	−0.112	−0.074***
	(0.051)	(0.007)	(0.122)	(0.015)
$Flood_{cjmy} \times ln(GDP/capita_{cj})$	0.006		0.005	
	(0.006)		(0.016)	
$Flood_{cjmy} \times High\ GDP/capita_{cj}$		0.017***		0.002
		(0.006)		(0.019)
Fixed Effects				
City	Yes	Yes	Yes	Yes
Country × Month × Year	Yes	Yes	Yes	Yes
Num obs.	693,872	693,872	593,776	593,776
Adj. R^2	0.789	0.789	0.804	0.804

Notes: Two-way clustered robust standard errors are in parenthesis. $^{***}p < 0.01$; $^{**}p < 0.05$; $^{*}p < 0.1$.
The dependent variable in all regressions, $ln(Night\ Lights_{cjmy})$, is the natural log of mean light intensity in city c in country j in month m of year y. We have used the cloud mask configuration of the NPP-VIIRS monthly composites, where data contaminated by stray light are removed. Missing data for $ln(Night\ Lights_{cjmy})$ was imputed using Predictive Mean Matching. $Flood_{cjmy}$ is a dummy indicating whether city c in country j was hit by a flood in month m of year y. $ln(GDP/capita_{cj})$ refers to the natural log of city c's GDP per capita, which is measured in PPP US$ (2007) and pertains to the year 2015. $High\ GDP/capita_{c}$ is a dummy indicating whether city c has a GDP per capita that ranks in the top 50^{th} percentile of the distribution of GDP per capita across all cities *i.e.* cities with a GDP per capita above US$5,567. Columns (1) and (2) only include observations from *High Income* and *Upper Middle Income* countries, whereas columns (3) and (4) only include observations from *Low Income* and *Lower Middle Income* countries. All regressions include the controls $Storm_{cjmy}$ and $Landslide_{cjmy}$, dummies indicating whether city c in country j was hit by a storm or landslide, respectively, in month m of year y. Two month leads and lags for all three disaster types have also been included as controls. Standard errors are clustered at the country and month-year level.

Table D.2: Adaptation Through Critical Infrastructure Across High- and Low-Income Countries

	Dependent Variable: $ln(Night\ Lights_{cjmy})$			
	High Income		Low Income	
	(1)	(2)	(3)	(4)
$Flood_{cjmy}$	-0.034^{***}	-0.031^{***}	-0.078^{***}	-0.079^{***}
	(0.007)	(0.006)	(0.018)	(0.016)
$Flood_{cjmy} \times CISI_{cj}$	0.206^{**}		0.084	
	(0.092)		(0.188)	
$Flood_{cjmy} \times High\ CISI_{cj}$		0.022^{**}		0.012
		(0.009)		(0.014)
Fixed Effects				
City	Yes	Yes	Yes	Yes
Country × Month × Year	Yes	Yes	Yes	Yes
Num obs.	693,872	693,872	593,640	593,640
Adj. R^2	0.789	0.789	0.804	0.804

Notes: Two-way clustered robust standard errors are in parenthesis. $^{***}p < 0.01$; $^{**}p < 0.05$; $^{*}p < 0.1$.
The dependent variable in all regressions, $ln(Night\ Lights_{cjmy})$, is the natural log of mean light intensity in city c in country j in month m of year y. We have used the cloud mask configuration of the NPP-VIIRS monthly composites, where data contaminated by stray light are removed. Missing data for $ln(Night\ Lights_{cjmy})$ was imputed using Predictive Mean Matching. $Flood_{cjmy}$ is a dummy indicating whether city c in country j was hit by a flood in month m of year y. $CISI_{cj}$ refers to the weighted average of the Critical Infrastructure Spatial Index (between 0 and 1) across all grid cells that fall within a city boundary, with weights equal to the area of the grid that falls within the city boundary. $High\ CISI_c$ is a dummy indicating whether city c has a weighted CISI that ranks in the top 50^{th} percentile of the distribution of CISI across all cities *i.e.*, cities with a weighted CISI above 0.051. Columns (1) and (2) only include observations from *High Income* and *Upper Middle Income* countries, whereas columns (3) and (4) only include observations from *Low Income* and *Lower Middle Income* countries. All regressions include the controls $Storm_{cjmy}$ and $Landslide_{cjmy}$, dummies indicating whether city c in country j was hit by a storm or landslide, respectively, in month m of year y. Two month leads and lags for all three disaster types have also been included as controls. Standard errors are clustered at the country and month-year level.